Hashemite Kingdom of Jordan

Scientific Research Support Fund

Hashemite University

Jordan Journal of Earth and Environmental Sciences

JJEES

An International Peer-Reviewed Scientific Journal

Financed by the Scientific Research Support Fund

http://jjees.hu.edu.jo/

Volume (8) Number (2) ISSN 1995-6681 December 2017 / Rabi' Al-Awwal 1439

Jordan Journal of Earth and Environmental Sciences (JJEES)

JJEES is an International Peer-Reviewed Research Journal, Issued by Deanship of Scientific Research, The Hashemite University, in corporation with, the Jordanian Scientific Research Support Fund, the Ministry of Higher Education and Scientific Research.

Editorial Board:

The International Advisory Board:

Editorial Board Support Team:

Submission address:

Manuscripts should be submitted electronically to the following e-mail:

jjees@hu.edu.jo

For more information and previous issues:

www.jjees.hu.edu.jo

Hashemite Kingdom of Jordan

Scientific Research Support Fund

Hashemite University

Jordan Journal of Earth and Environmental Sciences

JJEES

An International Peer-Reviewed Scientific Journal

Financed by the Scientific Research Support Fund

Volume 8 Number (2)

http:// jjees.hu.edu.jo/

ISSN 1995-6681

المجلة الأردنية لعلوم الأرض والبيئة
Jordan Journal of Earth and Environmental Sciences (JJEES)
http://jjees.hu.edu.jo

Hashemite University

Deanship of Scientific Research

TRANSFER OF COPYRIGHT AGREEMENT

Journal publishers and authors share a common interest in the protection of copyright: authors principally because they want their creative works to be protected from plagiarism and other unlawful uses, publishers because they need to protect their work and investment in the production, marketing and distribution of the published version of the article. In order to do so effectively, publishers request a formal written transfer of copyright from the author(s) for each article published. Publishers and authors are also concerned that the integrity of the official record of publication of an article (once refereed and published) be maintained, and in order to protect that reference value and validation process, we ask that authors recognize that distribution (including through the Internet/WWW or other on-line means) of the authoritative version of the article as published is best administered by the Publisher.

To avoid any delay in the publication of your article, please read the terms of this agreement, sign in the space provided and return the complete form to us at the address below as quickly as possible.

Article entitled:----------

Corresponding author: ----------

To be published in the journal: Jordan Journal of Earth & Environmental Sciences (JJEES)

I hereby assign to the Hashemite University the copyright in the manuscript identified above and any supplemental tables, illustrations or other information submitted therewith (the "article") in all forms and media (whether now known or hereafter developed), throughout the world, in all languages, for the full term of copyright and all extensions and renewals thereof, effective when and if the article is accepted for publication. This transfer includes the right to adapt the presentation of the article for use in conjunction with computer systems and programs, including reproduction or publication in machine-readable form and incorporation in electronic retrieval systems.
Authors retain or are hereby granted (without the need to obtain further permission) rights to use the article for traditional scholarship communications, for teaching, and for distribution within their institution.

☐ **I am the sole author of the manuscript**

☐ **I am signing on behalf of all co-authors of the manuscript**

☐ **The article is a 'work made for hire' and I am signing as an authorized representative of the employing company/institution**

Please mark one or more of the above boxes (as appropriate) and then sign and date the document in black ink.

Signed:_____ **Name printed:** _____

Title and Company (if employer representative) : _____

Date: _____

Data Protection: By submitting this form you are consenting that the personal information provided herein may be used by the Hashemite University and its affiliated institutions worldwide to contact you concerning the publishing of your article.

Please return the completed and signed original of this form by mail or fax, or a scanned copy of the signed original by e-mail, retaining a copy for your files, to:

Deanship of Scientific Research
The Hashemite University P.O. Box 150458, P.C.13115, Zarqa, Jordan
Tel.: 00962 53903333/ Ext. 4235
Fax: 00962 53826823
E-mail: jjees@hu.edu.jo

Subscription

Jordan Journal of Earth & Environmental Sciences (ISSN 1995-6681)
An International Peer- Reviewed Research Journal
Published by the Deanship of Scientific Research - The Hashemite University

Name:	الاســـــــــــم:
Specialty:.....	التخصـــــــــص:
Address:.....	العنـــــــــوان:
P.O. Box:.....	صنـــدوق البريـــــد:
City & Postal Code:	المدينة: الرمز البريدي:
Country:.....	الـــــــــــدولة:
Phone:.....	رقـــم الهاتـــــف:
Fax No:.....	رقـــم الفاكـــــس:
E-mail:.....	البريـــد الإلكترونـــي:
Method of payment:	طريقـــــة الدفـــع:
Amount Enclosed:.....	المبلـــغ المرفـــق:
Signature:.....	التوقيـــــــــع:

Cheques should be paid to Deanship of Research - The Hashemite University

I would like to subscribe to the Journal:

For

- ☐ One year
- ☐ Two years
- ☐ Three years

One year Subscription Rates

	Inside Jordan	Outside Jordan
Individuals	10JD	70$
Students	5JD	35$
Institutions	20JD	90$

Correspondence

Subscriptions and sales:

Professor Issa Makhlouf
Deanship of Scientific Research
The Hashemite University P.O. Box 150458, P.C.13115, Zarqa, Jordan
Tel.: 00962 53903333/ Ext. 4235
Fax: 00962 53826823
E-mail: jjees@hu.edu.jo

JJEES
Jordan Journal of Earth and Environmental Sciences

PAGES	PAPERS
55 - 60	Structural Evolution of the Area North of Ajloun Dome, Jordan *Mohammad Al-Tawalbeh, Mohammad Atallah and Mahmoud Al Tamimi*
61 - 67	Assessment of Heavy Metals in Topsoil of Al Hashmiyya City of Jordan *Kholoud Mashal, Mohammed Salahat, Mohammed Al-Qinna and Yahya Ali*
69 - 76	Does Forest Litterfall Nutrient Stocks Affect the Nutrient Supplying Capacity of Soils? *Azeez Jamiu Oladipupo*
77 - 89	The Need for a Quantitative Analysis of Risk and Reliability for Formulation of Water Budget in Jordan *Fayha M. Al-Shibli, William A. Maher and Ross M. Thompson*
91 - 96	How Precisely «Kaya Identity» Can Estimate GHG Emissions: A Global Review *Azadeh Tavakoli*
97 - 103	The Use of GIS Techniques and Geophysical Investigation for Flood Management at Wadi Al-Mafraq Catchment Area *Hani Al-Amoush, Abdel Rahman Al-Shabeeb, Rida Al-Adamat, A'kif Al-Fugara, Saad Al Ayyash, Akram Shdeifat, Eid Al-Tarazi and Jafar Abu Rajab*

JJEES
Jordan Journal of Earth and Environmental Sciences

Volume 8, (Number 2), Dec, 2017
ISSN 1995-6681
Pages 55 - 60

Structural Evolution of the Area North of Ajloun Dome, Jordan

Mohammad Al-Tawalbeh, Mohammad Atallah* and Mahmoud Al Tamimi

Department of Earth and Environmental Sciences, Yarmouk University, Irbid- Jordan

Received 24 January, 2017; Accepted 10 October, 2017

Abstract

The detailed mapping of the area north of Ajloun dome proved the existence of conglomerate beds (equivalent to Dana Conglomerate) of post Eocene (Post Umm Rijam). Other outcrops in the area range from Turonian to Miocene. The structures in the present study area consist of one Syncline (Ausara Syncline), a group of normal faults, one strike slip fault, and a group of systematic joint sets. The Ausara symmetric syncline is trending S65ºW, plunging 17º. It was formed during the second stage of the Syrian Arc Stress field (SAS), after the formation of Ajloun dome, which was formed in the Upper Cretaceous, during the first phase of the Syrian Arc folding. Normal faults, grabens and horsts trend NNW. They are parallel to the general Dead Sea Stress field (DSS) which trends NNW-SSE compression and ENE-WSW tension. They formed after the Ausara syncline because one of these fault truncated the syncline. Horizontal fault block rotation is indicated from the change in the general strike of the joint sets. The area close to the Jordan valley was tilting to the west as indicated from the general westward dipping of the Tertiary and the underlying Upper Cretaceous beds. The general structure of the area can be described as faulted flexure.

Keywords: Ausara syncline, Ajloun dome, Syrian Arc Stress (SAS), Dead Sea Stress (DSS).

1. Introduction

Most of the geological structures in Jordan are related either to the formation of the Dead Sea Transform (DST) or to the Syrian Arc Fold Belt (SAB). Example of the structures related to the DST is the fault system in east Jordan (Atallah, 1992; Diabat and Masri, 2005) (Figure 1). Examples of the structures related to the SAB are Ajloun Dome, Koura Basin, Amman-Hallabat structures and some fold structures east of DST (Abed, 2000). The formation of some folds can be related to the formation of the DST (Atallah, 1992) (Figure 1).

The Dead Sea Transform (DST) is a major sinistral strike slip fault. It extends more than 1000 km from the Gulf of Aqaba in the south to Taurus Mountains in the north. It separates the Arabian plate to the east from Sinai sub-plate to the west (Figure 2). In Jordan, the DST consists of three segments: Wadi Araba fault in the south, the Dead Sea basin in the middle and Jordan valley fault in the north (Figure 1). Jordan valley extends from the Dead Sea to the Lake Tiberias; it is crossed by the sinistral active Jordan Valley Fault (JVF) (Figure 1).

SAB is one of the most important geological systems in the Middle East. It controls the topography of the area to form heights and depressions. SAB extends in S shape from northern Sinai to Lebanon and southern Syria (Figure 2).Some fold structures in Jordan were considered as part of SAB (Abed, 2000). It was formed in two phases; the first phase was in the Late Cretaceous (Turonian to Masstrichtian) and the second phase in the Paleogene (Oligocene), where it was formed as a result of the closing of Neo-Tethys due to the northward movement of African-Arabian plate. The Levant was part of the plate which led to the Folding (Abed, 2000). Abed El Mota'al and Kusky (2003) suggested that the intensity of the folding and thrusting increased from Oligocene to Miocene with separation of the Arabian plate from the African plate.

Two main stress fields were identified in the Middle East since the Late Cretaceous (Eyal and Reches, 1983; Diabat et al., 2004). The Syrian Arc Stress field (SAS) trending ESE-WNW compressional stress, followed by the Dead Sea Stress field (DSS) trending SSE- NNW.

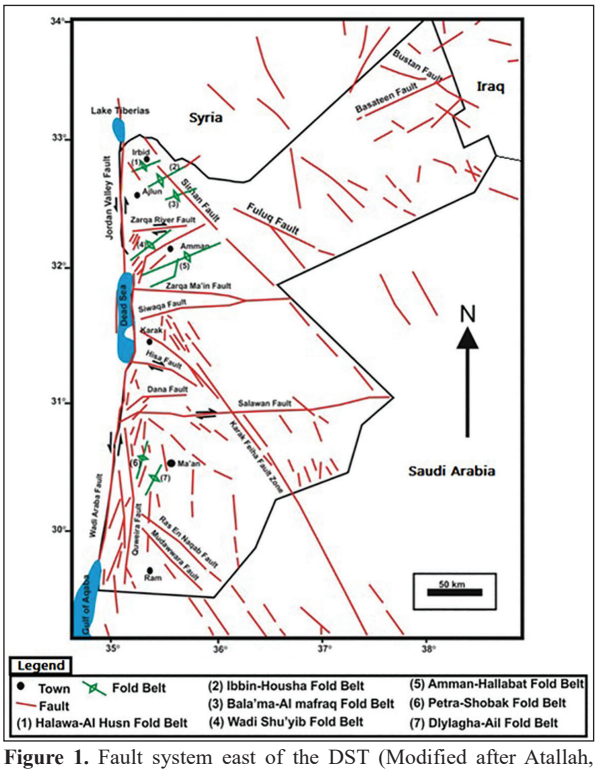

Figure 1. Fault system east of the DST (Modified after Atallah, 1992; Diabat and Masri, 2005)

* Corresponding author. e-mail: matallah@yu.edu.jo

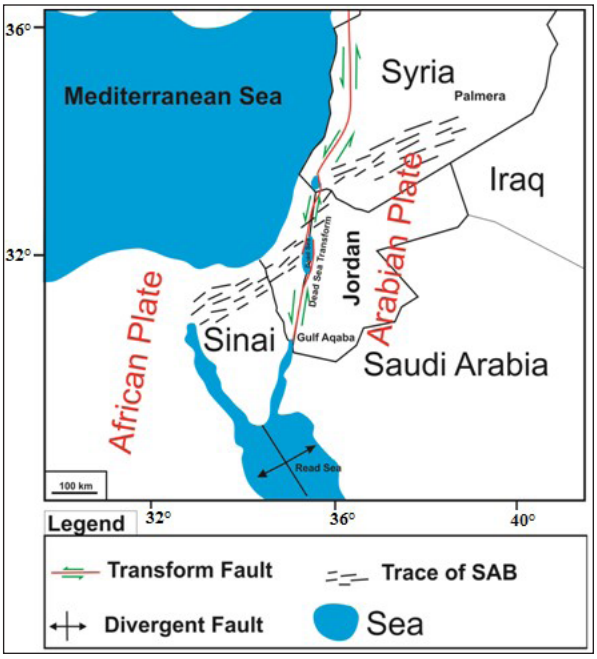

Figure 2. Tectonic setting of the Dead Sea Transform and the Syrian Arc Fold Belt (Modified after Garfunkel, 1981)

The present study area is located east of the Jordan valley fault, about 25 km southwest of Irbid (Figure 3). It extends from Ausara area (NW of Ajlun) passing through Halawa village to the Jordan valley (Figure 3).

The present study aims to map and analyze the structural elements in the area of investigation; in addition to understand the relationship between these structures and both the Syrian Arc System and the Dead Sea Transform. One of the interested features in the present study area is the folded Dana conglomerate. This study will describe this structure and find its relation with the Ajloun dome.

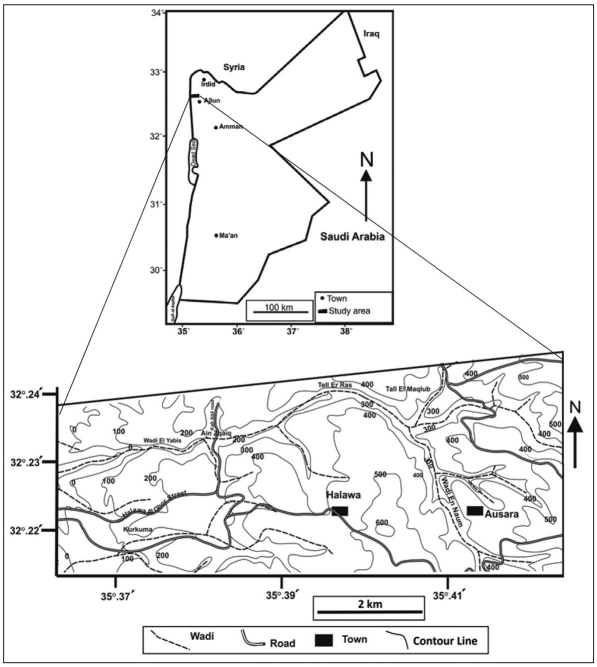

Figure 3. Location and topographic map of the study area.

2. Stratigraphy

The major outcrops in the present study area are Ajloun Group, Belqa Group and Jordan Group. Their age ranges from Late Cretaceous to Miocene (Figure 4). Ajloun Group consists basically of carbonate rocks. Belqa Group is composed mainly of chalk, chert, phosphate, limestone and marl. Jordan Group is composed mainly of conglomerate. Figure (4) is a geological map of the study area.

In the study area, the only outcropping formation of the Ajloun Group is the Wadi As Sir Limestone. It is of Turonian age and composed mainly of limestone, dolomite, and marly limestone. The thickness of this formation is 120 m (Abu Qudaira, 2005).

The Belqa Group consists of the following formations: Wadi Umm Ghudran Formation. It ranges from Coniacian to Santonian. Its thickness ranges from 25-40 m and comprises of white-gray massive chalk and chalky limestone. Amman Silicified Limestone and Al Hisa Phosphorite. They are of Campanian to Maastrichtian age and they are composed mainly of chert, limestone, and some phosphates. Their thickness is 70m. Muwaqqar Formation is of Maastrichtian to Paleocene age. It is composed of chalky limestone and marly limestone, its thickness reaches 150 m. Umm Rijam Chert Limestone is of Eocene age. It is 45 m thick and consists mainly of alternating of chalky and marly limestone and chert.

The Ausara conglomerate layers are exposed along the road from Ba'un to Judeta, Another outcrop of conglomerate exposed west of Ausara village, Here, the conglomerates are folded in a well-formed syncline. They lie on the Umm Rijam Formation (Figure 5). The age of Ausara Conglomerate is post Umm Rijam Formation (Post Eocene), which is equivalent to Dana Conglomerate. The thickness of the Ausara conglomerate reaches 40-60 m. It can be considered as part of the Jordan Group.

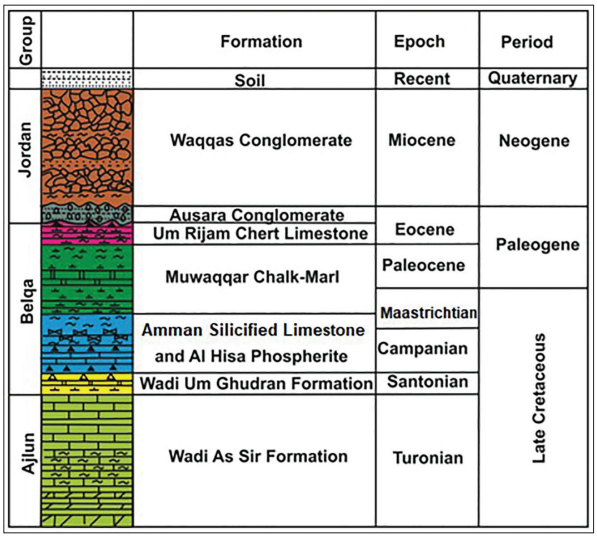

Figure 4. A general geologic column of the study area. (Modified after Abu Qudaira, 2005)

Waqqas Conglomerate as part of the Jordan Group is of Miocene age. It is composed mainly of gravel, silt and limestone (Abu Qudaira, 2005). The thickness of this unit reaches 150 m.

3. Structural Elements

3.1. Ausara Syncline

The Ausara Syncline locates northwest of Ausara village andeast of Halawa village along Wadi En Naum (Figure 5). The fold axis extends more than 4.5 km. The width of the syncline is about 4 km. The folded beds are Late Cretaceous-Paleogene. They are Muwaggar Formation, Umm Rijam Formation and the Ausara Conglomerate.

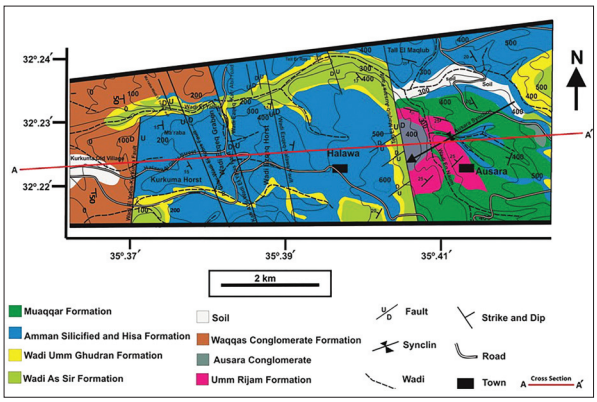

Figure 5. Geological map of the study area

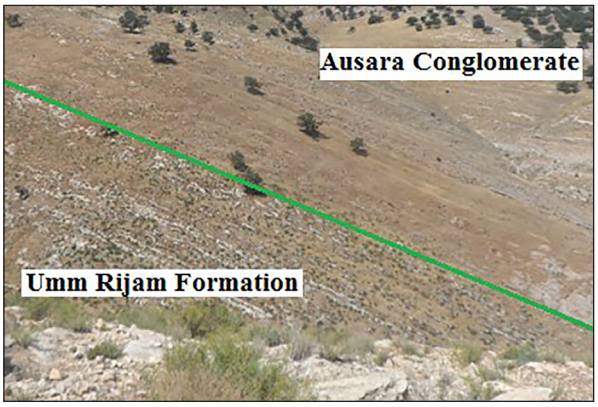

Figure 6. Conglomerate layers lie on the beds of the Umm Rijam Formation

Ausara Conglomerate form the core of the syncline (Figure 7). The Ausara Syncline is symmetric. The fold axis plunges17º and trends S65W. The inter limb angle is 64º, which means that it is an open fold (Figure 8) (Pluijm andMarshak, 2004).

3.2. Normal Faults

The study area was divided into three structural domains. Each domain contains a group of normal faults; they are: Kurkuma structural domain, Wadi Ezqeq-Tell ErRas structural domain, and Tell El Maqlub-Ausara structural domain.

3.2.1. Kurkuma Structural Domain

It is located in the western part of the study area, northeast of Kurkuma old village (Figure 3). The major faults in this structural domain are: Wadi El Yabis-Kurkuma Fault, Al Ghor-Wadi El Yabis Fault, KafrAbil-Wadi El Yabis Fault and Ma'raba-Wadi El Yabis Fault (Figures 5 and 9).

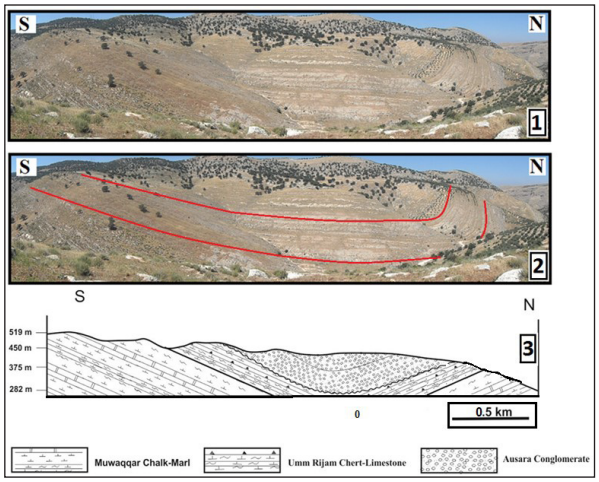

Figure 7. Part of Ausara Syncline (1, 2) and Cross section of Ausara Syncline (3)

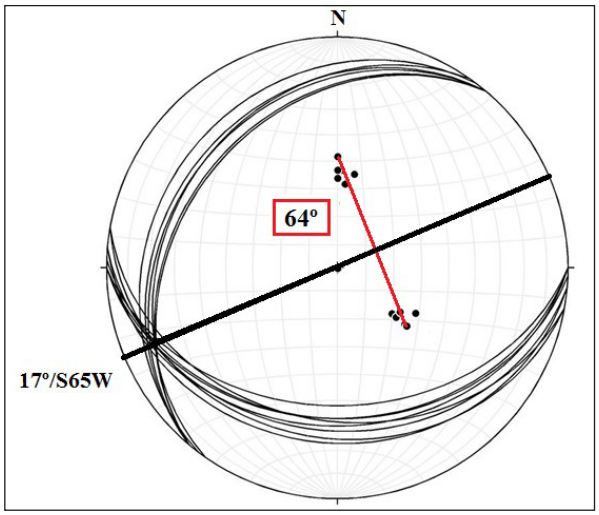

Figure 8. Stereonet diagram of Ausara Syncline. The fold axis trends S65W and plunges17º. The inter limb angle is 64º.

► *3.2.1.1. Wadi El Yabis-Kurkuma Fault*

This fault is located in the western side of the domain; it extends about 2.5 km (Figure 9). The strike of the fault plane is N5E with 140-180 m down throw to the west. This fault juxtaposes the Amman Silicified and Al Hisa Formations to the east against Waqqas Conglomerate to the west.

► *3.2.1.2. Al Ghor-Wadi El Yabis Fault*

It extends about 4 km. The strike of the fault plane is N20W (Figure 9); the downthrow is 70-90 m to the east. The Wadi Umm Ghudran Formation is downthrow relative to the Wadi As Sir Formation. It shows normal drag close to the fault plane (Figure 10).

► *3.2.1.3. Ma'raba-Wadi El Yabis Fault*

It is a small-scale normal fault and it is part of the Kurkuma Structural domain. The strike of fault plane is N20W. The downthrow is about 40-60 m. It juxtaposes Umm Ghudran Formation against Wadi As Sir Formation. Ma'raba-Wadi El Ybis Fault and Al Ghor-Wadi El Yabis Fault formed a horst between them (Figure 10).

3.2.2. Wadi Ezqeq-Tell Er Ras Structural Domain

It is located northwest of Halawa village. It extends from Tell Er Ras to Wadi Ezqeq (Figure 5). The major fault in this domain is the Wadi Ezqeq-Halawa fault; it extends about 3.5 km (Figures 5 and 11). The strike of the fault plane is N15ºW. The downthrow of the fault is about 70-100 m to the east. It juxtaposes Wadi As Sir Limestone against Amman Silicified Limestone.

Other small-scale normal faults trending NNW, they form small-scale horsts and grabens (Figure 12). They extend for about 80-100 m with downthrow about 30-40 m.

3.2.3. Tell El Maqlub-Ausara Structural Domain

This structure is located west of Ausara. It consists of one major normal fault and three subsidiary faults (Figures 5 and 13). Tell El Maqlub-Ausara fault represents the major fault. It strikes N15W. It crosses the study area from north to south. The downthrow of this fault is to the east, it reaches about 470 m. The maximum displacement occurred when the Ausara Conglomerate to the east were displacement against the Wadi As Sir Formation to the west (Figure 14).

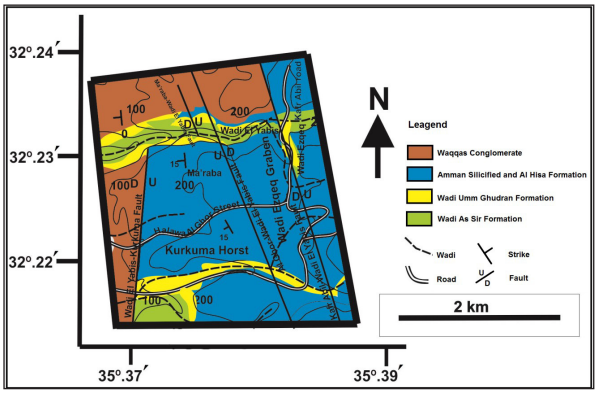

Figure 9. Kurkuma structural domain.

3.3. Strike Slip Fault

Located in the western part of Wadi El Yabis, north of the wadi, as a group of reverse and thrust faults dissecting the Wadi As Sir Formation (Figure 15). They form a positive flower structure. Positive flower structures are formed as bending of a strike slip fault. This fault can be traced in aerial photographs and in the field south of Wadi El Yabis. It strikes N60W (Figure 15). The horizontal displacement of this fault is not clear.

3.4. Joints

The study area is divided into three stations for interpretation of joints (Figure 16). The measured joints are represented in rose diagrams. All of the joints in the field were measured depending on the selection of the systematic joints. Stations were selected depending on the good exposure of systematic joints to cover the study area.

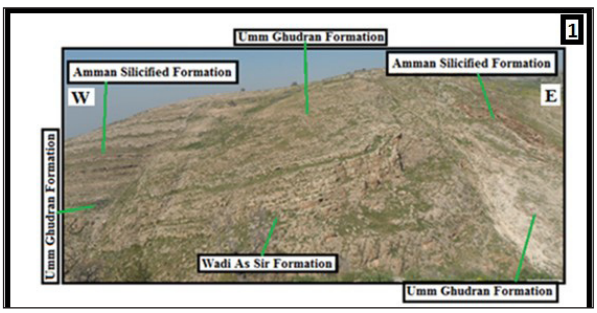

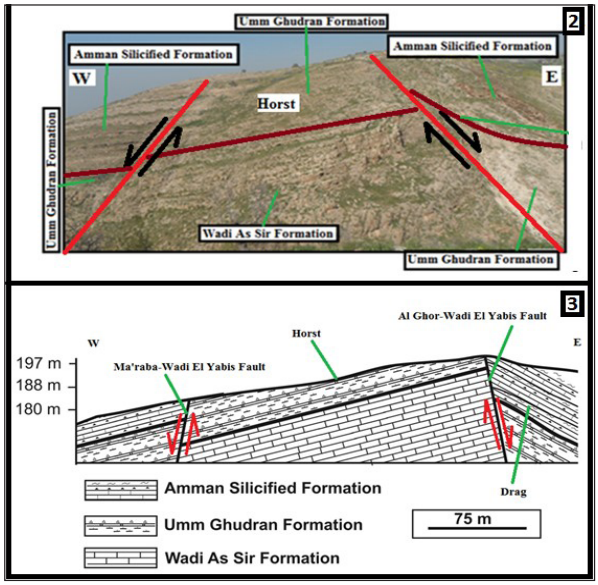

Figure 10. Al Ghor-Wadi El Yabis Fault to the right and Ma'raba-Wadi El Yabis Fault to the left, where they form a horst. The normal drag is close to the fault plane (1, 2). No. 3 is Cross section

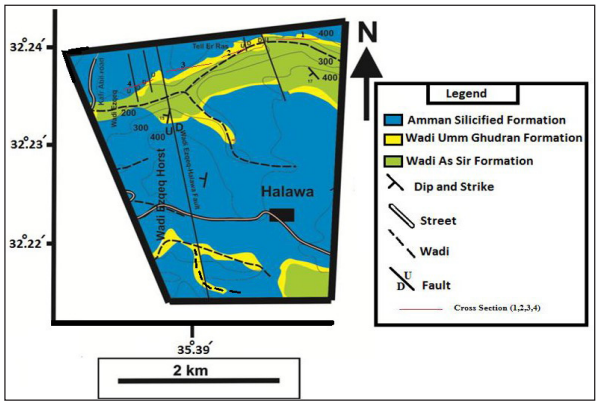

Figure 11. Wadi Ezqeq-Tell Er Ras structural domain.

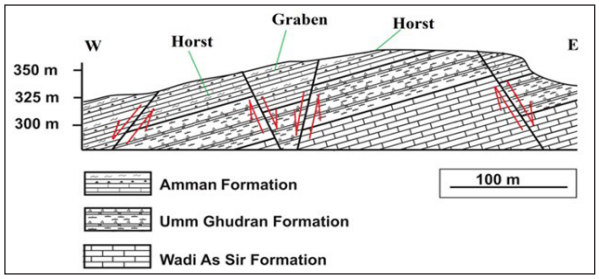

Figure 12. Cross section showing normal faults, horsts and grabensinWadiEzqeq–Tell ErRas structural domain

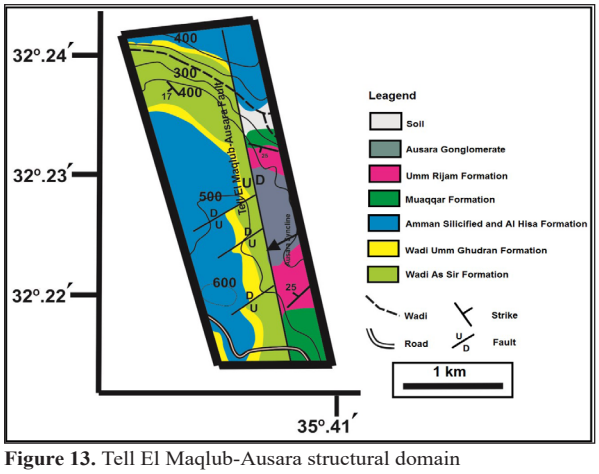

Figure 13. Tell El Maqlub-Ausara structural domain

3.4.1. Station 1

It is located around Ausara village east of study area (Figure 16). Joints were measured in Umm Rijam and Muwagger Formations. More than sixty joints were measured. The major trends are N60E and N30W (Figure 16). They are orthogonal sets of joints and the dihedral angle between the major joint trends is 90º (Figure 17).

3.4.2. Station 2

It is located in the middle part of study area (Figure 16). Joints were measured in Wadi Umm Ghudran Formation. Around sixty joints were measured. The measured joints show two major trends; N60W and N45E (Figure 16).

3.4.3. Station 3

It is located west of study area (Figure 16). Sixty joints were measured in the WadiAs Sir and Wadi Umm Ghudran Formations. The major trends are N60W and N30E (Figure 16). The dihedral angle between them is 90º (Figure 17).

The general trends of the total joints are S60W and N30E (Figure 18) other minor trends are also recorded.

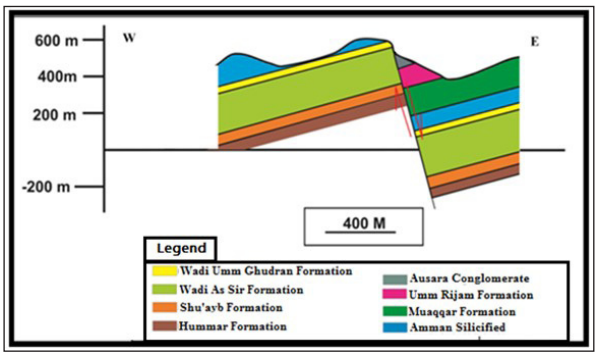

Figure 14. Cross section of Tell El Maqlub-Ausara Fault (Modified after Abu Qudaira, 2005)

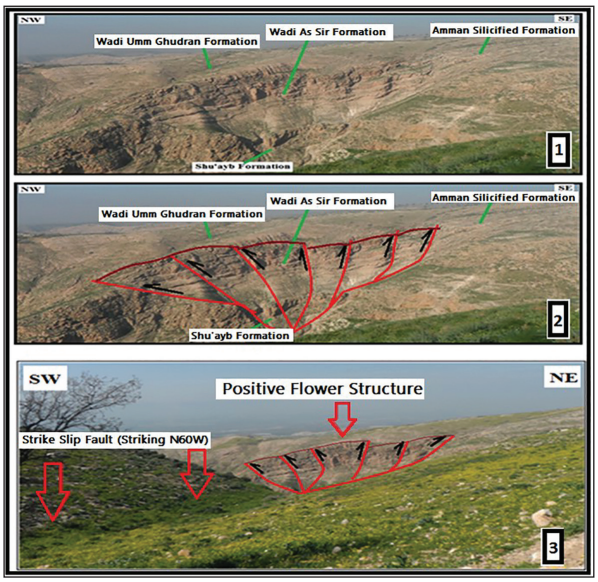

Figure 15. positive flower structure in the western part of study area (1, 2). The trace of the strike slip fault which causes the positive flower structure (3)

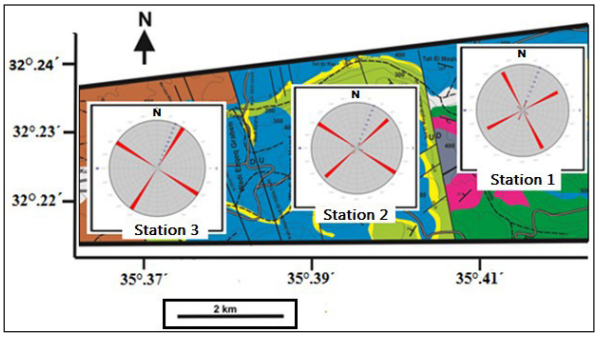

Figure 16. Joint trends in the different measured stations

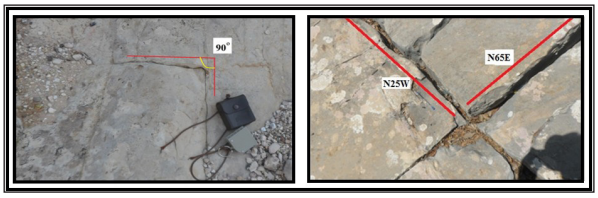

Figure 17. Orthogonal joint sets in the study area

4. Discussion

The major outcrops in the present study area are Ajloun Group, Belqa Group and Jordan Group. Their ages range from Late Cretaceous to Miocene. Ausara conglomerate is Post Eocene Age (which is equivalent to Dana Conglomerate).

The study area is located east of the Jordan Valley Fault and north of Ajloun Dome. The area is located on the northwestern flank of Ajloun Dome. The strata are gently dipping to the NW, but closer to the Jordan Valley; they are steeply dipping to the west. According to Abed (2000), Ajloun Dome and Koura Basin are part of the Syrian Arc Fold Belt.

The study area includes: one syncline, a group of normal faults, one strike slip fault and a group of systematic join sets. The folded beds of Ausara syncline are Late Cretaceous-Paleogene. The core of fold is Ausara Conglomerate. The fold axis trends S65ºW and plunges17º. The fold is symmetric and open. The fold is located on the northwestern flank of Ajloun dome. The general strike of the normal faults is S15ºE (Figure 19). The extension of the fault planes varies from tens of meters to few kilometers. The throw of these faults varies also from few meters to tens of meters and, in some cases, a hundred of meters were recorded. Some of the fault planes dip to the east and others dip to the west; therefore, different sizes of horst and grabens are formed between these faults. One of the prominent faults in the study area is the Tell El Maqlub-Ausara fault; it represents the maximum downthrow in the study area, which is 470 m. This fault is truncating the Ausara syncline (Figure 20). It means that these normal faults were formed after the formation of the folding. The major trend of the normal faults is 165º, which is parallel to the Dead Sea Stress field (DSS). Figure (21) shows a general W-E cross section in the study area. The general structure of the area can be considered as faulted flexure.

Comparing the major trends of joints in the rose diagrams in station (1) and station (2), it is noted that there is a block rotation of 30º. The rotation took place along Tell El Maqlub-Ausara fault domain (Figure 16).

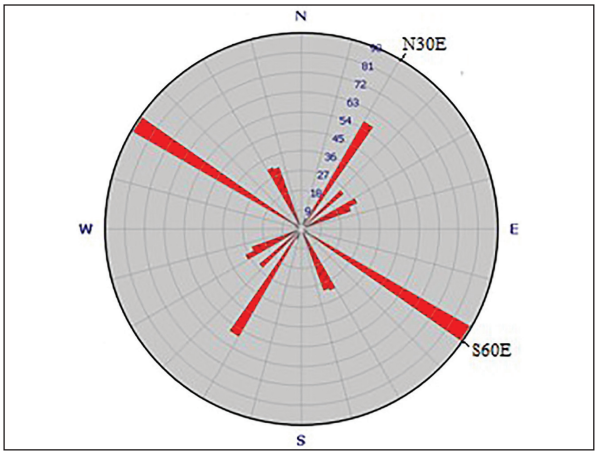

Figure 18. Rose diagram for joints in study area

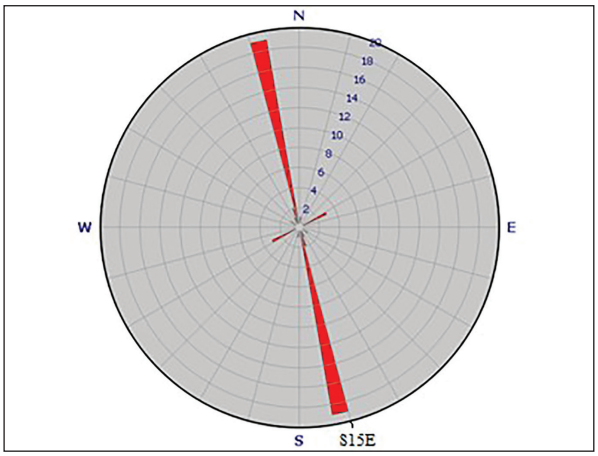

Figure 19. Rose diagram showing the main strike of normal faults in the study area

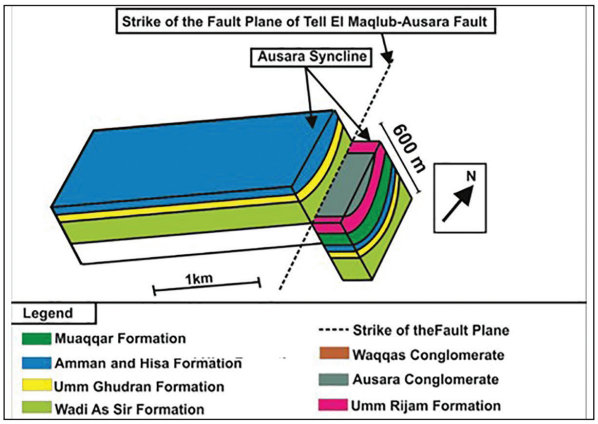

Figure 20. Block diagram showing the relation between Ausara syncline and Tell El Maglub-Ausara fault

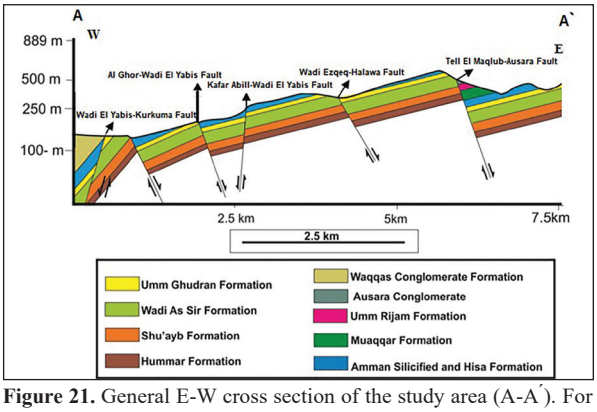

Figure 21. General E-W cross section of the study area (A-A´). For location see Figure (5)

5. Structural Evolution of the Study Area

The major structural features in north Jordan are the Ajloun Dome and the Koura Basin, in addition to other fold belts and faults. In the Late Cretaceous Ajlun Dome and Al-Koura Basin were formed during the first stage of the SAS. The Ausara conglomerate was deposited in certain basins that formed probably as a result of uplift of Ajloun area.

The area was subjected to compressional stresses forming the fold belts in north Jordan and forming the Ausara Syncline. The age of this folding is Post Eocene (the age of the Umm Rijam Formation). This folding could be associated with the second phase of the SAS (Abed, 2000; Abd El-Mota'al and Kusky, 2003).

A system of normal faults was formed after the Ausara Syncline. One of these faults truncated the syncline (Figure 20). The major strike of these faults is NNW-SSE, which is parallel to the trend of the DSS. The trend of faults, horsts and grabens is perpendicular to the main extension (ENE-WSW). The area close to the Jordan valley was tilted during the taphrogenesis associated with the formation of the Jordan Valley. The beds are generally dipping to the west (Figure 21).

Acknowledgment

The present study was supported by the Deanship of Scientific Research and Graduate Studies at Yarmouk University, under Grant Number (2014/23).

References

[1] Abd El-Mota'al, E. and Kusky, T. M., (2003). Tectonic Evolution of the Interplate S-Shaped Syrian Arc Fold-Thrust Belt of the Middle East Region in the Context of Plate Tectonic. The third InternationalConference on the Geology of Africa, 2, 139-157.

[2] Abed, A. M., (2000). Geology of Jordan, first edition. Jordanian Geologists Association. (In Arabic). Amman, Jordan.

[3] Abu Qudaira, M., (2005).Geological map of Dayr Abu Sa'id (3154IV).1:50,000.Natural Resources Authority. Amman, Jordan.

[4] Atallah, M., (1992). On the Structural Pattern of the Dead Sea Transform and its Related Structures in Jordan. Abhath Al-Yarmouk (Pure Sciences and Engineering), 1, 127-143.

[5] Atallah, M. and Mikbel, Sh.,(1992). Structural analysis of the folds between Wadi El Yabis and the Basalt Plateau, Northern Jordan. Dirasat, 19B (3), 43- 58.

[6] Diabat, A., Atallah, M. and Saleh, M., (2004). Paleostress analysis of Cretaceous rocks in the eastern margin of the Dead Sea transform. Jordan. Journal of African Earth Sciences, 38, 449-460.

[7] Diabat, A. and Masri, A., (2005). Orientation of the principal stresses along Zerqa- Ma'in Fault. Mu'ta Lil-Buhuth wad Dirasat, 20, 57- 71.

[8] Eyal, Y., Reches, Z., (1983). Tectonic analysis of the Dead Sea Rift region since the Late-Cretaceous based on mesostructures. Tectonics, 2, 167–185.

[9] Garfunkel, Z., (1981). Internal Structure of the Dead Sea Leaky Transform (rift) in Relation to Plate Kinematics. Tectonophysics, 80, 81- 108.

[10] Pluijm,B.V. and Marshak,S., (2004). Earth Structures: An Introduction to Structural Geology and Tectonics (Second edition).WW and Company. London.

JJEES
Jordan Journal of Earth and Environmental Sciences

Volume 8, (Number 2), Dec, 2017
ISSN 1995-6681
Pages 61 - 67

Assessment of Heavy Metals in Urban Areas of Al Hashmiyya City of Jordan

Kholoud Mashal[1], Mohammed Salahat[1], Mohammed Al-Qinna[1] and Yahya Ali[2]

[1]*Department of Land Management and Environment, Faculty of Natural Resources and Environment, Hashemite University;*
[2]*Department of Humanities and Social Sciences, Faculty of Arts, Hashemite university , Zarqa, Jordan.*

Received 26 May, 2017; Accepted 18 October, 2017

Abstract

The present study aims to assess the behavior of heavy metals (Pb, Zn, Cd, Cr, Cu and Ni) in the topsoil of Al Hashmiyya city in Jordan, their contamination level and the possible contamination sources. Heavy metals analyses were assessed using Krigging map, Enrichment Factor (EF), and geo-accumulation index (Igeo). The findings indicate that all heavy metals, except Cu, were present in higher concentrations above the safe limit. Multivariate analyses indicate that for all the tested heavy metals, soil pH was the most significant factor affecting heavy metal loads except for Cu, which was significantly related to iron oxides only. Moreover, the results indicate the presence of three major clusters: Pb, Zn, and Cr; Zn, Pb and Cr; and Cu, which does not behave differently from the other heavy metals. Most of the sites in the present study area are contaminated by heavy metals above threshold levels, reaching 100% probability. The present study shows the urgent need to monitor and control industrial emissions and remediate the heavily contaminated urban soils found in the study area.

Keywords: heavy metals, soil contamination, calcareous soil, krigging map, EF, Igeo urban areas.

1. Introduction

Heavy metals in soils have severe impacts on the environment and the local communities. Heavy metals accumulate in the human body via absorption, inhalation, and ingestion (Lim et al., 2008), and children and the elderly are the most strongly affected (Olawoyin et al., 2012). Several studies showed that anthropogenic activities lead to accumulation of heavy metals in topsoil (Tume et al., 2011; Li et al., 2013). Both vehicle emissions and industrial discharges have been identified as sources of heavy metals (Guo et al., 2012), and urban soils are known to behave as a sink for heavy metals from these sources (Tiller, 1992). Studies concerning heavy metal contamination in urban soils are needed to develop strategies to protect urban environments and human health against long-term accumulation of heavy metals. The present study represents a first attempt to identify the behavior, distribution, contamination and sources of heavy metals in urban topsoil in Jordan's highly-industrialized Al Hashmiyya City in Zarqa Governorate.

2. Materials and Methods

Soil samples (0-20 cm) were collected randomly to cover the areas around the highways in Al Hashmiyya city in Zarqa Governorate (described previously in Mashal et al., 2015) (Figure 1).

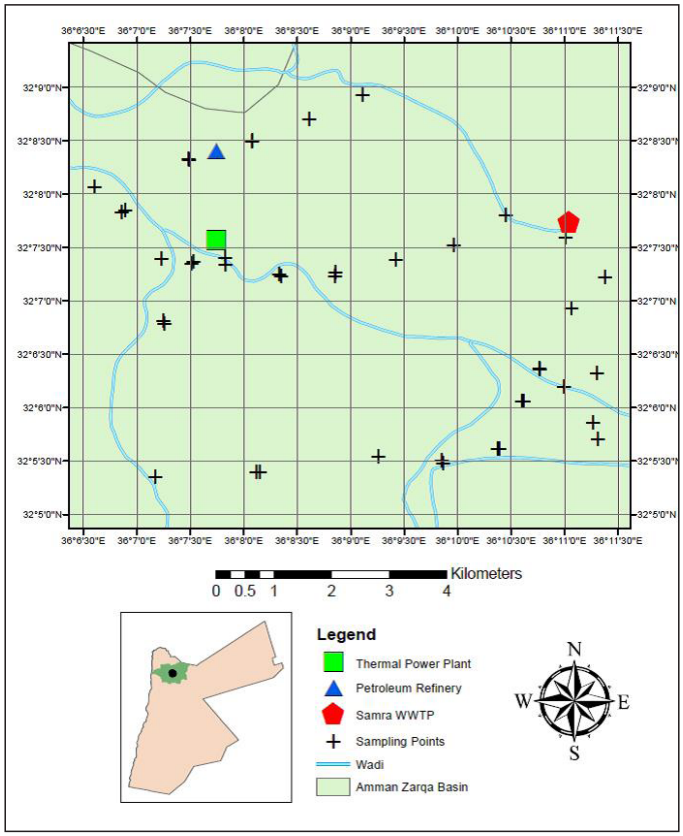

Figure 1. Sampling points and study area

* Corresponding author. e-mail: kmashal@hu.edu.jo

Four sub-samples were collected at each site to obtain a representative composite sample. A sampling density of two samples per km^2 was adopted wherever possible with a total of 43 samples. Al Hashmiyya area is susceptible to pollution from several industrial sources, including a Petroleum Refinery (PR), a Thermal Power Plant (TPP), and a Waste Water Treatment Plant (WWTP). The study area consists of highly dissected rocks with very gently undulating limestone parent material of the WadiesSir Limestone Formation, which represents the upper most of the Ajlun Group Formation (Ministry of Agriculture, 1994). Soil samples were obtained by mixing four subsamples from each site. The soil samples were collected using a stainless steel spade and were stored in self-sealing plastic bags. The spade was washed several times with distilled water and finally with deionized water and wiped dry with paper towels between each use. Geographical coordinates of sampling locations were recorded at each sampling point with a handheld GPS with 3m accuracy. Soil samples were air-dried, ground and sieved through a-2 mm sieve. The chemical properties, including pH_{se}, EC_{se} , Organic Matter (OM), percentage of total carbonates ($CaCO_3$), the active iron oxides (amorphous), and Cation Exchange Capacity (CEC), of all soil samples were measured according to appropriate analytical procedures reported in *Methods of Soil Analysis, part 3* (Sparks *et al*., 2001).The total concentration of metals in the soil was measured using aqua regia extracts. Total concentrations of Pb, Cd, Cu, Ni, Cr and Zn in the digestion solution were determined by PerkinElmer Analyst 300, with HGA 850 graphite furnace. The element standard solutions used for calibration were prepared by diluting stock solutions of 1000 mg/L of each element supplied by Sigma. Quality Assurance and Quality Control (QA/QC) procedures were assured through analyzing all samples in duplicate and the results were accepted when the relative standard deviation falls within 5%. Blank samples were also performed throughout all the experiments for correction of background and other sources of error.

Several ordinary (descriptive) and multivariate statistical analyses were performed for both soil chemical properties (pH_{se}, EC_{se}, OM, $CaCO_3$, CEC, and amorphous Fe oxide), and heavy metals contents (Cu, Zn, Pb, Cr, Cd, and Ni), using JMP statistical program (JMP 8, 2009). Descriptive statistical analyses included measures of central tendency, dispersion, and distribution, while multivariate analyses included correlation analysis, multivariate regression, stepwise regression, Principal Component Analysis (PCA), and cluster analyses. Stepwise Regressions (SWR) were selected according to Mallow's Cp (Cp) criterion (Mallow, 1973) and Akaike's Information (AIC) criterion (Akaike, 1974). Principal component analysis was achieved based on the correlation and the covariance matrix with a standardized original variable (Hawkins, 1974). Hierarchical cluster analysis (agglomerative clustering) was performed to investigate the presence of group factor effect on soil chemical properties and heavy metals contents (Milligan, 1980). In addition, the spatial distributions of soil properties and metal contents were investigated using the ArcMap program (ArcGIS 9.2, ESRI, 2006). The selection of the best empirical semivariance model was based on both cross-validation test and provided smallest nugget value (Goovaerts, 1997). The third stage involved the interpolation of the variable at unknown locations using kriging techniques with a simple linear weighted-interpolation scheme.

3. Results and Discussion

The descriptive statistical analyses of the chemical properties of urban topsoil samples and heavy metals content are summarized in Table (1). The soil described as highly calcareous soils with 62.4% maximum content of $CaCO_3$, most likely derived from underlying limestone. The CEC ranged from 0.79 to 11.8 $cmolkg^{-1}$, with a mean value of 5.3 $cmolkg^{-1}$. These low values are consistent with the low clay content and high calcite and quartz content in these soils. The mean OM was 2.4% and ranged from 0.53% to 16.3%.

Table 1. Statistical summary of chemical properties of soil samples and heavy metals content of the study area

	Unit	Maximum	Minimum	Mean	StdDev	CV
pH		8.5	6.7	7.6	0.40	5.3
EC	dSm^{-1}	63.8	1.3	15.2	15.1	98.7
$CaCO_3$	%	62.4	26.6	46.6	11.1	23.7
OM	%	16.3	0.5	2.4	2.6	107.9
Fe-oxide	$mgkg^{-1}$	2515.3	410.3	1558.3	754.9	48.4
CEC	$cmolkg^{-1}$	11.8	0.8	5.3	2.9	54.2
Pb	$mgkg^{-1}$	469.0	22.4	108.8	98.5	90.6
Zn	$mgkg^{-1}$	854.8	49.3	172.3	169.2	98.2
Cd	$mgkg^{-1}$	17.9	2.0	5.9	3.2	53.5
Cr	$mgkg^{-1}$	96.6	13.1	41.3	18.8	45.7
Cu	$mgkg^{-1}$	267.6	2.96	41.1	52.8	128.4
Ni	$mgkg^{-1}$	68.2	14.1	39.4	11.5	29.31

The heavy metal concentration in the urban topsoil samples were found in the following order: Zn > Pb > Cr >Cu >Ni >Cd (Table 1). However, Pb, Zn, Cd, and Cu concentrations varied greatly in the studied soils as indicated by the coefficient of variation, which exceeded 50%. For comparison of observed concentrations with geological baseline concentrations, the ranges of the baseline data estimated with the median ± 2MAD were used (Reimann *et al*., 2005). The observed concentration ranges of all trace metals (Table 2) were greater than their upper limits, suggesting the contamination of these soils with the studied heavy metals. The mean values of Cu, Cr and Ni in the analyzed soils are much lower than the critical mean concentrations (Table 2). Moreover, the contamination levels of soils with heavy metals and their sources in urban soils were assessed using two different pollution indices. The first is the geo-accumulation index (Igeo), an estimate of the enrichment of metal concentrations above geological baseline concentrations, according to the following equation (Muller, 1981):

$$I_{geo} = \log_2\left(\frac{[M]}{1.5[M_b]}\right)$$

where M is the measured concentration of the heavy metal in the study area, and M_b is the geochemical background value in a reference shale (Turekian and Wedepohl, 1961). Ranges of Igeo values are used to delimit levels of contamination. Igeo values with associated contamination levels for the study area appear in Table (2). Zinc, Cu and Cr appear to be of lowest concern, while Pb and Cd show the highest Igeo values.

The second pollution index is the Enrichment Factor (EF), using the following equation (Banat *et al*., 2005):

$$EF = \frac{[M]}{M_b}$$

EF values between 0.5 and 1.5 indicate the metal is entirely from crustal materials, whereas EF values greater than 1.5 suggest enrichment from anthropogenic sources (Zhang and Liu, 2002). Moreover, the degree of contamination is also classified based on ranges of EF values (Lacatuso, 1998). The results in Table (3) show that the EF values ranged from 0.40 to 19.6. The EF values calculated for Cr, Cu and Ni suggest very limited input from man-made sources, while the elevated Cd and Pb values indicating anthropogenic sources of pollution for these two metals. The big difference in EF values between these two anthropogenicaly-sourced metals may be due to the difference in the magnitude of input for each metal in the urban topsoil and/or the difference in the removal rate of each metal from the soil.

Table 2. Mean heavy metals concentrations and pollution indices of the sampled area

	Pb	Zn	Cd	Cr	Cu	Ni
Mean ($mgKg^{-1}$)	108.8	172.3	5.9	41.3	41.1	39.4
Baseline data* $mgkg^{-1}$	12.1–27.3	29.2–115	0.18–0.46	14.8–35.2	7.1–33.5	11.6–35.6
Average shale ($mgkg^{-1}$)	20	95	0.3	90	45	68
I_{geo} values	1.85	0.26	3.70	<0	<0	<0
Igeo classification	moderately contaminated	uncontaminated to moderately contaminated	heavily contaminated	Uncontaminated	uncontaminated	uncontaminated
EF	5.4	1.8	19.6	0.46	0.91	0.58
Degree of contamination	Sever	slight	excessive	Uncontaminated	uncontaminated	uncontaminated

* Reimann et al. (2005)

Heavy metals correlation varied from weak to strong at 95% confidence ($P<0.05$) (Table 3). The Pb has a moderate positive correlation with Zn, and Cr. Strong correlations were found between Ni and Cr, suggesting that these heavy metals may originate from a common source. Cr and Ni have similar ionic radii, and previous research suggests that Cr and Ni are associated mostly with the mineral phase in soils (e.g., Zhang *et al*., 1999). Moderate correlation exists between Zn and Fe, Pb, Cd, and Cu. The significant correlations between these elements support the idea that anthropogenic activities, such as traffic movement, are the main source of heavy metals in soils. Cu showed only weak positive correlations with the other heavy metals, suggesting a different source than other studied metals. In assessing the correlation between heavy metals and soil chemical properties, the results show that soil pH has a fairly moderate positive correlation with Pb, Zn, Cr and Ni (Table 3). Electrical Conductivity (EC) has no correlation with heavy metals. Soil OM showed a moderate positive correlation with Zn and Cu. Soil $CaCO_3$ showed only moderate positive correlation with Cd, and negative correlation with Cr, suggesting that Cd may be incorporated into calcite crystal structure by the formation of solid solutions (Shetye *et al*., 2009). The results show that CEC has a moderate positive correlation with Cr ad Ni while it has a moderate negative correlation with Pb, Zn and Cd. Zinc, Cd, and Cu elements were correlated positively with amorphous Fe oxide in the topsoil samples.

Table 3. Correlation between trace metal contents and soil properties in the urban topsoil samples (all heavy metals and amorphous Fe-oxide in $mgkg^{-1}$, EC in dSm^{-1}, and CEC in $cmolkg^{-1}$)

	Pb	Zn	Cd	Cr	Cu	Ni	pH	EC	%OM	$\%CaCO_3$	Fe-oxide	CEC
Pb	1.00											
Zn	0.51[b]	1.00										
Cd	0.14	0.35[a]	1.00									
Cr	0.37[a]	0.17	-0.06	1.00								
Cu	0.25	0.31[a]	0.12	-0.04	1.00							
Ni	0.28	0.08	0.02	0.73	0.09	1.00						
pH	0.23	0.28	-0.08	0.37	0.13	0.39[b]	1.00					
EC	0.12	-0.08	-0.16	-0.10	0.09	0.01	-0.46[b]	1.00				
% OM	0.21	0.58[b]	0.15	-0.08	0.34[a]	-0.03	0.06	0.21	1.00			
% $CaCO_3$	0.01	0.13	0.36[a]	-0.60[b]	0.26	-0.22	-0.22	0.20	0.18	1.00		
Fe-oxide	0.09	0.43[b]	0.56[b]	-0.38[a]	0.39[a]	-0.18	-0.26	0.07	0.37[a]	0.65[b]	1.00	
CEC	-0.34[a]	-0.33[a]	-0.33[a]	0.52[b]	-0.25	0.32[a]	0.25	-0.24	-0.28	-0.68[b]	-0.62[b]	1.00

[a] At the 0.05 level of significant correlation; [b] At the 0.01 level of significant correlation; p values in brackets

Multivariate analyses indicated that soil chemical properties significantly influence heavy metal loads. For all the tested heavy metals, soil pH was the most significant factor affecting their loads except Cu, which was significantly related to iron oxide only (Table 4). Soil EC had a negligible effect on heavy metal loads since it was omitted from all stepwise models, suggesting that soluble salts have no effect. On the other hand, soil CEC had a significant effect on Pb loads in urban soils, in which each one-unit increase in soil CEC reduced the pollution (load) of Pb in the soil by 14.4 mg kg^{-1}. Similarly, Fe oxide had a small but positive significant effect on the Zn, Cd, and Cu, suggesting that these elements are associated with the Fe (hydr)oxides in these soils. The Zn was highly related to OM content by which each one-unit increase in OM was subjected for increase in Zn load by 32.9 mg kg^{-1}, indicating that OM has a large sorption capacity towards these metals (Quenea *et al*., 2009). This effect is probably due to the cation exchange capacity of organic material (Martin and Kaplan, 1998).

Table 4. Statistical summary of full and stepwise multi-linear modeling

Parameter	Full Regression Model	Stepwise Regression Model				
	Math Model	R^2	RMSE	Math Model	R^{2*}	RMSE*
Pb	-428.691 + 103.381 pH + 1.566 EC -3.574 $CaCO_3$ + 0.639 OM -21.181 CEC + 0.007 Fe	0.337	86.64	-435.946 + 82.350 pH-14.419CEC	0.219	89.22
Zn	-817.703 +142.756 pH-0.463 EC -4.438 $CaCO_3$ + 31.190 OM -15.026 CEC + 0.086 Fe	0.568	120.13	-1126.785 + 146. 085 pH + 32.944 OM + 0.077 Fe	0.519	121.77
Cd	3.910+-0.163 pH -0.045 EC + 0.011 $CaCO_3$ -0.022 OM -0.017 CEC + 0.002 Fe	0.357	2.73	2.235 + 0.002 Fe	0.316	2.64
Cr	-66.845 + 17.086 pH + 0.286 EC- 0.881 $CaCO_3$ -0.440 OM + 1.641 CEC + 0.005 Fe	0.476	14.73	-7.008 + 12.068pH-0.919$CaCO_3$	0.416	14.75
Cu	-332.889+ 40.543 pH + 0.6145 EC + 0.121 $CaCO_3$+ 3.210 OM + 0.429 CEC + 0.028 Fe	0.259	49.05	-1.054 + 0.027Fe	0.150	49.24
Ni	-87.959+ 15.397 pH + 0.276 EC -0.096 $CaCO_3$ -0.580 OM + 1.309 CEC + 0.004 Fe	0.298	10.45	-47.087 + 11.461pH	0.156	10.74

*where R^2 is the coefficient of determination, and RMSE is the root mean square error of the prediction model.

According to PCA, Table (5) summarizes the variation of the specified variables with principal components and how the principal components absorb the variation in the data. Based on correlation, the first nine principal components account for 96.146% of the variation in the sample. This indicates the degree of diversity in the data and the relation between parameters included. While based on covariance, the first principal component accounts for 94.146% of the variation in the sample. This indicates a directional influence of the variables by which some are positively related or negatively related. The first PC that represents the linear combination of the standardized original variables that has the greatest possible variance can be written as follows:

$$PC_1 = -0.42404\ pH + 0.00861\ Ec + 0.03748\ CaCO_3 + 0.11371\ OM - 0.15276\ CEC + 0.00059\ Fe + 0.00103\ Pb + 0.00140\ Zn + 0.08448\ Cd - 0.01639\ Cr + 0.00421\ Cu - 0.01718\ Ni + 1.28088$$

On the other hand, each subsequent PC is the linear combination of the standardized original variable that has the greatest possible variance and is uncorrelated with all previously defined components. The second PC can be written as:

$$PC_2 = 0.94936\ pH - 0.00671\ Ec - 0.00973\ CaCO_3 + 0.10844\ OM + 0.00491\ CEC + 0.00007\ Fe + 0.00428\ Pb + 0.00259\ Zn + 0.04698\ Cd + 0.02187\ Cr + 0.00455\ Cu + 0.03351\ Ni - 10.60050$$

The slope of the parameters included in the PC indicates the importance of the parameter in explaining the variability within the data, and this coincides with regression models in which soil pH is the most dominant variable in all stepwise models affecting the variability of heavy metal loads.

Table 5. Statistical summary of principal component analyses based on correlation and covariance

	PC on Correlation	PC on Covariances				
Number	Eigenvalue	Percent	Cum Percent	Eigenvalue	Percent	Cum Percent
1	3.6956	30.797	30.797	576025.2	94.146	94.146
2	2.6413	22.011	52.808	26859.89	4.390	98.536
3	1.3587	11.322	64.130	6117.315	1.000	99.536
4	1.0282	8.568	72.698	2199.585	0.360	99.896
5	0.8591	7.159	79.858	323.9635	0.053	99.949
6	0.8180	6.817	86.674	208.3557	0.034	99.983
7	0.5673	4.727	91.402	69.0239	0.011	99.994
8	0.3236	2.697	94.098	26.1275	0.004	99.998
9	0.2457	2.048	96.146	5.7964	0.001	99.999
10	0.1949	1.625	97.770	2.7073	0.000	100.000
11	0.1631	1.359	99.129	2.1678	0.000	100.000
12	0.1045	0.871	100.000	0.0679	0.000	100.000

According to cluster analysis, the generated dendrogram and the scree plot indicates the presence of three major clusters at this study (Table 6). The three clusters actually represent three heavy metal loads (low, moderate, and high). The high metal loads of Pb, Zn, and Cr are grouped together and associated with soil pH above 8, iron oxides above 2000 and low soil EC. While Zn, Pb and Cr are grouped together and are associated with high OM above 5% with soil pH ranging between 7.5 and 8.3 and iron oxides above 2000. On the other hand, Cu is not grouped with any other heavy metal and thus acts differently. The high Cu loads are associated with soils with high $CaCO_3$ and low OM content. The mean of the generated clusters are presented in Table (6).

Table 6. Cluster Means as generated by Hierarchical cluster analysis

Cluster	pH	Ec	$CaCO_3$	OM	CEC	Fe	Pb	Zn	Cd	Cr	Cu	Ni
1	7.3	18.2	55.6	2.2	3.6	1935.8	76.6	143.7	6.2	25.3	26.8	30.2
2	7.6	13.8	34.9	1.3	8.2	731.9	94.1	84.2	3.5	53.8	18.7	44.0
3	7.8	12.6	48.5	3.8	4.1	2101.9	178.4	336.5	8.7	48.8	93.7	47.3

The spatial descriptions of soil variables are presented in Table (7). Generally, almost all soil chemical properties were characterized by anisotropic behavior indicating the oriented spatial dependence at variant associated angles as presented in the Table (8). Similarly, most soil heavy metals were having identical spatial trend of exponential semivariogrm with major independence ranges varied from 0.0561 to 0.0786 km and minor independence ranges varied from 0.0148 to 0.0298 km except for Ni that had isotropic behavior with independence spatial range of 0.0365 km. The similarity between soil chemical properties and heavy metals distributions suggests that the spatial distribution is controlled by pollution source and the transfer mechanism. Many contamination hotspots were identified in the krig maps (Figure 1a-e), some with potential contaminations of heavy metals up to 100 percent above threshold levels. Cadmium contamination is the most pronounced in the study area, followed by Pb. Lead is well known to be one of the less mobile elements in calcareous soils due to the precipitation of Pb carbonates as well as Pb adsorption to Fe oxides (Freyssinet *et al*., 2002). This could explain the high values still found in urban soils, even after the recent adoption of unleaded fuel in this area. Zinc, Cr, and Cu are the elements presenting the lowest degree of contamination.

Table 7. Descriptive analysis of soil variables spatial distributions

	Transformation	Isotropy	Model	Range (km)	Direction	Partial Sill	Nugget	
				Major	Minor			
pH	Normal	Aniso	Penta-spherical	0.0002	0.0001	297.0	0.248	0
EC	Lognormal	Aniso	Exponential	0.0104	0.0016	81.0	1.020	0.176
$CaCO_3$	Cox-Box (1.83)	Aniso	Circular	0.0786	0.0223	306.0	22958	50043
OM	Lognormal	Isotropy	Exponential	0.0786		0.168	0.356	
CEC	Cox-Box (0.24)	Aniso	Exponential	0.0786	0.0439	297.0	0.303	0.417
*Fe (mg/kg)	Normal	Isotropy	Spherical	0.0753		263858	570790	
Pb (mg/kg)	Lognormal	Aniso	Exponential	0.0786	0.0298	36.0	0.502	0.276
Zn (mg/kg)	Lognormal	Aniso	Exponential	0.0786	0.0121	288.0	0.274	0.184
**Cd (mg/kg)	Lognormal	Aniso	Exponential	0.0652	0.0214	36.0	0.118	0.109
Cr (mg/kg)	Lognormal	Aniso	Exponential	0.0561	0.0148	297.0	0.122	0.108
Cu (mg/kg)	Lognormal	Aniso	Exponential	0.0786	0.0123	18.0	0.470	0.235
Ni (mg/kg)	Normal	Isotropy	Exponential	0.0365		99.371	47.944	

Pb, Zn and Cu seem to follow the same pattern; where the highest concentrations are close to the highways and the lowest concentrations are in residential areas (Figures 2a, b and d). The Pb enrichment near highways most likely results from the burning of leaded fuel, Cu is likely derived from brakes, and Zn from worn out tires (Van Bohemen and Janssen Van, 2003). High Cd concentrations are found throughout the study area (Figure not shown). However, the lowest values were close to the residential areas, and the highest were near the Samra WWTP. The distribution of Cr and Ni were much more heterogeneous than the other metals (Figures 2c and e), suggesting that the concentration of Cr and Ni may not come from point pollution, such as industrial activities, and that natural factors, such as the soil parent materials, were also an important source of these two metals.

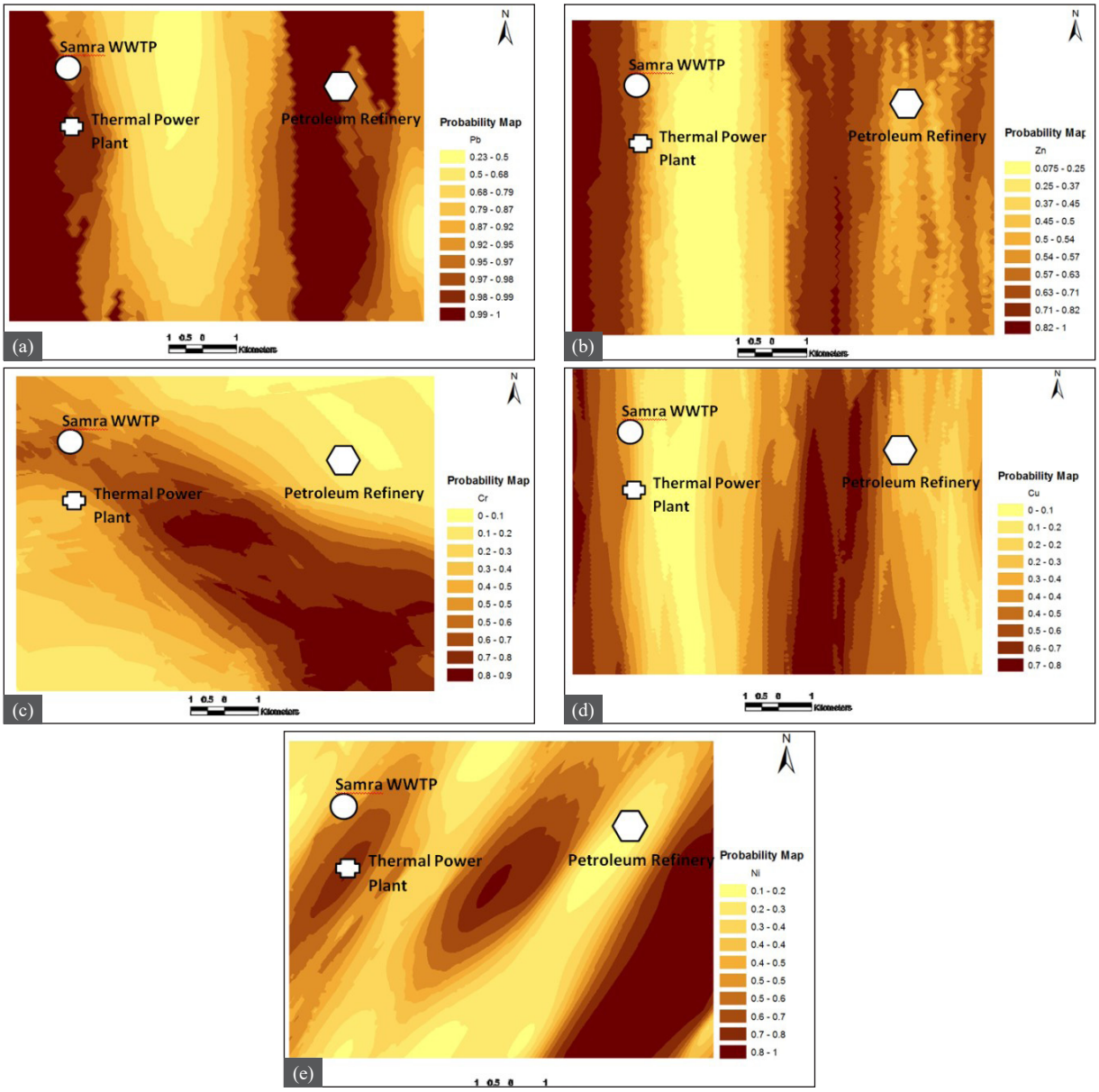

Figure 2. Probability maps of (a)Pb, (b) Zn, (c) Cr, (d) Cu, (e) Ni

Conclusion

Most of the sites in the present study area are contaminated by heavy metals reaching 100% probability above safe threshold levels. However, the Enrichment Factors (EFs) of the heavy metals showed that Cr, Cu and Ni are depleted by 0.46, 0.91, and 0.58, respectively, whereas Pb, Zn, and Cd are enriched by 5.4, 1.8 and 19.6, respectively. The calculation of Igeo index showed that the urban topsoil of Al-Hashemiyya is uncontaminated with Cr, Cu, and Ni, slightly contaminated with Zn, severely contaminated with Pb, and excessively contaminated with Cd. The contamination levels of Pb and Cd are higher than that for the other metals. Multivariate analyses indicate that soil pH is the most significant factor affecting the loads for the tested heavy metals except for Cu. Moreover, the results indicate the presence of three major clusters: Pb, Zn, and Cr; Zn, Pb and Cr; while Cu is not grouped with any other heavy metal and, thus, acts differently. The present study recommends adoption of monitoring, reporting and validation for the possible contamination so as to set appropriate strategies for controlling contaminants status and transports. Some of these strategies may include reduction in industrial emissions through improving their efficiencies, conducting periodical environmental impact assessments, creating zones and vulnerability maps for contaminated sites, and other related reclamation and rehabilitation programs.

Acknowledgment

The present work was funded by the Deanship of Research and Graduate Studies at the Hashemite University. We thank the Center of Environmental Studies at the Hashemite University for their assistance in analyzing the soil samples for the heavy metals. Also, we thank Eng. Hana Al-Nounah for her assistance in conducting the laboratory analysis.

References

[1] Akaiake H (1974) A new look at the statistical model identification, IEEE Transactions on Automatic Control, 19: 716-723.

[2] ArcGIS 9.2 (2006) Software Version 9.3. Redlands, California, USA: ESRI Inc.

[3] Banat K M, HowariF, Al-Hamada AA (2005) Heavy Metals in Urban Soils of Central Jordan: Should We Worry about Their Environmental Risks? Environmental Research 97: 258–273.

[4] Freyssinet PH, PiantoneP, AzaroualM, ItardY, Clozel-LeloupB, DGuyonnet, BaubronJC (2002) Chemical changes and leachate mass balance of municipal solid waste bottom ash submitted to weathering. Waste Manag. 22:159-172.

[5] Goovaerts P (1997)Geostatistics for natural resources evaluation. Oxford University Press, New York.

[6] Guo G, Wu F, XieF, Zhang R (2012) Spatial distribution and pollution assessment of heavy metals in urban soils from southwest China. Journal of Environmental Sciences 24: 410–418.

[7] Hawkins DM (1974) The Detection of Errors in Multivariate Data Using Principal Components. Journal of the American Statistical Association, 69: 340-344.

[8] Howell DC (1997) Statistical Methods for Psychology, Wadsworth Publishing Company, USA, 724 p.

[9] JMP 8 (2009) Statistics and graphics guide. SAS Institute Inc. Cary, NC, USA.

[10] Lacatuso R (1998) Appraising levels of soil contamination and pollution with heavy metals. European Soil Bureau Research Report Nº 4.

[11] Li X, LijuanL, YugangW, GepingL, Xi C, XiaoliangY, Myrna H P H, RuichaoG, HoujunW, JiehuaC, XingyuanH (2013) Heavy metal contamination of urban soil in an old industrial city (Shenyang) in Northeast China. Geoderma 192: 50–58.

[12] Lim H S, Lee JS, Chon HT, Sager M (2008) Heavy metal contamination and health risk assessment in the vicinity of the abandoned Songcheon Au-Ag mine in Korea. Journal of Geochemical Exploration 96: 223–230.

[13] Mallow CL (1973) Some comments on Cp, Technometrics 15: 661-675.

[14] Mashal K, Salahat M, Al-Qinna M, Degs Y (2015) Spatial distribution of cadmium
concentrations in street dust in an arid environment. Arab J Geosci 8:3171–3182.

[15] Milligan, GW (1980) An Examination of the Effect of Six Types of Error Perturbation on Fifteen Clustering Algorithms. Psychometrika, 45: 325-342.

[16] Ministry of Agriculture (1994) National soil map and landuse. Hunting Technical Services Ltd and Soil Survey and Land Research Centre, Amman, Jordan.

[17] Olawoyin R,Samuel A O, Robert LG (2012) Potential risk effect from elevated levels of soil heavy metals on human health in the Niger delta. Ecotoxicology and Environmental Safety 85:120–130.

[18] Quenea K, LamyI, WintertonP, BermondA, DumatC (2009) Interactions between metals and soil organic matter in various particle size fractions of soil contaminated with waste water. Geoderma149: 217–223.

[19] Reimann C, FilmozerP, Garret RG (2005) Background and threshold: critical comparison of methods of determination. Sci. Total Environ 346: 1–16.

[20] Shetye S, ShudhakarM, Mohan R, TyagiA (2009) Implications of organic carbon, trace elemental and CaCO3 variations in a sediment core from the Arabian Sea. Indian J. Mar. Sci.384:432–438.

[21] Sparks DL, Page AL, HelmkePA, RLoeppertH, SoltanpourPN, TabatabaiMA, Johnston CT, Sumner ME (Eds.), Methods of Soil Analysis, Part 3, Chemical Methods (2001), Soil Sci. Soc. Am. and Am. Soc. Agron., Madison, WI.

[22] Tiller KG (1992) Urban soil contamination in Australia. Australia Journal of Soil Research 30: 937–957.

[23] Tume P, Joan B, FerrranR, JaumeB, LluisL, Luis T, Bernardo S (2011) Concentration and distribution of twelve metals in Central Catalonia surface soils. Journal of Geochemical Exploration 109:92–103.

[24] Turekian KK, Wedepohl KH (1961) Distribution of the elements in some major units of the earth's crust. Geol. Soc. Am. 72:175–192.

[25] Van Bohemen HD, JanssenVLWH (2003) The influence of road infrastructure and traffic on soil, water, and air quality. Environ Manage 31:50 – 68.

[26] Wei YC, Bai YL, JinJY, Zhang F, Zhang L P, Liu XQ (2009) Spatial variability of soil chemical properties in the reclaiming marine foreland to yellow sea of China. Agricultural Sciences in China 8:1103-1111.

[27] Zhang C, SelinusO, KjellströmG (1999) Discrimination between natural background and anthropogenic pollution in environmental geochemistry — exemplified in an area of south-eastern Sweden. Sci. Total Environ 243:129–140.

[28] Zhang J, Liu CL (2002) Riverine composition and estuarine geochemistry of particulate metals in China – Weathering features, anthropogenic impact and chemical fluxes. Estuar. Coast. Shelf S 54:1051–1070.

JJEES
Jordan Journal of Earth and Environmental Sciences

Volume 8, (Number 2), Dec, 2017
ISSN 1995-6681
Pages 69 - 76

Does Forest Litterfall Nutrient Stocks Affect the Nutrient Supplying Capacity of Soils?

Azeez Jamiu Oladipupo

Department of Soil Science and Land Management, Federal University of Agriculture Abeokuta, Nigeria

Received 20 May, 2017; Accepted 22 October, 2017

Abstract

In order to understand nutrient stocks and dynamics of forest soils, the nutrient supplying capacity of forest soils and control soils were evaluated through greenhouse bioassay. Maize agronomy and nutrient uptake was assessed in 4 consecutive cycles, at 6 weeks/cycle. Results indicated that dry matter yield ranged from 4.25 to 10 g plant^{-1}. The mean plant height decreased from the 1st to the 3rd cycles. The organic carbon of the soils ranged from 0.61 to 1.80 % in soils from Leucaena leucocephala and Anogeissus leiocarpus, respectively. The soil total N ranged from 0.07 to 0.17 % while the maize N varied from 1.09 - 2.98 % in the 3rd and 1st cycle for soils under Treculia africana and Bambusa vulgaris. Bambusa vulgaris soil was better in nutrients supply considering the quantities of nutrients and their patterns of release to the soil.

Keywords: Agroforestry, maize, forest soils, soil nutrients, litter chemistry.

1. Introduction

The nutrient supplying capacity of a given soil type is essential for the growth and development of crops. High crop yield is partly dependent on the soil nutrient contents and its ability to supply these nutrients in adequate and available forms to the crops (Marschner, 2012). Many factors have, however, been recognised to influence the nutrient supplying capacity of soils. These factors include soil type, pH, organic matter content, soil cover or litter, and soil micro-organisms and the land-use system to which the soil is subjected to (Thiffault et al., 2011; Landon, 2014). Among these factors, soil cover or surface residues have been shown to contribute significantly both to the nutrient contents and to its supplying capacities particularly when under the same soil type (Meisner et al., 2012). The contributions of different soil surface residue to the soil nutrient supplying capacity are yet to be widely explored in research.

The capacity of trees to maintain and improve soil condition is shown by high soil fertility status and enriched nutrient cycling under natural forest, the restoration of fertility under forest fallow in shifting cultivation, and the experience of reclamation forestry and agroforestry (Attiwill et al., 1993). A range of properties have been identified which make tree species suited to soil improvement. These may include high biomass production, nitrogen fixation, a combination of fine feeder roots with tap roots and litter with high nutrient content (Attiwill et al., 1993).

It is recognized that forest trees contribute variable quantities of litters to the soil organic pool. This litter varies in their chemical compositions, the speed with which it breaks down in the soil and the diverse range of soil flora and fauna that inhabit it. The by-products of the litter breakdown are retained in the soil through chemical and biological processes (Ballard and Will, 1981). Nutrients, such as phosphorus, nitrogen, potassium, calcium, magnesium and trace elements, may be retained in a form that is not available for tree and plant growth (fixed pool), or may be in the plant available pool (Binkley et al., 2011).

Nutrients uptake in plants is influenced by the soil relative proportion of micro and macro-nutrients. Soil micro-nutrients are nutrients that are required by all plants for proper growth and productivity in minute amounts. They include copper, iron, manganese, and zinc. Each has several important and specific functions in plant cell metabolism and in photosynthesis. They are only rarely limiting to plant growth in soils because they are needed in trace amounts. A high proportion of these nutrients in the soil could lead to soil heavy metal pollution (Azeez et al., 2013). In contrast, macro-nutrients, such as nitrogen, phosphorus and potassium, are required in large quantity for optimum plant yield. These macronutrients, particularly, the NPK are highly limiting in most tropical soils. While it is clear that many tree litters could help supply these limiting nutrients and improve the soil chemical composition, the effects of different tree litters on the soil nutrient supplying capacity are yet to be effectively evaluated.

Similarly, the impact of trees on soil nutrients has been conventionally assessed by examining changes in soil nutrients (Baker, 1978) with fewer studies focusing on the nutrient concentrations of the crop grown in cycles on the forest soils. Different tree species could, however, differ in the quantity and quality of nutrients supplied to the soil. A good understanding of the impact of forest litters on the soil nutrient supplying capacity to subsequent crops grown on

* Corresponding author. e-mail: azeez2001ng@yahoo.com

that soil is imperative and could help promote the practice of agroforestry among smallholder farmers. Therefore, it is in this context that the present study aims to evaluate the nutrient supplying capacity of soils from different forest species by evaluating, through greenhouse bioassay, the agronomic response and nutrient concentration of successive maize plants grown on soils collected from forest sites.

2. Materials and Methods

2.1. The Study Location

The plantations used for the present study was located at the Federal University of Agriculture Abeokuta Nigeria forestry arboretum. The site is located adjacent to the University's main entrance on latitude 7^0 58' N and on the longitude 3^0 25' E. The general topography of the present study area was an undulating land terrain. The annual temperature ranges from 22^0 C to 33^0 C. The annual rainfall is about 1400 mm with wet season from April to October while the dry season is from November to March

2.2. History of the Forest Sites

The trees used for the present study and the non-tree spp. soils were of the same soil type. Gmelina arborea was established in 2000 at an elevation of 159 m above sea level (ASL). The trees are located at 7.22738°N, 3.44742°E. Tectona grandis plantation was established in 1998 at an elevation of 156 m ASL; the trees are located at 7.22713°N; 3.44773°E; Leucaena leucocephala was established in 1998 at 159 m ASL and located at 7.22738°N, 3.44742°E. Bambusa vulgaris is probably the oldest plantation; estimates showed that it was established in 1990 at 150 m ASL at 7.22737°N, 3.44717°E. Treculia africana was established in 2001 at an elevation of 149 m ASL at 7.2263°N, 3.44909°E. Anogeissus leiocarpus was established in 2001 at an elevation of 149 m ASL and located at 7.2265°N, 3.44038°E.

2.3. Soil Sample Collection and Preparation

The soil samples were taken under the seven tree species which included: Gmelina arborea, Tectona grandis, Leucaena leucocephala, Bambusa vulgaris, Treculia africana, Anogeissus leiocarpus and fallow land (non tree spp.). Soil samples were collected at 0-15 cm depth with a shovel at the basement of each tree species. The trees established a continuous cluster of trees with litters of the same tree on the ground. Soil samples were collected from few meters from the base of trees randomly at depth of 0-15 cm (surface soil). The systematic sampling points were selected to fall at center points where at least four trees shoot-biomass interlock. Details of the sampling positions are shown in Figure (1). The soils were collected from the central dark spots on Figure (1). The samples were collected into well-labelled sampling bags. The samples were air dried and sieved with a 2 mm sieve. Routine soil analysis was carried out on those samples. Thirty-two experimental pots were prepared; 5 kg soil from each of the tree species was dispensed into the pots.

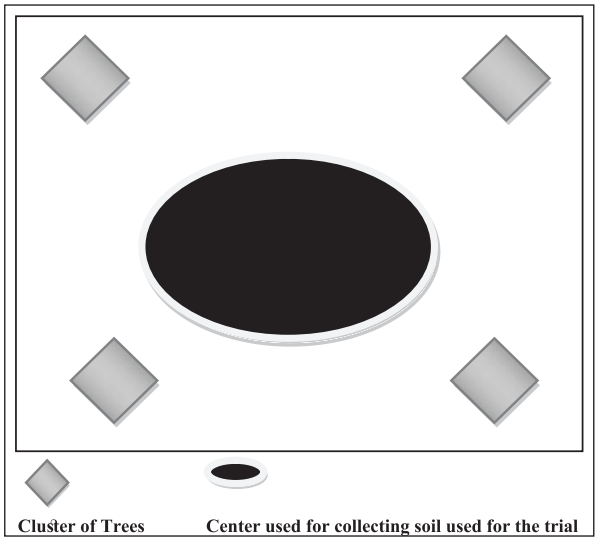

Figure 2. Sampling design of soil collection.

2.4. Soil Analysis

The soil pH was determined using glass electrode pH meter (McLean et al., 1982). Total nitrogen was determined using macro-Kjeldahl method (Bremner and Mulvaney, 1982). Phosphorus was determined by Bray 1 method (Nelson and Sommers, 1996). Organic carbon was determined using chromic acid oxidation procedure method (Nelson and Sommers, 1996). Exchangeable cations (potassium, calcium, sodium and magnesium) were extracted using 1N ammonium acetate. K and Na in the extract were read on a flame photometer while Ca and Mg were read on Atomic Absorption Spectrophotometer (AAS). The available Zn, Cu, Mn and Fe, extracted with HCl, were determined on an Atomic Absorption Spectrophotometer (Donisa et al., 2000).

2.5. Experimental Design, Planting and Data Collection

The experimental design was completely randomized design carried out in the screen house. Maize was planted in each of the thirty-two pots containing the soil samples from the tree species with no fertilizer or manure. Major soil nutrient, NPK (20-10-10) fertilizer (120 kg ha^{-1}), was added to the control soil samples taken from the non-tree spp). The vegetation of the non-tree spp was predominantly Chromolaena odorata. The maize was planted and thinned to one maize stand per pot after emergence. At the second, fourth and sixth weeks of planting, the plant height was measured with a meter rule.

2.6. Plant Sample Preparation and Analysis

At the end of four consecutive cycles, each cycle of six weeks, the maize plant was cut at ground level, oven-dried at 65^0 C to constant weight. The dry weight was recorded; this was immediately followed by milling. The plant samples were analyzed for total nutrient (N, P, K, Ca, Mg, Zn, Fe, Mn, Cu) concentrations at the end of each cycle after the samples were digested in ternary mixture of sulphuric, nitric and perchloric acids.

2.7. Statistical Analysis

The soil and plant data were subjected to the analysis of variance (ANOVA) using the SAS statistical package. The means were separated by Duncan's Multiple Range Test (DMRT) at 5 % probability level.

3. Results

3.1. The Oven Dried Weights of the Maize Plants under the Various Treatments

The maize plants oven dried weight is presented in Table (1). In the first and second cycles, the mean oven-dried weights of the maize plant varied from 4.25 to 6.25 kg and 6.5 to 8.5 kg in non-tree spp and Bambusa vulgaris; non-tree spp. and Gmelina arborea for the first and second cycles, respectively. At the 3rd planting cycle, Gmelina arborea also gave the highest mean oven-dried weight, while the lowest value was observed in non-tree spp. In most cases, Bambusa vulgaris soil, without fertilizer application, gave greater oven-dried weight, and in all, the non-tree spp recorded the least. It was observed that the maize plant oven dried weight increased from the first to the third cycles across the treatments. The cumulative mean weight of maize shows that the soils all enhanced the biomass accumulation in maize plant. However, the significant lowest yield was recorded in soil from Tectona grandis and the non-tree spp. without fertilizer application

3.2. The Effect of Tree Types on Maize Plant Height at 3 Cycles of Planting

The mean maize plant heights at different growth stages and at different cycles of planting are presented in Table (2). At the first cycle, the plant height, at 4 weeks of planting, varied from 58.88 cm to 74.38 cm with the tallest and lowest plants found in soil under Anogeissus leiocarpus and non-tree spp., respectively. At 6 weeks of planting, plant height ranges from 62.75 cm to 84.63 cm with non-tree spp. having the lowest (62.75 cm) and non-tree spp. + NPK fertilizer having the highest height (84.63 cm). In all, the Anogeissus leiocarpus and the non-tree spp. soils significantly produced the tallest and shortest plants, respectively. In the second planting cycle at 4 WAP, the non-tree spp. + NPK fertilizer soil gave the tallest plant (59.25 cm) while the lowest was in soil from Bambusa vulgaris (46.50 cm) but at 6 WAP, the tallest plant was found in Treculia africana (85.38 cm) soil while the lowest was in non-tree spp. (73.63 cm). At the third planting cycle during the 4 WAP, soil from the non-tree spp gave significantly ($P < 0.05$) higher taller plants than all other treatments. The soils from Bambusa vulgaris plantation produced the shortest maize plants both at the 4 and 6 WAP. The non –tree fertilizer gave the highest mean plant height of 78.50 cm at the 6 WAP.

Table 1. Effect of tree types on height and oven dried weight of maize plant

Plantation type	Dry weight (g pot^{-1})			
	Cycle 1	Cycle 2	Cycle 3	Mean
Bambusa vulgaris	6.25a	8.50a	8.50ab	7.75a
Tectona grandis	4.75a	8.00ab	6.50c	6.42c
Leucaena leucocephala	5.75a	8.00ab	8.00bc	7.25ab
Gmelina arborea	5.25a	8.25ab	8.75ab	7.42ab
Anogeissus leiocarpus	6.00a	8.00ab	10.00a	8.00a
Non-tree spp	4.25a	6.50b	7.50bc	6.08c
Treculia africana	5.50a	8.25ab	7.75bc	7.17abc
Non-tree spp + NPK fertilizer	5.75a	8.00ab	9.00ab	7.42ab

Means with the same alphabet(s) in a column are not significantly different from each other at $p < 0.05$

Table 2. Effect of soils under different tree species on maize plant height at 3 cycles of planting

	First cycle		Second cycle		Third cycle	
	4WAP	6WAP	4WAP	6 WAP	4WAP	6WAP
	cm					
Bambusa vulgaris	63.63bc	67.75c	46.50b	77.75ab	37.00c	61.75c
Tectona grandis	62.63bc	66.88c	51.00ab	76.25ab	43.50b	63.25c
Leucena leucocephala	65.30bc	69.13bc	52.25ab	80.00ab	41.50bc	75.75a
Gmelina arborea	62.13bc	66.50c	56.25a	79.50ab	39.50bc	66.00bc
Anogenous spp	74.38a	78.55ab	58.50a	84.00a	44.25b	71.75ab
Non-tree spp	58.88c	62.75c	46.63b	73.63b	50.25a	73.25ab
Treculia Africana	68.88ab	72.75bc	58.50a	85.38a	40.50bc	66.00bc
Non-tree spp + NPK fertilizer	65.25bc	84.63a	59.25a	83.00ab	42.00bc	78.50a

Means with the same alphabet(s) in a column are not significantly different from each other at $p < 0.05$

3.3. Chemical Properties of Soils from Different Trees Species

The soil was characterized before planting and the result revealed that many of the soils under the different trees varied significantly in their nutrients concentrations (Table 3). Generally, the soil was moderately acidic and the pH ranged from 5.81 to 6.13 in the Gmelina arborea and non-tree spp., respectively. The organic carbon of the soils ranged from 0.61 to 1.80 % in soils from Leucaena leucocephala and Anogeissus leiocarpus, respectively. The total N varied from 0.07 to 0.17 %. The total N recorded in soils under the Bambusa vulgaris and Gmelina arborea was 143 % greater than that of Leucaena leucocephala and the non-tree spp. Gmelina arborea soil had a significantly higher available P of 19.46 mg kg^{-1} among the soils of the tree types; the lowest P (9.40 mg kg^{-1}) was obtained in soils under the Treculia africana and non-tree species. The exchangeable K slightly varied from 0.25 mg kg^{-1} in the soil from Bambusa vulgaris to 0.37 mg kg^{-1} in the Tectona grandis. The different tree species had no significant effect (P>0.05) on the soil exchangeable calcium. Tectona grandis, Treculia africana and non-tree species soils had significantly greater magnesium contents. The amount of sulphur varied from 0.05 to 0.41 %. Soils under Gmelina arborea had a significantly higher sulphur content. Some of the soil micronutrients in each of the forest soils also varied significantly. The non-tree species, Tectona grandis and Treculia africana had a significantly greater Cu content. The Mn content ranged from 1.68 mg kg^{-1} in the non-tree spp. to 14.36 mg kg^{-1} in the soils under Anogeissus leiocarpus. Anogeissus leiocarpus and Bambusa vulgaris recorded significantly high acid extractable Fe while Leucaena leucocephala had the least Fe content. The Zn content ranged from 0.02 to 5.82 mg kg^{-1} in the Bambusa vulgaris and Gmelina arborea, respectively.

Table 3. Chemical properties of soils from different trees species before the experiment

Tree types	pH	Org. C	Total N	S	P	K	Ca	Mg	Cu	Mn	Fe	Zn
		---------- % ----------			mg kg^{-1}	cmol kg^{-1}	---------- mg kg^{-1}----------					
Anogeissus leiocarpus	5.89bc	1.80a	0.11a	0.11b	14.37b	0.26b	1.15a	0.38abc	3.29ab	14.36a	123.38a	0.93b
Bambusa vulgaris	6.12a	0.72ab	0.17a	0.21ab	15.93ab	0.25b	0.82a	0.43abc	2.56bc	19.02b	118.38ab	0.02b
Gmelina arborea	5.81 c	0.97ab	0.17a	0.41a	19.46a	0.30ab	0.98a	0.42abc	1.93c	5.81c	5.65c	5.82a
Leucaena leucaephala	5.95abc	0.61b	0.07a	0.05b	3.18d	0.35a	1.05a	0.33bc	2.25c	2.79d	0.29c	0.05b
Tectona grandis	6.08ab	0.84ab	0.09a	0.09b	5.11dc	0.37a	0.85a	0.53a	3.66a	1.86d	89.00b	2.31b
Treculia africana	5.82c	1.07ab	0.11a	0.05b	9.40 c	0.35a	1.18a	0.51ab	3.70a	1.84d	1.06c	0.38b
Non tree specie	6.13a	0.68b	0.07a	0.05b	9.40c	0.35a	1.17a	0.51ab	4.13a	1.68d	1.39c	1.40b

Means with the same alphabet(s) in a column are not significantly different from each other at $p < 0.05$

3.4. Effect of Tree Types on Maize Nutrient Concentrations in the First Cycle

The maize plant nutrient concentrations, under the different treatments in the first cycle, are presented in Table (4). The mean total N concentration ranged from 2.04 to 2.98 % in the soil from non-tree spp. + NPK fertilizer and Bambusa vulgaris, respectively. Total N in the maize plants, under the Bambusa vulgaris soil, was significantly ($P < 0.05$) higher than all the other treatments with the exception of those under Tectona grandis. The N concentration was in the order: Bambusa vulgaris > Tectona grandis > Leucaena leucocephala > Gmelina arborea > Anogeissus leiocarpus > non-tree spp. > Treculia africana > non-tree spp. + NPK fertilizer. The P concentration in maize varied from 0.05 to 0.40 mg kg^{-1}. Maize plants in the Gmelina arborea soil had higher P concentrations, though not significantly different from the other treatments. The non-tree spp. + NPK fertilizer was significantly higher ($P < 0.05$) in K and Ca concentrations of the maize plants than all other treatments. The Mg concentration of the maize plants, with different treatments, ranged from 0.49 to 1.45 mg kg^{-1}. Treatment with non-tree spp has the highest Mg value of 1.45 mg kg^{-1}, though not significantly ($P < 0.05$) different from other treatments except for the plants in Bambusa vulgaris, Leucaena leucocephala and non-tree spp. + NPK fertilizer soils.

The Zn concentration of the maize plant under the Treculia africana soil was significantly ($P < 0.05$) higher than all the other treatments. The Fe and Mn concentrations of maize plants in the Bambusa vulgaris soil were significantly ($P < 0.05$) higher than all the other treatments except for plants in Anogeissus leiocarpus soil. The Fe and Mn concentrations varied from 413 mg kg^{-1} to 881 mg kg^{-1} and 153 to 253 mg kg^{-1}, respectively. Maize plants in the non-tree spp soil had the highest concentration of Cu (29.25 mg kg^{-1}) with the least of 19.75 mg kg^{-1} in Bambusa vulgaris. Maize Cu concentrations under the non-tree spp was not significantly ($P > 0.05$) different from that of Leucaena leucocephala, Gmelina arborea and Anogeissus leiocarpus. Other differences were, however, significant ($P < 0.05$).

Table 4. Effect of tree types on Maize nutrient concentrations in the first and second cycles

Plantation type	N (%)	P	K	Ca	Mg	Zn (mgkg^{-1})	Fe	Mn	Cu
First Cycle									
Bambusa vulgaris	2.98a	0.18a	0.20b	0.22c	0.87bc	73.25b	881.25a	252.75a	19.75c
Tectona grandis	2.81ab	0.08a	0.23b	0.26bc	0.94abc	48.00b	498.75cd	134.50bcd	21.25bc
Leucaena leucocephala	2.59bc	0.05a	0.30b	0.25bc	0.84bc	45.00b	415.00d	96.25cd	23.75abc
Gmelina arborea	2.48cd	0.40a	0.28b	0.31b	1.27ab	58.75b	396.25d	137.50bc	26.25ab
Anogeissus leiocarpus	2.36cd	0.25a	0.25b	0.26bc	0.92abc	117.75b	871.25a	175.25b	27.25ab
Non-tree spp	2.34cd	0.22a	0.31b	0.21c	1.45a	68.00b	542.50bc	134.25bcd	29.25a
Treculia Africana	2.27de	0.22a	0.28b	0.24bc	0.96abc	336.50a	625.25b	152.50bc	20.00c
Non-tree spp + NPK fertilizer	2.04e	0.18a	0.67a	0.40a	0.49c	43.38b	413.63d	70.88d	20.00c
Second Cycle									
Bambusa vulgaris	2.57a	1.59ab	0.89b	0.68a	0.68b	69.94b	435.88a	81.56c	13.95abc
Tectona grandis	2.18b	2.69a	0.73c	0.68a	0.60b	49.25de	377.00ab	88.00bc	13.00abc
Leucaena leucocephala	2.07bc	0.90bc	1.02a	0.53bc	0.81a	56.75cd	393.13ab	104.88bc	10.81cd
Gmelina arborea	2.23b	1.48b	1.05a	0.68a	0.89a	84,31a	382.94ab	110.50ab	12.63bcd
Anogeissus leiocarpus	2.00bc	1.38bc	0.81bc	0.70a	0.85a	48.38e	311.00bc	133.75a	11.63cd
Non-tree spp	2.01bc	0.74bc	1.03a	0.64ab	0.85a	60.00c	360.00ab	109.25ab	17.56ab
Treculia Africana	1.76d	0.52bc	0.59d	0.44cd	0.65b	48.88e	256.13c	87.63bc	7.88d
Non-tree spp + NPK fertilizer	1.93cd	0.33c	0.72c	0.40d	0.41c	31.77f	346.55abc	55.17d	17.98a

Means with the same alphabet(s) in a column are not significantly different from each other at $p < 0.05$

3.5. Effect of Tree Types on Maize Nutrient Concentrations in the Second Planting Cycle

The concentration of maize nutrients, with different treatments in the second planting cycle, is presented in Table (4). The result indicated the nutrient concentrations in maize plant varied significantly under the various treatments. The N concentration of maize plant with different treatments ranged from 1.76 % to 2.57 % in the Bambusa vulgaris and Treculia Africana, respectively. Maize plants on the Bambusa vulgaris soil were significantly higher ($P < 0.05$) in their N and P concentrations than all the other treatments except for P with Tectona grandis. The K concentration of maize plant, treated in the non-tree spp. soil without fertilizer, was significantly higher ($P < 0.05$) than all the other treatments except for those in Leucaena leucocephala and Gmelina arborea soil. The mean Ca concentration of maize plants with different treatments ranged from 0.40 mg kg^{-1} to 0.70 mg kg^{-1} in non-tree spp. + NPK fertilizer and Anogeissus leiocarpus, respectively. The Mg concentration of maize plants under non-tree spp. + NPK fertilizer was significantly lower ($P < 0.05$) than all other treatments.

Maize plants, treated with Gmelina arborea soil, were found to be significantly higher ($P < 0.05$) in Zn concentrations than all the other treatments. The Fe concentration of maize plants in the Bambusa vulgaris was not significantly different ($P > 0.05$) from the other treatments except for Anogeissus leiocarpus and Treculia africana. The Mn concentration of maize plants with different treatments ranged from 55.17 to 133.75 mg kg^{-1} for non-tree spp and Anogeissus leiocarpus, respectively. The concentrations of Cu varied from the lowest value in Leucaena leucocephala to the highest in non-tree spp. + NPK fertilizer soils. The differences were statistically significant at $P < 0.05$.

3.6. Effect of Tree Types on Maize Nutrient Concentrations in the Third Cycle

Table (5) shows the mean concentration of maize nutrients under the different treatments at the third planting cycle. The N concentrations of maize plants differ significantly under the various treatments and this varied from 1.09 to 2.23 % in the Treculia africana and Bambusa vulgaris, respectively. Phosphorus concentration was not significant under the different treatments ($P > 0.05$). The treatment had a significant impact on K concentrations in the maize plant and it varied from 0.47 mg kg^{-1} to 1.08 mg kg^{-1} in the non-tree spp. + NPK fertilizer and Gmelina arborea, respectively. Maize plants in the Leucaena leucocephala and Anogeissus leiocarpus recorded the lowest Ca concentrations of 0.36 mg kg^{-1} and 0.64 mg kg^{-1}, respectively. Non-tree spp. + NPK fertilizer and non-tree spp. recorded the least and highest Mg concentrations in the maize plant.

Table 5. Effect of tree types on Maize nutrient concentrations in the third and fourth cycles

Plantation type	N (%)	P	K	Ca	Mg	Zn(mgkg^{-1})	Fe	Mn	Cu
Third Cycle									
Bambusa vulgaris	2.23a	1.33a	0.87abc	0.60a	0.63abc	60.13b	299.97a	69.98cd	12.63b
Tectona grandis	2.01ab	1.22a	0.62bc	0.54ab	0.42d	41.61cd	330.07a	77.92bc	10.14bc
Leucena leucocephala	1.86b	0.58a	0.61bc	0.36b	0.55cd	46.24c	324.13a	83.25bc	9.41c
Gmelina arborea	2.04ab	1.13a	1.08a	0.56ab	0.74ab	72.58a	325.35a	97.45ab	10.71bc
Anogeissus leiocarpus	1.73b	1.24a	0.91ab	0.64a	0.74ab	39.68cd	152.73b	121.36a	9.88bc
Non-tree spp	1.79b	0.54a	0.89ab	0.42ab	0.76a	47.53c	272.54a	99.43ab	12.90b
Treculia Africana	1.09c	0.46a	0.83abc	0.59ab	0.56bcd	32.20d	134.09b	59.09cd	5.29d
Non-tree spp + NPK fertilizer	1.75b	0.42a	0.47c	0.44ab	0.40d	29.98d	315.43a	48.51d	18.05a
Fourth Cycle									
Bambusa vulgaris	2.93a	0.40de	1.58ab	0.68ab	0.61bc	40.75c	411.90a	70.75b	Data not available
Tectona grandis	0.98cd	0.33e	1.56ab	0.71ab	0.40d	61.13a	315.20a	75.80b	
Leucena leucocephala	2.47ab	0.49cd	2.16a	0.68ab	0.81a	40.75c	556.90a	52.50c	
Gmelina arborea	1.60bc	0.51cd	1.94ab	0.63ab	0.73ab	62.75a	315.80a	82.44ab	
Anogeissus leiocarpus	0.54d	0.57bc	1.43b	0.62ab	0.84a	47.13bc	501.40a	82.38ab	
Non-tree spp	0.92cd	0.65b	1.86ab	1.14a	0.52cd	69.13a	498.80a	38.38d	
Treculia Africana	1.69bc	0.43de	1.44b	0.38b	0.46cd	61.13a	511.10a	90.15a	
Non-tree spp + NPK fertilizer	2.69a	0.87a	1.56ab	0.57b	0.50cd	70.00a	390.00a	52.50c	

Means with the same alphabet(s) in a column are not significantly different from each other at $p < 0.05$.

3.7. Effect of Tree Types on Maize Nutrient Concentrations in the Fourth Cycle

The mean concentration of maize nutrients under the different treatments at the fourth planting cycle is shown in Table (5). The total N concentrations in the maize plants ranged from 0.54 to 2.93 % in the Anogeissus leiocarpus and Bambusa vulgaris soils, respectively. Differences in N concentrations of maize plants found under the Bambusa vulgaris, Leucaena leucocephala and non-tree spp. with NPK fertilizer soils were not significant (P>0.05). The non-tree spp. recorded significantly the highest P concentrations of 0.87 mg kg^{-1} among the various treatments. The lowest P value of 0.33 mg kg^{-1} was observed in maize plants in the Tectona grandis soil. Differences in K concentrations of the maize plants were not significant (P>0.05) under the Leucaena leucocephala, Gmelia arborea, Bambusa vulgaris, Tectona grandis, non-tree spp. and the non-tree spp. with NPK fertilizer. Anogeissus leiocarpus, however, recorded the least K concentration which was significantly lower than that obtained under the Leucaena leucocephala. Calcium concentrations varied slightly under the different treatments and ranged from 0.38 to 1.14 mg kg^{-1} in maize plants under the Treculia Africana and the non-tree spp. Higher Mg concentration (0.84 mg kg^{-1}) was observed in Anogeissus leiocarpus soil. Tectona grandis gave the least mean Mg concentration of 0.40 mg kg^{-1} in the maize plants.

The mean zinc concentrations varied from 40.75 to70 mg kg^{-1} in Bambusa vulgaris and non-tree spp. with NPK fertilizer soils. Maize Zn concentrations grown on soils from non-tree spp with NPK fertilizer, non-tree spp., Gmelina arborea, Treculia Africana and Tectona grandis were not significantly different at 5 % probability level. The iron concentration ranged from 315.20 to 556.90 mg kg^{-1} in the Tectona grandis and Leucaena leucocephala soils. These differences were, however, not significant (P>0.05). The non-tree spp. gave the lowest mean Mn concentration of 38.38 mg kg^{-1} while Treculia africana gave the highest Mn concentration (90.15 mg kg^{-1}) in the maize plants.

4. Discussion

The present study shows that there is a positive synchrony between the soil chemical composition and maize nutrients concentrations grown on soils taken under different trees and non-tree species. The present study used nutrient concentrations in maize plants and maize›s oven-dried weight under the various treatments as a proxy for the nutrient supplying capacity of soils under different tree spp. The soils from each of the tree spp. varied in their nutrient supplying capacities. Kumar (2008) noted that different trees had different effects on soil nutrients. There exist significant differences between the quantities of each nutrient released due to the different forest spp. It was also observed that planting cycles affected the nutrient release. The nutrients release varied depending on the number of planting cycles. The mean oven-dried weight of the maize plant increased

steadily from the first to the third planting cycles in all the treatments while the plant›s height followed the reverse order.

The total N decreased as the number of planting cycles increased from the first to the fourth cycle in most of the treatments. The N supplied by Gmelina arborea soil to the maize plants declined steadily from the 1st to the 4th planting cycle, though initially had a relatively high total N. This confirms earlier reports that in low-input farming system N deficient is a challenge due to the N removed in crops, season after seasons without replenishment (Scow et al., 1994; Ledgard, 2001). This system of agriculture is, however, not encouraged in the view of the need to promote sustainable use of soil resources and the urgent need to achieve food security in Sub-saharan Africa. In all the four planting cycles, N declined in the different tree soils with the exception of Bambusa vulgaris and non-tree spp. with NPK fertilizer. In most cases, the different forest soils supplied more N than the non-tree spp. This implies that forest soils are better N suppliers than non-tree soils. Soils taken under the Bambusa vulgaris plantation gave a higher total N during all the planting cycles among the different treatments even greater than the non-tree spp amended with NPK fertilizer. This demonstrates that soils obtained under the Bambusa vulgaris plantation are better N supplier and could maintain their N supply for at least 4 planting cycles without any mineral amendments than other tree spp. investigated in the present study. This could perhaps be due to the old age of the Bambusa vulgaris plantation and the several years of litter deposition. Anand and Anand (1999) reported nutrient build up from litters of Bambusa vulgaris.

The P concentration in the maize plants did not vary significantly with respect to the number of planting cycles and tree spp., while the second planting cycle and Tectona grandis appeared to give a slightly higher P in the maize plants. Since the amount of P, absorbed in the plant, is proportionate to the amount of soil available P; this could explain why the different tree spp. did not have a visible effect on the P concentration of the tested maize crop. The amount of P in the maize declined with increasing cropping cycles with the exception of those in Bambusa vulgaris and Tectona grandis soils. This indicates a decline in soil available P under the different forest soils. This is an expected trend because previous research has shown that soil nutrients decline in low input agriculture as cropping intensifies (Bommarco et al., 2013). Conversely, the stability in the amount of P supplied by the Bambusa vulgaris and Tectona grandis after four planting cycles was a demonstration of their ability to improve to soil phosphorus fertility under low input farming system or in degraded soils.

The supply of K did not follow any particular trend among the tree spp. In addition, the planting cycle did not exact significant impact on the K concentrations in the maize crop. It was observed that K supplied in all the tree and non-tree soils was slightly higher at the 4th planting cycle. In all, Bambusa vulgaris proved to be a better supplier of NPK than the other tree species. This is in agreement with the earlier findings of improved nutrient status under Bambusa vulgaris plantations (Rahangdale et al., 2014). Calcium concentration in the maize plants was very high both in the Anogeissus leiocarpus and at the second cycle, compared to the other treatments and planting cycles. Similar results were obtained by Casals et al. (2013). In all, the first cycle gave the least Ca concentrations in each of the treatments. It was interesting to note that soils from the Treculia africana gave increased Ca concentrations in the maize plants from the first to the third cycle. This shows that Treculia africana has the potential to be a sustainable supplier of cations both for proper plant growth and for neutralizing acid soils. Such tree species are, thus, desirable in sustainable soil fertility strategies. The non-tree spp., amended with NPK fertilizers, had no influence on the Ca concentrations in the maize plant as calcium concentrations in the maize plant did not follow a particular pattern under the different treatments. The supply of Mg from the soils under the different trees decreased steadily from the first cycle to the 4th cycle. The non-tree spp. had greater Mg concentrations particularly in the first cycle and slightly higher when amended with NPK fertilizer at the 4th planting cycle. Considering all the treatments as soil nutrient suppliers, the non-tree spp. amended with NPK was found to be the poorest irrespective of the number of planting cycles.

The micro-nutrients of the maize plants decreased at the 4th cycle compared to the 1st planting cycle. Soils from different trees do not have profound influence on the Zn concentrations in the maize plant. The non-tree spp., however, had a significantly greater Zn release at the first and fourth planting cycles. There was a decrease in the amount of Zn supplied from the 1st to the 3rd cycle with a slight increase in the 4th cycle under the non-tree spp. soil. The least Fe concentration occurred in the third cycle and in the Leucaena leucocephala. Bambusa vulgaris and Anogeissus leiocarpus soils were better in supplying Fe to the maize plant particularly in the first planting cycle. The Fe supplying capacity of the different tree spp. dropped with increasing number of planting cycles. Soils from Bambusa vulgaris had a significantly greater Mn concentration in the first cycle than the other tree and non-tree spp. which were found not to be significantly different from each other. The maize Cu concentrations under both the tree and non-tree spp. followed the same pattern. The amount of Cu was significantly higher in the first cycle than the 2nd and 3rd cycles under the various treatments. In most cases, the non-tree spp. was a better Cu supplier than the tree spp. It was recognized that the soils from each tree and non-tree spp. supplied sufficient quantities of micro-nutrients to the maize plant for proper growth and development. Quantities higher than those supplied may result in heavy metal bioaccumulation in the plant tissues which could be dangerous to human health.

Conclusions

The present study demonstrates that different soils under different tree species have varying effects on the dry matter yield and nutrient concentrations of maize plant. The maize dry matter weights, plant height and the nutrients concentrations varied depending on the type of tree species. In all, soils from Bambusa vulgaris and Anogeissus leiocarpus were found to be better nutrient suppliers in considering the quantities of nutrients and their patterns of release. It was observed, and must be emphasized, that agroforestry or farming systems with no or low external input result in declining yields through nutrients mining and chemical degradation. A higher crop yield was observed in the first planting cycle, and more nutrients were extracted. However, in subsequent cropping

cycles, both the yield and nutrient concentrations could be significantly reduced. Farmers are, therefore, advised to supplement their agroforestry practices with other soil fertility management options, like nutrients addition, to maintain and increase their yield sustainably.

References

[1] Anand, N., and Anand, J. S., 1999. Bambusa vulgaris tree and nutrient built up from litter. Forest Ecology and Management 119 (1 – 3): 105 – 207.

[2] Attiwill, P. M., and Adams, M. A., 1993. Nutrient Cycling in Forests. New Phytocology 124: 561-582.

[3] Azeez, J. O., Mesele, S. A, Sarumi, S. O., Ogundele, J. A., Uponi, A. O., Hassan, A. O. 2013. Soil metal pollution as a function of traffic density and distance from road in emerging cities: a case study of Abeokuta, southwestern Nigeria. Archives of Agronomy and Soil Science 60(2): 275-295.

[4] Baker, J.B., 1978. Nutrient drain associated with hardwood plantation culture. In Proceedings, Second Symposium on Southeastern Hardwoods, p. 48-53. USDA Forest Service, Southeastern Area State and Private Forestry, Atlanta, GA

[5] Ballard, R., and Will, G. M., 1981. Accumulation of organic matter and mineral nutrients under a Pinus radiata stand. New Zealand Journal of Forest Science 11(2): 145-151.

[6] Binkley, D., Driscoll, C. T., Allen, H. L., Schoeneberger, P., and McAvoy, D., 2011. Acidic deposition and forest soils: context and case studies of the Southeastern United States. Springer Publishing Company, Incorporated

[7] Bommarco, R., Kleijn, D., and Potts, S. G., 2013. Ecological intensification: harnessing ecosystem services for food security. Trends in Ecolology Evolution 28(4): 230-238.

[8] Bremner, J. M., and Mulvaney, C. S., 1982. Pages 600-601 in A. L. Page et al., Eds. Methods of soil analysis. Part 2. 2nd ed. Am Soc Agron, Madison, WI.

[9] Casals, P., Romero, J., Rusch, G. M., and Ibrahim, M., 2013. Soil organic C and nutrient contents under trees with different functional characteristics in seasonally dry tropical silvopastures. Plant and Soil. DOI 10.1007/s11104-013-1884-9

[10] Donisa, C., Mocanu, R., Steinnes, E., and Vasu, A., 2000. Heavy metal pollution by atmospheric transport in natural soils from the northern part of eastern Carpathians. Water Air and Soil Pollution 120:347–358.

[11] Kumar, B. M., 2008. Litter dynamics in plantation and agroforestry systems. In: Batish DR, Kohli RK, Singh HP, Jose S (eds) Ecological basis of agroforestry. CRC Press, Boca Raton, pp 181–216.

[12] Landon, J. R., 2014. Booker tropical soil manual: a handbook for soil survey and agricultural land evaluation in the tropics and subtropics. Routledge

[13] Ledgard, S. F. 2001. Nitrogen cycling in low input legume-based agriculture, with emphasis on legume/grass pastures. Plant and Soil 228(1): 43-59.

[14] Marschner, H., 2012. Marschner›s mineral nutrition of higher plants. P. Marschner (Ed.). Academic press.

[15] McLean, E. O., Dumford, F., and Coronel, S. W., 1982. A comparison of several methods of determining lime requirements of soil. Soil Science Society of America Proceedings 30:26-30

[16] Meisner, A., De Boer, W., Cornelissen, J. H., and van der Putten, W. H., 2012. Reciprocal effects of litter from exotic and congeneric native plant species via soil nutrients. PloS one, 7(2), DOI: 10.1371/journal.pone.0031596.

[17] Nelson, D. W., and Sommers, L. E., 1996. Total carbon, organic carbon, and organic matter. pp. 961-1010, In D. L. Sparke (ed) Methods of soil analysis. Part 3. Chemical Methods SSSA Book Series no. 5. ASA and SSSA., Madison, W I.

[18] Rahangdale, C. P., Pathak, N. N., and Koshta, L. D., 2014. Impact of Bambusa vulgaris based agroforestry system on organic matter built - upand nutritional status of soil. International Journal of Agroforestry and Silviculture 1 (3): 31-36.

[19] Scow, K., Somasco, O., Gunapala, N., Lau, S., Venette, R., Ferris, H., and Shennan, C., 1994. Transition from conventional to low-input agriculture changes soil fertility and biology. California Agriculture 48(5): 20-26.

[20] Thiffault, E., Hannam, K. D., Paré, D., Titus, B. D., Hazlett, P. W., Maynard, D. G., Brais, S., 2011. Effects of forest biomass harvesting on soil productivity in boreal and temperate forests—A review. Environmental Review 19: 278-309.

JJEES
Jordan Journal of Earth and Environmental Sciences

Volume 8, (Number 2), Dec, 2017
ISSN 1995-6681
Pages 77 - 89

The Need for a Quantitative Analysis of Risk and Reliability for Formulation of Water Budget in Jordan

Fayha M. Al-Shibli*, William A. Maher, Ross M. Thompson

Institute for Applied Ecology – University of Canberra, Bruce, ACT, 2601 Australia

Received 21 May, 2017; Accepted 25 Aug, 2017

Abstract

Jordan is one of the most water-deficient countries globally, with a water demand consistently exceeding the water availability. The present paper reviews the state of current water resources and programmes being implemented to tackle this challenge. The authors of the present paper identify the recent trends and potential risks of maintaining a reliable water supply, discuss the past and the recent developments and extrapolate future water needs. The analysis found that the largest pressures on water supply come from population increases, the likely long-term consequences of climate change and groundwater over-abstraction. The authors conclude that, to date, projections of water use, supply and demand have not considered the different socio-economic factors and the various environmental and technological changes in a quantitative way. A new approach is suggested to quantify the future available water emphasising the need for quantitative assessment of the most influential pressures determining future water availability and use.

Keywords: Water system, Change in climate, Population growth, Groundwater over-abstraction.

1. Introduction

Jordan occupies an arid and semi-arid Mediterranean climatic zone, and is undergoing natural and human-driven changes that could have negative consequences for current and future water availability (Iglesias et al., 2011). Jordan is already suffering substantial water shortages because of limited natural water supplies (FAO, 2012) which are not sufficient for potable usage. UNEP (2007) has determined that annual freshwater needs will be 420 m^3 per capita by 2050. In Jordan, it is predicted that by 2025, freshwater supply could decrease to 90 m^3 per capita compared with 3600 m^3 per capita in 1946 (El-Naser, 2012; MWI, 2014). With no substantive reuse of water in Jordan currently, drivers, which increase water demand, are of critical importance (MWI, 2013c).

Many natural factors determine the amount of water, which is available for human use. These include hydro-climatic characteristics such as climate, geography, soil type, latitude, and vegetation cover. There are also significant human-pressures which determine water availability. These include groundwater over-abstraction, rapid population growth and the resulting changes in living patterns, technological advances, and land degradation due to overgrazing, deforestation, urbanization, and industrialization.

These pressures can act individually or in combination to affect water availability (Gleick, 1998; Zimmerman et al., 2008; FAO, 2012). Due to the threat of water shortages in Jordan, a number of efforts have been taken to manage the gap between the limited supply and high demand. Increasing demands of water across competing sectors have led to a growing need to develop policy and management solutions to ensure adequate water supply. Jordan has developed institutional, technological and strategic solutions to cope with water scarcity within the local cultural environment. The Jordanian government currently has focussed on large-scale water supply projects, such as inter-basin water transfers, dam construction, extraction of fossil groundwater aquifers, enhancing physical infrastructure and exploring for groundwater in the private sector (Al-Jayyousi, 2012). The government has issued more licences for groundwater well drilling and has imposed surveillance on existing wells. As a part of this initiative, 3043 legal wells were gauged for industrial, agricultural, municipal and livestock usage and 141 illegal wells were closed (MWI, 2013b). Moreover, a water pricing policy has been implemented to keep the extraction rates within recharge rates (MWI, 2013a), combined with increasing sewage connections, increasing wastewater and households tariffs, and reducing non-revenue water volume. At the household level, staggered water delivery times have been introduced, and compulsory water storage is required in new buildings. Water has been rationed for each economic sector and there is an expanding reliance on water trade for potable usage (Toppo, 2014). A range of measures has been applied to increase the efficiency of water use in irrigated agriculture. Farmers have been encouraged to rely on the reuse of treated wastewater and/or to purchase water from private wells. Efforts have been made to secure the rights to crops in neighbouring countries in order to reduce water consumption in agriculture, especially water consuming crops. Prioritization of water uses for drinking is the focal issue rather than water for irrigational or industrial uses (MWI, 2016d).

* Corresponding author. e-mail: fayha.al-shibli@canberra.edu.au

Nevertheless, reforming of water rights and allocations as well as water pricing probably have not succeeded in meeting water saving targets (Bengoechea, 2013).

Despite substantial reform of water policy, governance arrangements and management, it remains uncertain whether these measures will guarantee the future water needs for Jordan. Quantification of long-term future water system components including; demand, supply, future deficits, and the effects of the main drivers have been inadequately addressed by water industry planners.

This review evaluates the effects of pressures on water availability through water accounting, and uses quantitative analysis to estimate their effects on the water budget. We show the importance of quantitative studies for evaluating the consequences of interacting drivers in order to provide the basis for future management of Jordan›s water resources.

Due to the threat of water shortages in Jordan, a number of efforts have been taken to manage the gap between the limited supply and high demand. Increasing demands of water across competing sectors have led to a growing need to develop policy and management solutions to ensure adequate water supply. Jordan has developed institutional, technological and strategic solutions to cope with water scarcity within the local cultural environment. The Jordanian government currently has focussed on large-scale water supply projects, such as inter-basin water transfers, dam construction, extraction of fossil groundwater aquifers, enhancing physical infrastructure and exploring for groundwater in the private sector (Al-Jayyousi, 2012). The government has issued more licences for groundwater well drilling and has imposed surveillance on existing wells. As a part of this initiative, 3043 legal wells were gauged for industrial, agricultural, municipal and livestock usage and 141 illegal wells were closed (MWI, 2013b). Moreover, a water pricing policy has been implemented to keep the extraction rates within recharge rates (MWI, 2013a), combined with increasing sewage connections, increasing wastewater and households tariffs, and reducing non-revenue water volume. At the household level, staggered water delivery times have been introduced, and compulsory water storage is required in new buildings. Water has been rationed for each economic sector and there is an expanding reliance on water trade for potable usage (Toppo, 2014). A range of measures has been applied to increase the efficiency of water use in irrigated agriculture. Farmers have been encouraged to rely on the reuse of treated wastewater and/or to purchase water from private wells. Efforts have been made to secure the rights to crops in neighbouring countries in order to reduce water consumption in agriculture, especially water consuming crops. Prioritization of water uses for drinking is the focal issue rather than water for irrigational or industrial uses (MWI, 2016d). Nevertheless, reforming of water rights and allocations as well as water pricing probably has not succeeded in meeting water saving targets (Bengoechea, 2013).

Despite substantial reform of water policy, governance arrangements and management, it remains uncertain whether these measures will guarantee the future water needs for Jordan. Quantification of long-term future water system components including; demand, supply, future deficits, and the effects of the main drivers have been inadequately addressed by water industry planners.

This review evaluates the effects of pressures on water availability through water accounting, and uses quantitative analysis to estimate their effects on the water budget. We show the importance of quantitative studies for evaluating the consequences of interacting drivers in order to provide the basis for future management of Jordan›s water resources.

2. Geo-Climatologically Characteristic

Jordan has a hot climate characterized by dry summers, and the annual average temperature exceeds 18°C. According to the Köppen-Trewartha climate classification (KCC) (Belda et al., 2014) that considers types, subtypes and rainfall/ temperature regime; the climate of Jordan can be classified as a BSh climate. BS refers to the semi-arid or steppe climates, and is found where the mean annual precipitation is lower than R (annual precipitation threshold), but higher than 0.5R. If mean annual precipitation is lower than 0.5R, the KCC defines the area as having an arid or desert climate BW. The eastern and southern areas of Jordan have a BWh climate: a hot, dry desert climate with annual average temperatures above 18°C.

Jordan is 88,778 km^2 in area with surface water occupying approximately 540 km^2 (DoS, 2015). Most of the land cover is aridisols and rich in carbonates. Low rainfall zones are covered with sand and silt which results in arid-adapted vegetation. The predominant land cover is pasture, with forest and cultivated fields covering less than 9% of the total area. Desert and semi-desert cover 85% of the total territory area and three quarters of the land is covered with rocks, granite rocks, sand and bare soil (Ababsa et al., 2012; MoEnv, 2006). Soil moisture regimes range from xeric to arid, while the soil temperature ranges between thermal and hyper-thermal.

Jordan can be sub-divided into nine identifiable climatic regions: cool arid Mediterranean, warm arid Mediterranean, very warm arid Mediterranean, very warm Saharan Mediterranean, warm Saharan Mediterranean, cool Saharan Mediterranean, cool semi-arid Mediterranean, warm semi-arid Mediterranean and mild sub-humid Mediterranean (MoEnv, 2006). The Jordan climate possesses these characteristics due to its transitional location between the Mediterranean climate in the west and the arid and semi-arid climate in the east and south. Across all zones, drought coincides with maximum temperatures to bring summer dryness. The Mediterranean climate within the highland regions is differentiated by moderate and dry summers and cold and rainy winters. The Desert zone prevails in Badia with total area of 70,000 km^2, which is characterized by hot summers and cold winters. A Semi-tropical climate is dominant in the Ghor area (Jordan Valley) which is differentiated by hot summers and warm winters (Figure 1).

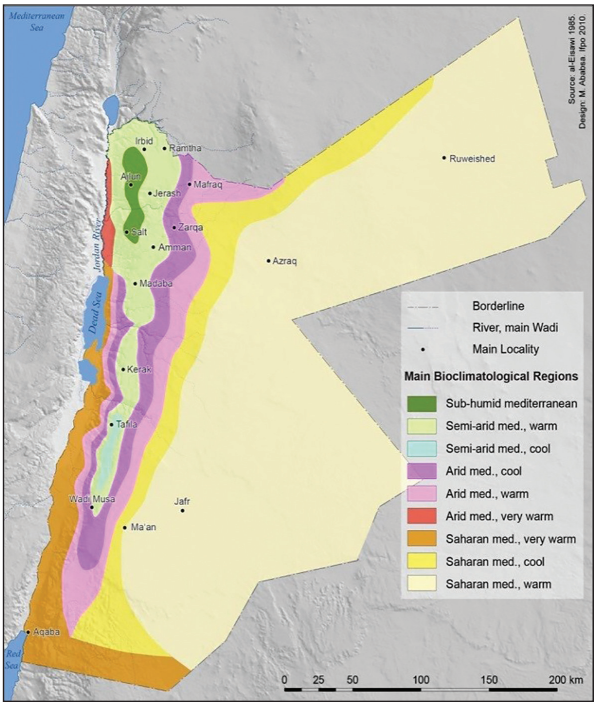

Figure 1. Main bioclimatological zones of Jordan; source: Ababsa and Kohlmayer (2013).

3. Annual Water Budget

The main water resources of Jordan consist of surface water resulting from precipitation (rainfall and snow), groundwater aquifers and/or fossil water in deep aquifers, and treated wastewater resources (Fig. 2). Currently, data on these resources quantities only exist for 2014 water year, so all calculations are based on that year.

Rainfall is the main water resource; the long-term average rainfall is about 8200 Million Cubic Meters (MCM; MWI, 2016g). Most rainfall evaporates (94.7%) and the remainder flows into rivers and other catchments, such as dams (2.3%) or infiltrates into underground aquifers (3.0%). In 2000-2013, it was estimated that the long-term average for total consumptive water use was 823.8 MCM consisting of municipal (429 MCM) that included domestic, refugee water use, commercial & tourism, agricultural (503 MCM) and industrial consumption (43.8 MCM; MWI, 2012; MWI, 2013a; MWI, 2014). In 2014, municipal consumption included 369.9 MCM for domestic and 59 MCM for non-domestic uses (commercial & tourism) but did not incorporate the 52.4 MCM used by refugees (MWI, 2016g). The Government›s aim is to reduce the gross volume used for irrigation in order to meet domestic demand. At present, most surface water is allocated for irrigation, primarily in the Jordan Valley (Raddad, 2005). Agriculture accounts for more than 60% (MWI, 2013b) of the total water withdrawal. Similar to global usage (Kassam et al., 2007), agriculture accounts for more than 90% of water consumption (FAO, 2012). It has been estimated that the distribution efficiency of irrigation conveyance systems across Jordan in 2013 was 87% (MWI, 2013b).

In terms of domestic water consumption, houses expend most water usage on bath, shower, washing machine, irrigated yards, and leaks (Jacobs and Haarhoff, 2007). This means that significant domestic consumption is of non-potable water. The peak daily outdoor water demand corresponds more closely to rainfall frequency rather than rainfall amount (Adamowski, 2008).

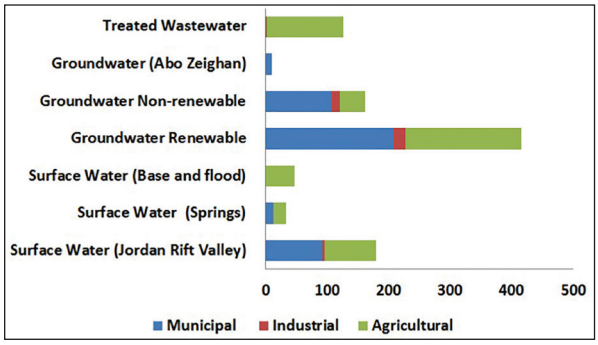

Figure 2. Main available water resources: surface water resources including base and flood, springs and Jordan Rift Valley, groundwater resources including Abo Zeighan aquifer, renewable and non-renewable aquifers, and treated wastewater. The main allocations of each resource to municipal, agricultural and industrial usages in MCM (million cubic meters), source (MWI, 2016d)

An estimate of the water budget of the Zarqa River Basin showed that the annual rainfall is lost as evapotranspiration (73.73%), infiltration (21.20%) and direct runoff (3.86%) (Shatnawi et al., 1999). It has been suggested that water supply systems in Jordan may also be characterised by high rates of loss (Table 1) (MWI, 2013a). Latest estimations by MWI (2016g) showed that the volume of supplied water for drinking purposes is equal to 126 L/day per capita, compared to the billed water volume of 59 L/day per capita; suggesting high waste and inefficiencies in water supply system.

Table 1. Supply, sold and wasted water volumes for drinking purposes during water years 2008-2014. The difference between water volume supplied through conveyance systems and water volume billed to consumers generates the wasted water volume (non-revenue water) in cubic meters; source: (MWI, 2010); (MWI, 2012); (MWI, 2013a); (MWI, 2016d).

	Water Supply (into distribution system) (m^3)	Water Sold (billed to consumers) (m^3)	Non-revenue water amount (m^3)	Percent of wasted (%)
2008	332410250	192400200	140010050	42%
2009	335500100	195210114	140289986	42%
2010	342500100	199500100	143000000	42%
2011	340500600	201100500	139400100	41%
2012	345616340	182424522	163191818	47%
2013	374742031	195632169	179109862	47%
2014	428100000	198800000	229300000	54%

Molden (1997) pointed out «water that is being lost is not always necessarily wasted.» Knowing the main drivers of water loss, however, are essential to identify best practices for avoiding non-revenue water. Van den Berg (2015) investigated the factors that affect high loss rates through leakage and identified the condition of the water supply system, defective water management, climate, topography, and high costs of maintenance as key contributing factors. For Jordan, non-revenue water may be the result of the considerable disorganized hydraulic infrastructure and planning. In other words, water losses could be due to leakages whether from defective pipes, meters and tanks and/or water theft. The large number of prosecutions for water theft suggest illegal use of irrigation water is widespread; there were 2688 cases in 2014 (MWI, 2014). Still, limited research on water losses in Jordan, in addition to the lack of leakage records and literature

on real and apparent water losses, means that the problem has been over- or under-estimated. Measures being used in Europe suggest best management practises would prioritize quantifying and managing water leakage (Lambert et al., 2014). In particular, determining whether losses are due to the distribution system and service connections or to variability in inflow rates is critical (Lambert et al., 2014).

Managing these challenges in Jordan has led to a number of initiatives. New water plans suggest renovation of the ageing water distribution systems and development of detailed non-revenue water reduction plans. There is also significant effort aimed at engaging local communities, groups and institutions to achieve more efficient water usage (MWI, 2016d). The new water plans establish a target that the total water volume being sold to consumers will be just above 350 MCM by 2023, largely through reducing non-revenue water volume by 4% each year until 2018, and then by 3% annually through to 2023 (MWI, 2013c). These plans require investment of more than 7.8 billion USD including refugee backup plans and the Red Sea-Dead Sea Conduit (RS-DS; MWI, 2016d). In Table 2, water production and supply amounts for drinking purposes and per capita consumption regardless of the waste amounts due to leakage or infringements are shown.

Table 2. Water production and supply volumes for municipal uses and per capita allotments that fluctuating over water years (2003-2014) in MCM; sources: (MWI, 2010; MWI, 2012; MWI, 2013a; MWI, 2014)

Year	Water Production (MCM)	Water Supply (MCM)	Per capita consumption (Litre/day)
2014	428.1	339.2	172
2013	374.8	341.3	123
2012	345.4	339.1	145
2011	341.3	330.1	145
2010	339.2	327.7	147
2009	na	313.4	144
2008	na	na	na
2007	320.5	300.9	144
2006	298.2	286.3	139
2005	294.7	282.0	140
2004	287.0	275.8	134
2003	268.0	258.7	143

Regarding water use over sectors by time, it seems that competition among different sectors (as previously shown in Figure 1) for water has increased. Irrigation usage encroaches on the rights of domestic and potable usage since all systems must share the scarce available water. The new surface water utilization policy (MWI, 2016e) reallocates water shares among sectors based on the economic output per cubic metre of water consumed. Moreover, government has specified the maximum amounts of water usage in new buildings and settlements (MWI, 2016f). Decreasing agricultural water use will affect food production and food security in the face of a growing population with growing food requirements. These effects can be mitigated by improving water productivity in agriculture (Molden et al., 2003), with water savings prioritized for human use (Kassam et al., 2007).

4. Current Water Supplies

4.1. Surface Water Resources

Jordan has 15 surface water basins which drain into three different water bodies: the Dead Sea, the Red Sea and desert mudflats (Figure 3). The largest catchment by area is Hammad basin (19270 km^2) while the smallest catchment is the south side wadis of the Jordan River (434 km^2). Yarmouk basin has 39.3% of the total annual discharge from all basins followed by 9% sourced from the Zarqa basin. High annual rainfall is received by both catchments (375mm and 262mm, respectively). Only 50% of surface water is consumed with the remainder flowing in to wadis, springs and rivers. Surface water constitutes 65% of the available fresh water in Jordan (MWI, 2016e).

Jordan abides by international political treaties to provide specific water allocations and allowable storage to the Jordan River and its tributaries based on mean annual flow volume. Due to political conflicts, diversion schemes, drought and constructed dams; the mean annual flow volume of the Jordan River has declined over the last decades, decreasing the allotments to each neighbouring country (Comair et al., 2012; UN-ESCWA&BGR, 2013). Although Jordan possesses 40% of the Jordan River basin and receives 36% of the total precipitation into the basin, Jordan receives only 100 MCM via the King Abdullah Canal (0.1% of the total withdrawal amount from the basin) due to high losses through evaporation (Comair et al., 2012). The King Abdullah Canal is fed by the Yarmouk River and some of the water is sourced from Lake Tiberias, the wadis of Arab and Ziqlab, and the Mukheibeh wells. Flow in the Yarmouk River is decreasing as a result of Syrian upstream abstractions by 25 constructed dams, with discharge declining from 430 MCM in 1970 to 260 MCM in the early 1990s (MoEnv, 2006).

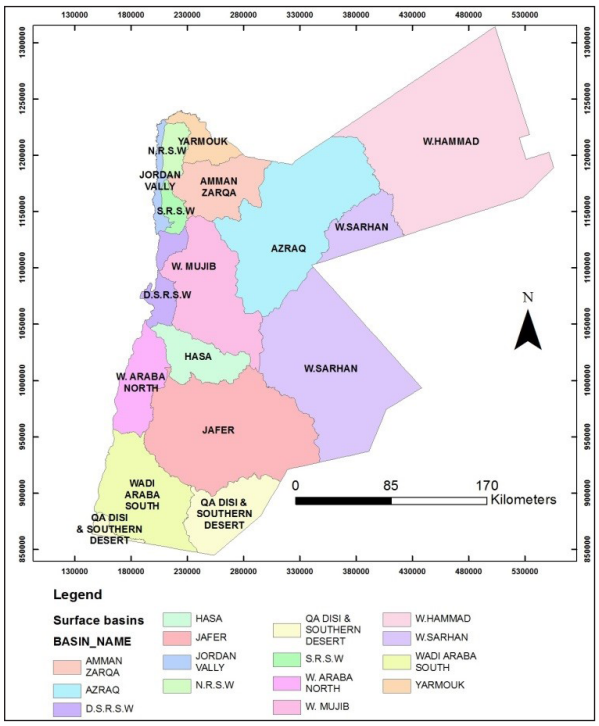

Figure 3. Jordan 16 surface water basins; (source, the Ministry of Water and Irrigation, Directorate of Water Studies, 2017)

The total capacity of large dams in the Jordan Valley is 330 MCM, with small dams and excavations storing approximately 111.43 MCM. King Talal Dam is the largest dam (86 MCM), harvesting the flow of Zarqa River for agricultural and industrial use .The Al-Wala dam (15.12 MCM), Al-Mujib dam (10.34 MCM) and Al-Tannour dam (5.38 MCM) are used for multiple purposes. Eighteen desert dams have been constructed for livestock and artificial groundwater recharge with a total capacity 31 MCM (MoEnv, 2006).

4.2. Groundwater Resources

Jordan has 12 main groundwater water basins (Figure 4). Eighty percent of groundwater of Jordan is contained within three aquifers; Disi, Amman-Wadi Es Sir aquifer and the Basalt aquifer (El-Naser, 2012). Groundwater contributes approximately 60% of water for all uses (79% of GW supplies for municipal uses) (MWI, 2016c). Groundwater bodies are classified as renewable and non-renewable. Geologically, groundwater aquifers are basalt bedrock, carbonate (e.g., Amman) or sandstone (e.g., the Ram aquifer). Unconsolidated aquifers also occur in riverine deposits, such as in the Jordan Valley. Depth of aquifers also varies, alluvial deposits are considered to be shallow aquifer, while Hummar aquifer exemplifies an intermediate aquifer, and Kurnuba deep aquifer (Jassim et al., 2015).

The largest groundwater extractions occur from the Disi- Mudawwara Basin (approximately 125 MCM/Year (MoEnv, 2006)). Due to over-abstraction, depression of the water level from 0.1m to 1.31m has occurred (MWI, 2014). In comparison, the Wadi Araba Basin, which yields 3.5 MCM/Year (MoEnv, 2006), has only recorded a water level decline of 0.46m (MWI, 2014). Most groundwater aquifers in Jordan are being over-pumped; the abstraction rate is higher than the safe yield except for the Hammad Basin and Sirhan Basin where abstraction is aligned to the safe yields. The Yarmouk (59 MCM), Amman-Zarqa (154 MCM), Dead Sea (71 MCM), and Azraq basins (80 MCM) are all considered over-extracted. Although the Jafr basin has a large catchment area (12710 km^2), it yields only 27 MCM due to low annual rainfall (45 mm) (MoEnv, 2006). Latest estimates by MWI (2016c) show that an additional 225 MCM of GW are pumped for agricultural use within highland plateaus. The total safe yield quantity available from renewable ground water is 275.5 MCM but the over-pumping volume is about 244.5 MCM according to Raddad (2005), with a government target to reduce to this 156 MCM in 2016 (MWI, 2016d).

Quantifying groundwater recharge rates is essential to determine the natural renewable component of any aquifer by precipitation and it has been estimated that 3.3% of the total rainfall groundwater recharge (Margane et al., 2002). A study of the Hasa basin water balance (Abu-Saleem et al., 2010) revealed that only 15.4% and 0.64% of the effective precipitation annually contributed in generating groundwater recharge and surface runoff, respectively, while the remainder was lost as evapotranspiration. Likewise, another study determined the recharge rate of the Zarqa Basin (Schulz et al., 2013) to be approximately 21.0mm annually.

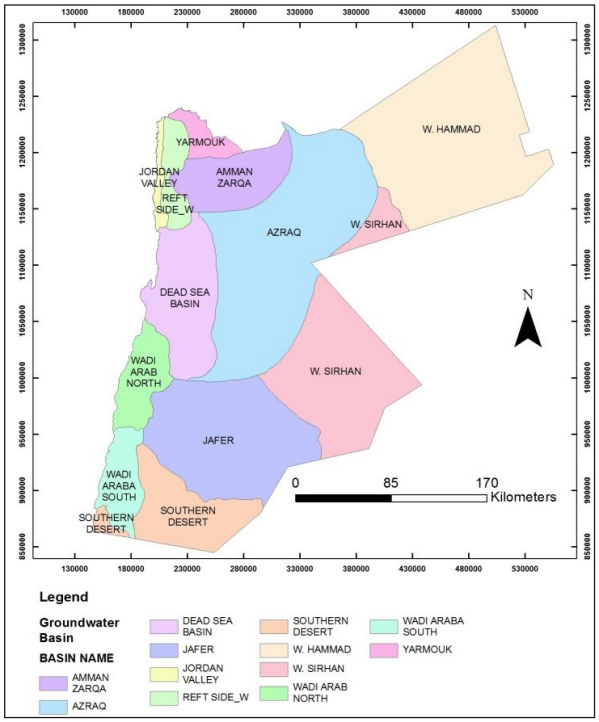

Figure 4. The twelve main groundwater basins of Jordan (The Ministry of Water and Irrigation, Directorate of Water Studies, 2017)

4.3. Treated Wastewater

Treated wastewater and brackish water are non-conventional resources which can be utilized for industrial and agricultural purposes. The high salinity content of reclaimed wastewater is the main limiting factor for agricultural use (Ammary, 2007). According to MWI (2016d), 125MCM of treated water is produced for agricultural use annually from 137 MCM of wastewater. Desalinization provides 50 MCM from brackish aquifers for urban use. Since the generated volume of wastewater in 2015 was 140 MCM, the 11 million projected population is estimated to produce 240 MCM by 2025 (MWI, 2016d); but unevenly distributed across the country (MWI, 2013a).

5. Water Availability and the Potential Risks

A number of factors influences the water availability, including population distribution, density, and growth rates, patterns of urbanisation and services to urban centres, climate variability and change, and a range of other anthropogenic impacts including land-use change (Gleick, 1993; Heathwaite, 2010; Molden, 1997; Wada et al., 2010; Pla et al., 2016). In order to effectively manage pressures on water supplies, there is a need to determine the separate and interacting effects of all relevant factors influencing water availability (Jooste, 2000).

5.1. Population Growth

Jordan has high rates of population growth due to both intrinsic factors and immigration. According to the latest official census (DoS, 2016), Jordan›s population is estimated to have reached 9,531,712, with only 69.4% of people being born in Jordan. The total population growth rate between the years 2004 and 2015 was approximately 5.3%. Amman the capital has the largest population with 4 million, with other major urban centres at Irbid and Zarqa (DoS, 2016). It is

not only lifestyle and developmental changes that have caused water scarcity in Jordan (Schutte and Pretorius, 1997; Kassam et al., 2007; O›Brien, 2014) but also population growth. Increased population presents significant challenges for water management in urban areas, compounding the effects of environmental conflicts and resource deterioration (Toppo, 2014). This leads to inequities in access to water and water provided services. Jordan also faces considerable population pressure due to the influx of refugees from the surrounding politically unstable countries. Over 1,400,000 Syrians have entered the country (DoS, 2016) since 2011 and have been in competition with locals for their scarce water resources and exacerbated water shortages. There have been significant challenges in supplying water to refugees; MWI (2013c) estimated that each person in the Zaatari refugee camps is supplied with 37 L/day where the required amount is 50 L/day/person according to WHO standards. This rapid population growth has lift inadequate time to align with sustainable consumptive water rates, which its demand depending on alternate external supplies (Fischer and Heilig, 1997).

5.2. Change in Climate

At the global level, the effects of climate change on fresh water resources have been analysed by IPCC (Shaman et al., 2004; Van den Berg, 2015). Oki and Kanae (2006) estimated that the effect of sea level rise and the mixing of saline sea water with groundwater aquifers would have profound effects on quality and quantity of groundwater resources. Projections through to 2090 show that populous regions will be susceptible to high water stress globally due to decreased water availability (Arnell, 2004). These effects may be compounded by changes in availability of freshwater as a consequence of changes in rainfall patterns and higher evapotranspiration rates (Oki and Kanae, 2006; Van den Berg, 2015).

Threats to water availability due to climate change include higher intensive precipitation which may lead to surface flooding and increased surface runoff with lower rates of groundwater recharge. Climate change may also affect drought frequency and consequently effect water demand and aquatic ecosystems. Long-term observations on eastern Mediterranean climate zones (Solomon et al., 2007) indicate warming of surface air temperature by 1-3ºC. Effects on precipitation, distribution and variability are as yet uncertain. Climate change has a perceptible effect on water availability and as a consequence affects the whole hydrological cycle (Morrison et al., 2009; Quevauviller, 2010; Quevauviller, 2011).

The effects of changing climate are exacerbated by Jordan›s location in the north mid-latitude climate between the subtropics and the equator. Previous studies have clearly shown declining rainfall of approximately 1.2 mm/year, although this is spatially variable across Jordan (Rahman et al., 2015). The western side of Jordan has had an increase in daily rainfall of approximately 2-3%, mostly in north western parts (Rahman et al., 2015). In terms of temperature over the last 30 years, Donat et al. (2014) noted drying trends in eastern parts of Arab countries due to the stronger effect of ENSO. The latest projections by MoEnv (2014) conclude that Jordan will experience warmer summers, drier winters, drier autumns, more droughts and more heat waves, but no clear trend towards increased precipitation or wind intensity. Therefore, MWI (2016b) forecasted a decrease in water availability which will be severe after 2040 due to climate change.

MoEnv (2009) concluded that water availability and quality will be the main stress on Jordan›s society and the environment due to climate change. These consequences would be compounded by the effects of demographic growth (Sowers et al., 2011). The variability of water flows in the Jordan and Yarmouk Rivers is predicted to increase. For example, the Jordan River flow was 620 MCM but recently decreased to 270 MCM (Verner, 2013; Verner et al., 2013). Climatic change might cause an increase in desertification, exacerbate inputs and withdrawals of water, decrease water availability, and thus; contribute to future water deficits as much as the human-driven increases in water demand (Verner et al., 2013; MWI, 2016b). Down-scaled General Circulation Models across all climate scenarios predict water demand will increase for all sectors, whilst water supply will decrease (MoEnv, 2014). Subsequently, the annual water deficit is predicted to reach 769 MCM by 2050 (MoEnv, 2014). Other studies have also highlighted the susceptibility of Jordan to more frequent drought periods (Menzel et al., 2007; Shatanawi et al., 2013).

Few studies have been conducted to assess the expected effects of climate change on water resources in Jordan. Abu-Allaban et al. (2015) used incremental climate scenarios to assess the influence of climate change on water resources of the Mujib basin. The study concluded that the main driver of decreasing runoff is air temperature. A decrease in rainfall and surface runoff to about 20 to 50% during the dry seasons was predicted. Another study assessed the effect of climate change on water resources in the Yarmouk and Amman-Zarqa Basins (Hammouri, 2015). The study predicted future possible change in temperature from +1 to + 4 ºC, and in precipitation from -20% to +20% while monthly surface runoff will decline by 41% by 2049; except during February when it will witness an increase by +1.7% and -21.9% for Yarmouk and Amman - Zarqa Basins, respectively (Abu-Allaban et al., 2015).

In terms of climate variability, the timing and quantity of the rainfall season is characterized by yearly and seasonal fluctuations of rainfall and uneven distribution across Jordan. For a country with a small area, like Jordan, non-uniformity of stream flow increases in time and space. The variability of flow depends on moisture and water resources including precipitation (Gleick, 1993). The higher the aridity index (dryness index), the greater variability of water resources occurs annually and seasonally across the region.

5.3. Human Use

5.3.1. Groundwater Over-Abstraction

Due to its importance, availability and management of groundwater resources have become a key issue in Jordan. Global groundwater depletion is a major issue globally; ground water volume extracted worldwide was $126x10^3$ MCM per year in 1960 and exceeded $283x10^3$ MCM per year in 2000 (Wada et al., 2010). In some countries, groundwater is considered to be a non-renewable resource (Kalf and Woolley, 2005). Characteristically, in Jordan, groundwater is the most

reliable, accessible, and cheapest freshwater resource which makes it the favoured supply especially for urban and rural use. This has led to some aquifers being over-exploited. Overexploitation is defined as intensive groundwater use, either planned or unplanned, which has negative effects (Villarroya and Aldwell, 1998), or where the abstraction rate is greater than the recharge rate (Custodio, 2002). The end point of over-abstraction is the depletion of groundwater storage during a specific time and depends on aquifer size, storage and permeability (Custodio, 2002).

Since groundwater is the main water resource in Jordan, in some water basins abstracted volumes have sometimes exceeded safe yields threefold (Raddad, 2005; Al-Zyoud et al., 2015). Over-exploitation of aquifers can lead to a reduction or cessation of surface-water discharges. In Jordan, it is expected that most groundwater dependent creeks will be exhausted within the upcoming 20 years (Salameh, 2008). Therefore, over-abstraction of groundwater aquifers beyond their annual rechargeable quantities constitutes a major threat to future water availability and resource sustainability.

A simulation of average groundwater recharge for the Jordan River basin has estimated rates to be about (2-20) mm /per year while the rest of the Jordanian groundwater aquifers are estimated to be recharging at (0-2) mm per year (Wada et al., 2010). The south eastern aquifers of Jordan are particularly vulnerable to over-extraction, as they have a high groundwater footprint/area ratio (GF/A), indicating ecosystems which are strongly dependent on groundwater (Gleeson et al., 2012).

Previous research has indicated that most of groundwater resources in Jordan are already depleted beyond their safe yields (El-Naqa et al., 2007). Some groundwater basins have been lost; for example, Dhuleil and Agib (Salameh, 2008). Studies using remote sensing to measure cumulative drawdown of water level for the Amman-Zarqa basin have shown a depletion of 1.6-2.0 m/year (El-Naqa et al., 2007; Al-Zyoud et al., 2015). In that system, the basin safe yield is considered to be around 88 MCM, while the current pumping rate is approximately 156 MCM, with an estimated depletion volume of about 69 MCM by the end of 2013 (MWI, 2013b). Al-Zyoud et al. (2015) called for urgent changes in groundwater management practices to reduce deterioration of groundwater resources. Such effective management requires adequate information about the geology of aquifers and soil layer characteristics (Datta and Kourakos, 2015; Tessitore et al., 2016).

Overconsumption of groundwater has threatened not only the quantity but also the quality, especially shallow aquifers and moderately steep areas (Al Kuisi et al., 2014; Jassim et al., 2015). The main source of groundwater contamination in the Amman-Zarqa basin is contaminated water percolating into aquifers. Nitrate and selenium concentrations reached 157 mg/L and 580 µg/L, respectively, in some aquifers (Al Kuisi et al., 2014). Contamination sources ranged from very low hazard sources, such as from excavations and low intensity farming, to oil refinery waste. Wadi As-Sir and Kherbit As-Samra wastewater plants are located in areas that may contaminate groundwater. Another example of groundwater quality deterioration is at Disi and As-Swwan aquifers as a consequence of fertilizers and biocides from agriculture uses (Jassim et al., 2015).

5.3.2. Urbanization

Land misuse, urbanization, and land settlement patterns are important pressures on water availability (Song et al., 2016; Liu and Long, 2016). In semi-arid regions, large rivers have dried up because of reducing flows due to urbanization (Guo et al., 2000; Rosegrant et al., 2002). In the eastern and southern Mediterranean countries urbanisation is occurring five times faster than it is in Europe, threatening reliable supplies of drinking water (Shatanawi et al., 2007). Urban expansion affects surface runoff and stream discharge, in terms of quantity, the timing and frequency of high flows and quality (Burns et al., 1998), in addition to influences on the sustainability of water resources in the transitional urban areas (Grafton et al., 2015).

Over the last decades, Jordan has been developing major cities through expanding and modifying urban areas, and the process of urban sprawl is continuing. Urbanization is characterised by development of ‹hard› infrastructure, such as roofs, roads and divided highways, creation of landfills and waste dumps, and alteration to land cover for housing, industry, transport infrastructure and recreation areas. A typical example of such urbanization that caused desertification and biodiversity degradation is in the woodlands of northern Jordan. The northern woodland area has decreased from 30,895 ha in 1956 to 19,080 ha in 1987 (MoEnv, 2006). Urbanization has changed the quality of soils in the small areas that are suitable for vegetation (MoEnv, 2006). Regardless of land-use regulation, housing developments, including those based on illegal occupation of land have increased. This problem has been exacerbated by increased migration with major impacts on urban expansion and land tenure (Douglas, 2006). Supplying urban areas with services, such as water is a major challenge for administrators.

Although only 40% of Jordan›s agricultural lands are irrigated areas (about 102.5 million hectares) 90% of agricultural products are produced in these areas (MWI, 2016d). ACS (2007) recorded that in 1975 the total area of cultivated land in Jordan was 975000 hectares; with 82500 hectares as irrigated land. In 1997, the total area of irrigated and rain-fed cultivated lands had decreased due to urbanization to 187500 hectares and 575000 hectares, respectively. DoS (2014) estimated the total cultivated area was 260600 hectares in 2002 and 187200 hectares in 2007. In 2014, the total cultivated areas were 273950 hectares, which included 105050 hectares of irrigated land and 168900 hectares considered as rain-fed areas. Alsaaideh et al. (2012) showed that during the period from 1987 to 2005, urban areas increased by 220 km^2. This was largely at the cost of loss of natural vegetation (8.7 km^2) bare lands (101.4 km^2), forest (12.7 km^2), and agricultural land (98.9 km^2)

Menzel et al. (2009) applied a hydrological model with a land use/cover module to the Jordan River Basin (northern part of Jordan, Palestine and Israel), in order to determine available water (runoff and groundwater recharge only) and irrigation demands in the region. They found that using an assumption of no economic development and steady state political conditions, the population growth for Jordan would lead to widespread loss of natural vegetation by 2050, and an increasing shortfall in meeting water needs.

6. Interactions between Drivers

While there is a growing understanding of the effects of single pressures on water availability, there is a need at national scales to understand the combined and interacting effects of multiple pressures. For example, changes in land use have multiple effects on water including; deterioration of groundwater quality due to agrochemicals percolating into aquifers (Jasem and Alraggad, 2010), fertilizer contamination, salinization and changes in rates of runoff and recharge. They are also likely, however, to be associated with changes in population, demands for potable water and risk of illegal abstraction. These effects are then overlain by the consequences of climate change. Collectively there are multiple complex interactions between all of these pressures.

Human activities, unplanned urban growth, land misuse and concrete areas, interactively prevent rainfall reaching the ground and hence being infiltrated to recharge groundwater aquifers (Fikos et al., 2005). In turn, this combination cause deterioration of groundwater quality and overexploitation of groundwater resources (Datta and Kourakos, 2015). It is not only that the extreme-hazards of contamination caused by industries is considerable (Al Kuisi et al., 2014) but also the effects of growing population on groundwater quality. In Jordan, the wells that are situated directly beneath Zaatari Camp are contaminated due to the infiltration of discharges toward the saturated zone of groundwater wells (MWI, 2016c).

Physical characteristics of soil and land cover affect the amount of evaporation, surface runoff and hence the groundwater recharge. These effects also link climate influences, surface runoff, evaporation, groundwater recharge and abstraction. An assessment of the effects of climate change on the recharge of central western aquifers in Jordan revealed that increasing the temperatures by 1 °C and 2 °C will cause a decrease in groundwater recharge by 11% and 23%, respectively (Jassim and Alraggad, 2009), while the change to precipitation, decreasing by 10% and 20%, will result in decreasing groundwater recharge by 24% and 48%, respectively.

An analysis of the effects of climate change, population growth and increasing migration on water resources showed that Jordan is classified as a high water stress nation regarding the population growth and the medium to high stress regarding the climate change. This means that population and economic growth will drive water demand and supply rather than a changing climate (Vörösmarty et al., 2000). Hoff et al. (2011) compared the changes in future water demands in the Jordan River basin under five different scenarios combining climate change with socio-economic and technological factors. Their study showed that socio economic factors and the climate change projections will significantly affect the future unsatisfied water demands until 2050. The study expects that unsatisfied water demands within the basin will exceed 500 MCM due to socio-economic development compared to 1600 MCM by 2050. In addition, 1000 MCM of unsatisfied demands are caused by climate change (MWI, 2016b).

These factors may interact continuously through time or discretely depending on the complexity of the water basin and its conditions. Although numerous water supplies are used to meet water needs, the combined effects of these multiple interacting pressures can result in deterioration of water resources and cause water scarcity (Figure 5).

7. Future Water Supplies

The International Water Management Institute issued a report in 1998 that estimated the water

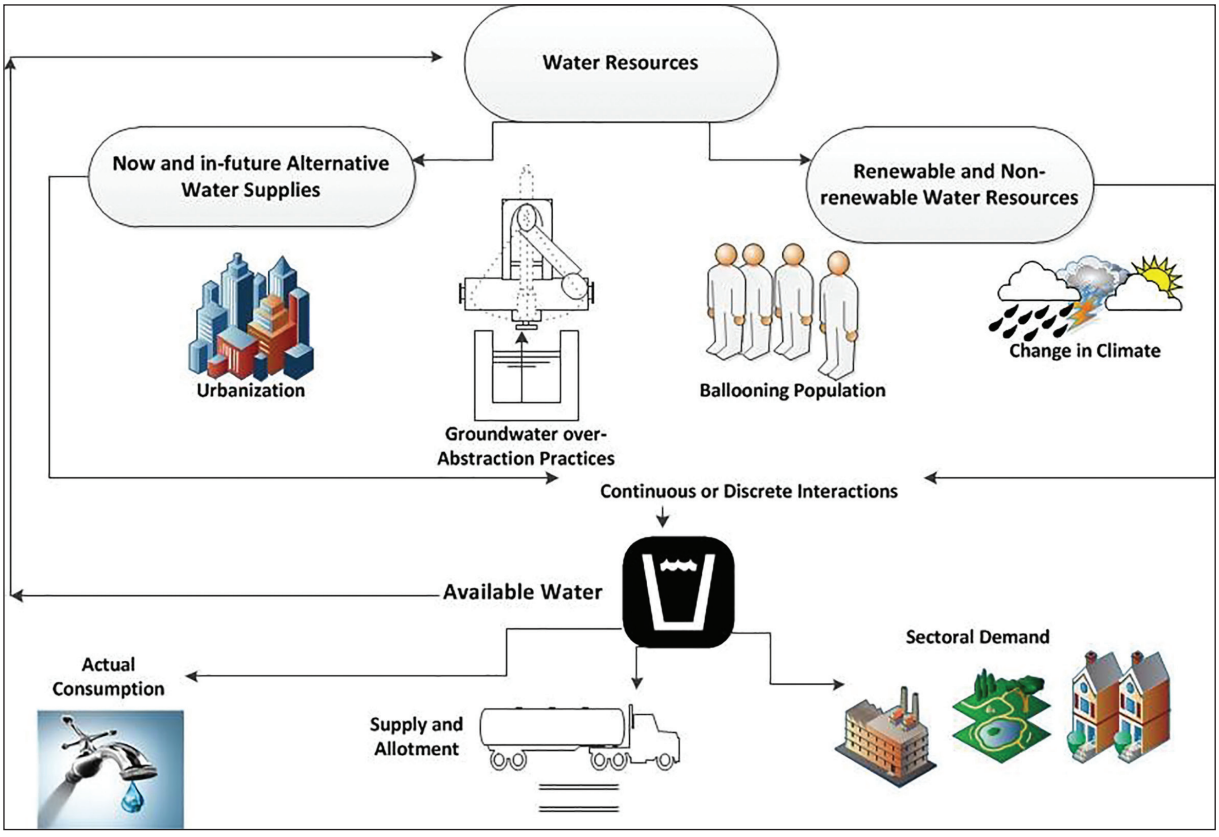

Figure 5. Schematic description of interacting pressures affecting water availability

scarcity of 118 countries by simulating annual total water withdrawals through the period 1990 to 2025 (Seckler, 1998). Jordan is one of the countries identified as being ‹water scarce›. The report concluded that Jordan should reduce withdrawals of water for irrigation in order to meet domestic and industrial water needs. By 2025, the report predicted that projected population growth will be 283% which will restrict the renewable water supply to 73 m^3 per capita and the total water withdrawals will equal 292% of the available water resources.

During 2016 to 2025, a new water strategy will be implemented in Jordan to increase water supplies for different uses (Table 3). This will provide about 187.5 MCM for drinking purposes by setting up new wells, deep aquifers, dams, desalination plants, and household water harvesting. The additional gross amount of water will be about 552.5 MCM (MWI, 2016d).

Table 3. Jordan future water supplies and its contributions to national water budget in total volume equals to 552.5 MCM (MWI, 2016a)

Additional Water Supplies Projects	Supply volume (MCM)	Purposes
Setting up new wells, deep aquifers, dams, desalination plant, and water harvesting techniques	187.5	For potable uses
RS-DS project	235	For potable uses
Dams, dams expansions as in Wala and Mujib Dams, water harvesting setups	36.35	For different uses especially flood regulation and irrigation
Treated wastewater plants – expansion projects; for examples: Samra & Southern Amman WWTP	94	Not specified

Currently, projects, such as the Disi groundwater conveyor from the Disi aquifer, provide the Amman annually with 100 MCM conveying good quality water via a 325 km (El-Naser, 2009; Al-Amir et al., 2012). Recently, the Jordanian government has decided to utilize Disi water for drinking water rather than irrigation in order to satisfy water demands (Salameh et al., 2014). Other projects suggested by MWI (2009) include extracting water from Jafr, Hisban and Lajoun aquifers. This will provide additional amounts of non-renewable groundwater of 9% of the total water resources by the year 2022. Also, building and expanding wastewater plants will provide 15% of the total water resources used for irrigation and industry purposes. Moreover, desalination will supply 520 MCM of non-conventional water by 2022, for example, desalination of brackish water from Hisban Kufranjeh Dam and Wahdah Dam.

Another major project, the main mega Conduit (RS-DS), which connects the Red Sea with the Dead Sea, is still under construction. This project will tackle the rapid drop in water levels of the Dead Sea due to evaporation rates and increasing temperatures (Oroud, 2011). Water from the Red Sea will be desalinised, producing drinking water and hypersaline brine which will be used to augment the Dead Sea. Through this resource-sharing system, the amount of water allocated to Jordan will be around 580 MCM per year from the canal. The main obstacle for the project, however, is the financial cost (10 billion US dollars) (MoEnv, 2009). According to Al-Salihi and Himmo (2003), seawater desalination seems to be the most suitable development option for Jordan.

The Wahdah Dam is a bilateral project between Syria and Jordan and was built to generate hydropower as well as to provide irrigation water for both countries. The dam has been constructed in order to catch rainfall within the Yarmouk river basin which receives 2065 MCM of rainfall on average. Although the dam capacity is 225 MCM/year, the maximum stored volume recorded in 2014 was only 70 MCM/yr. The reasons behind the low annual level of the Wahdah dam could be due to drought and dams retaining water from Yarmouk Wadis and groundwater abstraction upstream (UN-ESCWA&BGR, 2013).

The view of Gleick (2003) is that, in Jordan, gains from seeking new sources of water supplies will be insignificant in comparison with improving water use by implementing water efficiency approaches. For example, in Israel, Australia, New Zealand and Japan, significant water savings have been gained by the introduction of dual flush toilets.

8. Quantitative Analysis of Potential Risks and Reliability of Undertaken Measures

Despite major reforms, Jordan is still encountering a significant water crisis. This requires a strategic approach to water resources management including the use of water pricing schemes, water trading and renovation of old water systems and restructuring of stakeholders. Future water plans will require detailed quantitative information as shown in (Figure 6).

This present review has shown that the future projections of water use, supply and demand might not take various challenges into consideration. The new water allocation initiatives will require data on socio-economic factors and environmental and technological assumptions. The new water allotments will be based on the following assumptions:

1. Domestic water demands needs to meet 80-120 L/day for locals as well as for refugees;
2. A constant annual population growth for all residents (1.94%) except for refugees (3%),
   refugees are resettled in the country;
3. Seasonality of water demand during summer (additional 17% of water amount);
4. Potential to reduce non-revenue water volume by 4% each year until 2018, and then by 3% annually through to 2023;
5. Changes in patterns of irrigation; irrigation demand is increasing in the Jordan valley and decreasing in highlands and therefore the irrigation future demands are constant by (700) MCM through the next 10 years;
6. The effects on consumption of changing demographics such as increasing family members in a single house are taken into consideration; and
7. The additional of annual 2% water amount for abrupt changes.

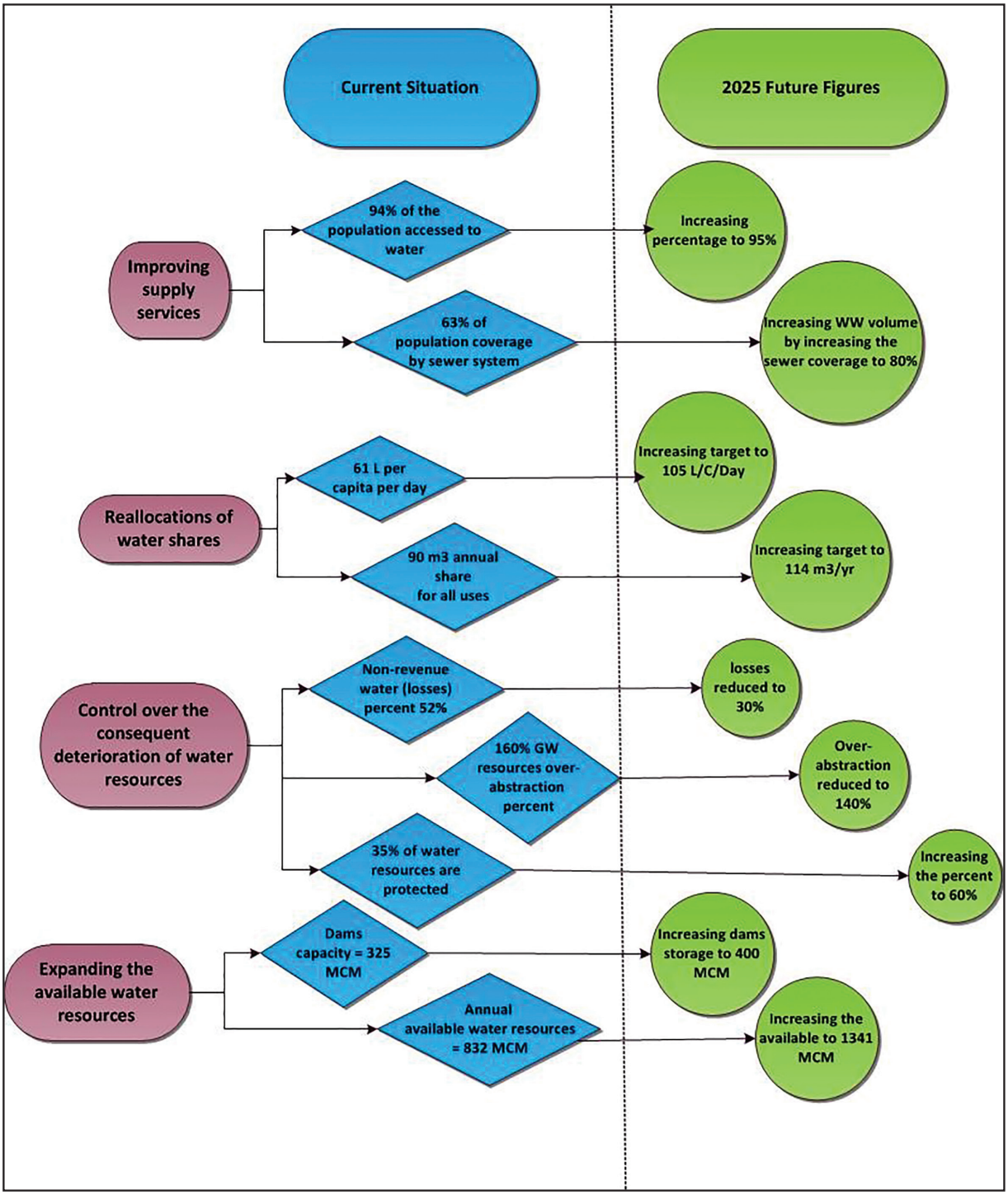

Figure 6. Quantitative analysis of potential risks and reliability of water supply based on water allotments. Reallocation of water predicts that the total available resources will provide 1459 MCM, where the total demands will be 1548 MCM, and hence, 89 MCM is the expected deficit (MWI, 2016g)

Conclusions:

It appears that current initiatives will unlikely guarantee water security. Certain estimates of water quantity, use and availability suffer from significant concerns; for example, errors in measurements and calculations that aligned with data scarce region, consequent over-allocation of water shares, uncertain predictions, complexity of water system modelling issues, and limited research on the factors affecting available water volumes.

Current and future water planning for Jordan has not rigorously tested the consequences of all major pressures and their cumulative and interactive effects. Since water scarcity and the consequent deterioration of water resources are major issues that require not only thematic research but also reliable applied outcomes, there is an urgent need for investigation of these pressures. The latest studies have focused on a single hydrological assessment and water balance of single water unit i. e. the use of a one-off water accounting method. Research is needed to identify water accounting measurement components in the light of water quantity, occurrence and intensity. Those measurements need to take into consideration the differences between supply and demand, and the consequently effects on

users, sustainability of resources and hydrological cycle.

The concept of water quantification provides a useful approach within which the response to main pressures changes can be studied. This approach requires adequate information on multiple pressures and their interactions at the regional level especially in the long term. The emphasis on one pressure within short period would limit the readiness for sudden changes in other pressures.

References

[1] ABABSA, M., DUPRET, B. & DENNIS, E. 2012. Popular Housing and Urban Land Tenure in the Middle East: Case Studies from Egypt, Syria, Jordan, Lebanon, and Turkey, American University in Cairo Press.

[2] ABABSA, M. & KOHLMAYER, C. 2013. Atlas of Jordan: history, territories and society, Inst. Française du Proche-Orient.

[3] ABU-ALLABAN, M., EL-NAQA, A., JABER, M. & HAMMOURI, N. 2015. Water scarcity impact of climate change in semi-arid regions: a case study in Mujib basin, Jordan. Arabian Journal of Geosciences, 8, 951-959.

[4] ABU-SALEEM, A., AL-ZU›BI, Y., RIMAWI, O., AL-ZU›BI, J. & ALOURAN, N. 2010. Estimation of water balance components in the Hasa basin with GIS based WetSpass model. Journal of Agronomy, 9, 119-125.

[5] ACS 2007. Alrai Center for Studies. Arabic Article: SEMINAR - Agricultural sector in Jordan.

[6] ADAMOWSKI, J. F. 2008. Peak daily water demand forecast modeling using artificial neural networks. Journal of Water Resources Planning and Management, 134, 119-128.

[7] AL-AMIR, S. M., AL-HAMARNEH, I. F., AL-ABED, T. & AWADALLAH, M. 2012. Natural radioactivity in tap water and associated age-dependent dose and lifetime risk assessment in Amman, Jordan. Applied Radiation and Isotopes, 70, 692-698.

[8] AL-JAYYOUSI, O. R. 2012. Islam and sustainable development: new worldviews, Gower Publishing, Ltd.

[9] AL-SALIHI, A. H. & HIMMO, S. K. 2003. Control and management study of Jordan›s water resources. Water international, 28, 1-10.

[10] AL-ZYOUD, S., RÜHAAK, W., FOROOTAN, E. & SASS, I. 2015. Over Exploitation of Groundwater in the Centre of Amman Zarqa Basin—Jordan: Evaluation of Well Data and GRACE Satellite Observations. Resources, 4, 819-830.

[11] AL KUISI, M., MASHAL, K., AL-QINNA, M., HAMAD, A. A. & MARGANA, A. 2014. Groundwater vulnerability and hazard mapping in an arid region: case study, Amman-Zarqa Basin (AZB)-Jordan. Journal of Water Resource and Protection, 6, 297.

[12] ALSAAIDEH, B., AL-HANBALI, A. & TATEISHI, R. 2012. Assessment of land use/cover change and urban expansion of the central part of Jordan using remote sensing and GIS. Asian Journal of Geoinformatics, 11.

[13] AMMARY, B. Y. 2007. Wastewater reuse in Jordan: Present status and future plans. Desalination, 211, 164-176.

[14] ARNELL, N. W. 2004. Climate change and global water resources: SRES emissions and socio-economic scenarios. Global environmental change, 14, 31-52.

[15] BELDA, M., HOLTANOVÁ, E., HALENKA, T. & KALVOVÁ, J. 2014. Climate classification revisited: from Köppen to Trewartha. Climate research, 59, 1-13.

[16] BENGOECHEA, E. P. 2013. Water scarcity and climate change impact and vulnerability in irrigated agriculture in Mediterranean river basins. Agronomos.

[17] BURNS, D. A., MURDOCH, P. S., LAWRENCE, G. B. & MICHEL, R. L. 1998. Effect of groundwater springs on NO3− concentrations during summer in Catskill Mountain streams. Water Resources Research, 34, 1987-1996.

[18] COMAIR, G., MCKINNEY, D. & SIEGEL, D. 2012. Hydrology of the Jordan River Basin: Watershed delineation, precipitation and evapotranspiration. Water resources management, 26, 4281-4293.

[19] CUSTODIO, E. 2002. Aquifer overexploitation: what does it mean? Hydrogeology journal, 10, 254-277.

[20] DATTA, B. & KOURAKOS, G. 2015. Preface: Optimization for groundwater characterization and management. Hydrogeology Journal, 23, 1043-1049.

[21] DONAT, M., PETERSON, T., BRUNET, M., KING, A., ALMAZROUI, M., KOLLI, R., BOUCHERF, D., AL-MULLA, A. Y., NOUR, A. Y. & ALY, A. A. 2014. Changes in extreme temperature and precipitation in the Arab region: long-term trends and variability related to ENSO and NAO. International Journal of Climatology, 34, 581-592.

[22] DOS 2014. DoS Yearbook. In: STATISTICS, D. O. (ed.). Amman- Jordan.

[23] DOS 2015. Jordan in Figures. In: STATISTICS, D. O. (ed.). Amman-Jordan.

[24] DOS 2016. The national population and housing census of 2015, Official Report. In Arabic In: STATISTICS, D. O. (ed.). Amman - Jordan

[25] DOUGLAS, I. 2006. Peri-urban ecosystems and societies transitional zones and contrasting values. Peri-urban interface: Approaches to sustainable natural and human resource use, 18-29.

[26] EL-NAQA, A., AL-MOMANI, M., KILANI, S. & HAMMOURI, N. 2007. Groundwater Deterioration of Shallow Groundwater Aquifers Due to Overexploitation in Northeast Jordan. CLEAN- WILEY-VCH Verlag GmbH & Co. KGaA, Weinheim, 35 (2), 156 – 166.

[27] EL-NASER, H. 2009. Management of scarce water resources: a Middle Eastern experience, WIT Press.

[28] EL-NASER, H. 2012. Jordan›s Precious Groundwater Resources Is the Term Sustainability Applicable under Extreme Water Scarcity Conditions? 5Th ACWUA Best Practice Conference (Utilities Perspective on Water Resources Management in the Arab Region). Muscat - Oman.

[29] FAO 2012. Coping with water scarcity: An action framework for agriculture and food security. Food and Agriculture Organization of the United Nations - Rome.

[30] FIKOS, I., ZIANKAS, G., RIZOPOULOU, A. & FAMELLOS, S. 2005. Water balance estimation in Anthemountas river basin and correlation with underground water level. Global nest. The international journal, 7, 354-359.

[31] FISCHER, G. & HEILIG, G. K. 1997. Population momentum and the demand on land and water resources. Philosophical Transactions of the Royal Society of London B: Biological Sciences, 352, 869-889.

[32] GLEESON, T., WADA, Y., BIERKENS, M. F. & VAN BEEK, L. P. 2012. Water balance of global aquifers revealed by groundwater footprint. Nature, 488, 197-200.

[33] GLEICK, P. H. 1993. Water in crisis: a guide to the world›s fresh water resources, Oxford University Press, Inc.

[34] GLEICK, P. H. 1998. Water in crisis: paths to sustainable water use. Ecological applications, 8, 571-579.

[35] GLEICK, P. H. 2003. Global freshwater resources: soft-path solutions for the 21st century. Science, 302, 1524-1528.

[36] GRAFTON, Q., DANIELL, K. A., NAUGES, C., RINAUDO, J.-D. & CHAN, N. W. W. 2015. Understanding and Managing Urban Water in Transition, Springer.

[37] GUO, Z., XIAO, X. & LI, D. 2000. An assessment of ecosystem services: water flow regulation and hydroelectric power production. Ecological Applications, 10, 925-936.

[37] HAMMOURI, D. N. 2015. Assessment of Climate Change Impacts on Water Resources of North Jordan. online presentation: Faculty of Natural Resources & Environment - The Hashemite University.

[39] HEATHWAITE, A. 2010. Multiple stressors on water availability at global to catchment scales: understanding human impact on nutrient cycles to protect water quality and water availability in the long term. Freshwater Biology, 55, 241-257.

[40] HOFF, H., BONZI, C., JOYCE, B. & TIELBÖRGER, K. 2011. A water resources planning tool for the Jordan River Basin. Water, 3, 718-736.

[41] IGLESIAS, A., GARROTE, L., DIZ, A., SCHLICKENRIEDER, J. & MARTIN-CARRASCO, F. 2011. Re-thinking water policy priorities in the Mediterranean region in view of climate change. Environmental Science & Policy, 14, 744-757.

[42] JACOBS, H. & HAARHOFF, J. 2007. Prioritisation of parameters influencing residential water use and wastewater flow. Journal of Water Supply: Research and Technology-AQUA, 56, 495-514.
[43] JASEM, A. H. & ALRAGGAD, M. 2010. Assessing groundwater vulnerability in Azraq basin area by a modified DRASTIC index. Journal of Water Resource and Protection, 2010.
[44] JASSIM, A. H. M., ALMOMANI, T. & ALHEJOJ, I. 2015. Groundwater Vulnerability for the Surface Outcropping Aquifers in Jordan. Journal of Environmental Protection, 6, 250.
[45] JASSIM, A. H. M. & ALRAGGAD, M. M. 2009. GIS modeling of the effects of climatic changes on the groundwater recharge in the central western parts of Jordan. Jordan J. Civil Eng, 3, 347-356.
[46] JOOSTE, S. 2000. A model to estimate the total ecological risk in the management of water resources subject to multiple stressors. WATER SA, 26, 159-166.
[47] KALF, F. R. & WOOLLEY, D. R. 2005. Applicability and methodology of determining sustainable yield in groundwater systems. Hydrogeology Journal, 13, 295-312.
[48] KASSAM, A., MOLDEN, D., FERERES, E. & DOORENBOS, J. 2007. Water productivity: science and practice—introduction. Irrigation Science, 25, 185-188.
[49] LAMBERT, A., CHARALAMBOUS, B., FANTOZZI, M., KOVAC, J., RIZZO, A. & ST JOHN, S. G. 14 years experience of using IWA best practice water balance and water loss performance indicators in Europe. IWA WaterLoss 2014 Conf., Vienna, Austria, 2014.
[50] LIU, Y. & LONG, H. 2016. Land use transitions and their dynamic mechanism: The case of the Huang-Huai-Hai Plain. Journal of Geographical Sciences, 26, 515-530.
[51] MARGANE, A., HOBLER, M., ALMOMANI, M. & SUBAH, A. 2002. Contributions to the Hydrogeology of Northern and Central-Jordan.
[52] MENZEL, L., KOCH, J., ONIGKEIT, J. & SCHALDACH, R. 2009. Modelling the effects of land-use and land-cover change on water availability in the Jordan River region. Advances in Geosciences, 21, 73-80.
[53] MENZEL, L., TEICHERT, E. & WEISS, M. Climate change impact on the water resources of the semi-arid Jordan region. Proc. 3rd International Conference on Climate and Water, Helsinki, 2007. 320-325.
[53] MOENV 2006. National Strategy and Action Plan to Combat Desertification 2006. In: ENVIRONMENT, M. O. (ed.). Amman - Jordan: UNDP.
[55] MOENV 2009. Jordan›s Second National Communication to the United Nations Framework Convention on Climate Change (UNFCCC). In: ENVIRONMENT, M. O. (ed.).
[56] MOENV 2014. MoEnv . Jordan›s Third National Communication on Climate Change. Amman-Jordan (Ministry of Environemnt)
[57] MOLDEN, D. 1997. Accounting for water use and productivity, Iwmi.
[58] MOLDEN, D., MURRAY-RUST, H., SAKTHIVADIVEL, R. & MAKIN, I. 2003. A water-productivity framework for understanding and action. Water productivity in agriculture: Limits and opportunities for improvement.
[59] MORRISON, J., MORIKAWA, M., MURPHY, M. & SCHULTE, P. 2009. Water Scarcity & climate change. Growing risks for business and investors, Pacific Institute, Oakland, California.
[60] MWI 2009. Water for Life. Jordan›s Water Strategy (2008-2022). In: DIRECTORATE, M. O. W. A. I. O. J.-A. A. M. (ed.). Amman-Jordan.
[61] MWI 2010. Ministry of Water and Irrigation, Jordan. Annual Report. Amman, Jordan: Ministry of Water and Irrigation - Awareness and Media Directorate
[62] MWI 2012. Ministry of Water and Irrigation, Jordan. Annual Report. Amman, Jordan.
[63] MWI 2013a. Annual Report2013. Amman: Ministry of Water and Irrigation - Awareness and Media Directorate
[64] MWI. 2013b. Jordan Water Sector Facts and Figures Bulletin [Online].
[65] MWI 2013c. Structural Benchmark/ Action Plan to Reduce Water Sector Losses. In: JORDAN, M. O. W. A. I. O. (ed.). Amman.
[66] MWI 2014. 2014 Annual Report. Amman- Jordan: Ministry of Water and Irrigation - Awareness and Media Directorate
[67] MWI 2016a. Annex 1, Additional Water Supply CIP. In: JORDAN, M. O. W. A. I. O. (ed.). Amman
[68] MWI 2016b. Climate Change Policy for a Resilient Water Sector. In: JORDAN, M. O. W. A. I. O. (ed.). Amman
[69] MWI 2016c. Groundwater Sustainability Policy. In: JORDAN, M. O. W. A. I. O. (ed.). Amman.
[70] MWI 2016d. National Water Strategy of Jordan, 2016 – 2025. In: JORDAN, M. O. W. A. I. O. (ed.). Amman.
[71] MWI 2016e. Surface Water Utilization Policy. In: JORDAN, M. O. W. A. I. O. (ed.). Amman.
[72] MWI 2016f. Water Demand Management Policy. In: JORDAN, M. O. W. A. I. O. (ed.). Amman
[73] MWI 2016g. Water Reallocation Policy. In: JORDAN, M. O. W. A. I. O. (ed.). Amman.
[74] O›BRIEN, M. 2014. The Worth of Water: A Look at the Water Scarcity Crisis and the Perceptions of the Basic Need of Water in South Africa. Senior
[75] OKI, T. & KANAE, S. 2006. Global hydrological cycles and world water resources. science, 313, 1068-1072.
[76] OROUD, I. M. 2011. Evaporation estimates from the Dead Sea and their implications on its water balance. Theoretical and applied climatology, 106, 523-530.
[77] PLA, C., VALDES-ABELLAN, J., TENZA-ABRIL, A. J. & BENAVENTE, D. 2016. Predicting Daily Water Table Fluctuations in Karstic Aquifers from GIS-Based Modelling, Climatic Settings and Extraction Wells. Water Resources Management, 1-15.
[78] QUEVAUVILLER, P. 2010. Water sustainability and climate change in the EU and global context–policy and research responses.
[79] QUEVAUVILLER, P. 2011. Adapting to climate change: reducing water-related risks in Europe–EU policy and research considerations. Environmental Science & Policy, 14, 722-729.
[80] RADDAD, K. 2005. Water supply and water use statistics in Jordan. International water session water statistics, Vienna, Austria.
[81] RAHMAN, K., GORELICK, S. M., DENNEDY-FRANK, P. J., YOON, J. & RAJARATNAM, B. 2015. Declining rainfall and regional variability changes in Jordan. Water Resources Research, 51, 3828-3835.
[82] ROSEGRANT, M. W., CAI, X. & CLINE, S. A. 2002. World water and food to 2025: dealing with scarcity, Intl Food Policy Res Inst.
[83] SALAMEH, E. 2008. Over-exploitation of groundwater resources and their environmental and socio-economic implications: the case of Jordan. Water International, 33, 55-68.
[84] SALAMEH, E., ALRAGGAD, M. & TARAWNEH, A. 2014. Disi Water Use for Irrigation–a False Decision and Its Consequences. CLEAN–Soil, Air, Water, 42, 1681-1686.
[85] SCHULZ, S., SIEBERT, C., RÖDIGER, T., AL-RAGGAD, M. M. & MERZ, R. 2013. Application of the water balance model J2000 to estimate groundwater recharge in a semi-arid environment: a case study in the Zarqa River catchment, NW-Jordan. Environmental earth sciences, 69, 605-615.
[86] SCHUTTE, C. & PRETORIUS, W. 1997. Water demand and population growth. WATER SA-PRETORIA-, 23, 127-134.
[87] SECKLER, D. W. 1998. World water demand and supply, 1990 to 2025: Scenarios and issues, Iwmi.
[88] SHAMAN, J., STIEGLITZ, M. & BURNS, D. 2004. Are big basins just the sum of small catchments? Hydrological Processes, 18, 3195-3206.
[89] SHATANAWI, K., RAHBEH, M. & SHATANAWI, M. 2013. Characterizing, monitoring and forecasting of drought in Jordan River basin. Journal of Water Resource and Protection, 2013.
[90] SHATANAWI, M., HAMDY, A. & SMADI, H. 2007. Urban wastewater: Problems, risks and its potential use for irrigation. The use of non-conventional water resources, 15.

[91] SHATNAWI, M., RAHBEH, N. & AL-KHARABSHEH, A. 1999. Rainfall-Runoff Relationship and water budget for Zarqa river basin. International Refereed Research Journal-Dirasat (Jordan).

[92] SOLOMON, S., QIN, D., MANNING, M., CHEN, Z., MARQUIS, M., AVERYT, K., TIGNOR, M. & MILLER, H. 2007. IPCC, 2007: Summary for Policymakers, Climate Change 2007: The Physical Science Basis. Contribution of Working Group I to the Fourth Assessment Report of the Intergovernmental Panel on Climate Change. Cambridge University Press, New York.

[93] SONG, Y., LIU, H., WANG, X., ZHANG, N. & SUN, J. 2016. Numerical simulation of the impact of urban non-uniformity on precipitation. Advances in Atmospheric Sciences, 33, 783-793.

[94] SOWERS, J., VENGOSH, A. & WEINTHAL, E. 2011. Climate change, water resources, and the politics of adaptation in the Middle East and North Africa. Climatic Change, 104, 599-627.

[95] TESSITORE, S., FERNÁNDEZ-MERODO, J., HERRERA, G., TOMÁS, R., RAMONDINI, M., SANABRIA, M., DURO, J., MULAS, J. & CALCATERRA, D. 2016. Comparison of water-level, extensometric, DInSAR and simulation data for quantification of subsidence in Murcia City (SE Spain). Hydrogeology Journal, 1-21.

[96] TOPPO, D. 2014. Political Agitation and Water Shortages in the Hashemite Kingdom of Jordan. Claremont McKenna College.

[97] UN-ESCWA&BGR 2013. Inventory of Shared Water Resources in Western Asia. . In: FÜR, U. N. E. A. S. C. F. W. A. B. & ROHSTOFFE)., G. U. (eds.). Beirut. : Online version. .

[98] UNEP 2007. Global Environment Outlook GEO4 - environment for development Malta.

[99] VAN DEN BERG, C. 2015. Drivers of non-revenue water: A cross-national analysis. Utilities Policy, 36, 71-78.

[100] VERNER, D. 2013. Adaptation to a changing climate in the Arab countries.

[101] VERNER, D., LEE, D., ASHWILL, M. & WILBY, R. 2013. Increasing Resilience to Climate Change in the Agricultural Sector of the Middle East: The Cases of Jordan and Lebanon, World Bank Publications.

[102] VILLARROYA, F. & ALDWELL, C. 1998. Sustainable development and groundwater resources exploitation. Environmental Geology, 34, 111-115.

[103] VÖRÖSMARTY, C. J., GREEN, P., SALISBURY, J. & LAMMERS, R. B. 2000. Global water resources: vulnerability from climate change and population growth. science, 289, 284-288.

[104] WADA, Y., VAN BEEK, L. P., VAN KEMPEN, C. M., RECKMAN, J. W., VASAK, S. & BIERKENS, M. F. 2010. Global depletion of groundwater resources. Geophysical research letters, 37.

[105] ZIMMERMAN, J. B., MIHELCIC, J. R., SMITH & JAMES 2008. Global stressors on water quality and quantity. Environmental science & technology, 42, 4247-4254.

JJEES
Jordan Journal of Earth and Environmental Sciences

Volume 8, (Number 2), Dec, 2017
ISSN 1995-6681
Pages 91 - 96

How Precisely «Kaya Identity» Can Estimate GHG Emissions: A Global Review

Azadeh Tavakoli*

Assistant Professors, Civil & Environmental Engineering, Department of Environmental Sciences, University of Zanjan, Zanjan, Iran

Received 27 May, 2017; Accepted 25 August, 2017

Abstract

Climate change is the greatest environmental threat facing our planet, endangering health, communities, economy and national security. Many models tried to evaluate influencing factors, estimate emission rates or any parameter can effect on this phenomena. «Kaya identity» is a mathematical equation that relates economic, demographic and environmental factors to estimate anthropogenic emissions in global scale. In the present study, «Kaya identity» is developed for 215 countries around the world (national scale) during 1990-2011. Then model predictions are compared with real data to evaluate how well Kaya identity can estimate emissions and how results accuracy changed over time. Based on the results, energy intensity and carbon intensity follow a decline; population and Gross Domestic Product (GDP) per capita follow an increasing path. More than 80% of emissions, about 74% of GDP and 52% of the population around the world can be estimated precisely (< 20% error) by Kaya identity. The model predictions show an improvement in accuracy of results over time. Eight out of top ten emitter countries could be estimated well (usually between -20% < error < +20%) by Kaya identity from emission point of view. Results confirm that Kaya identity can be used widely and reliably for estimation of emissions and identification of effective factors globally to help in achieving emission reduction targets by helping governments to better predict emission rates.

Keywords: Climate change, Emission, Kaya identity, Accuracy, World.

1. Introduction

During the past decades, a distinct body of researches has started to investigate the relationship between climate change impacts and human influences on the climate system. The Fourth Assessment Report of the Intergovernmental Panel on Climate Change (IPCC) states that human activities, with more than 90% certainty, are responsible for «most of the observed increase in globally averaged temperatures since the mid-20th century» (IPCC, 2007a). These activities would lead to emission of four principal greenhouse gases: carbon dioxide (CO_2), methane (CH_4), nitrous oxide (N_2O) and the halocarbons. Accumulation of these components in the atmosphere will cause significant effects on global temperature, weather, food security, water supply and will take its toll on the economy (Tavakoli et al., 2016). People are affecting climate, primarily through emission of greenhouse gases from fossil fuels and other resources. As a consequence, climate change can impact on almost all aspects of human lives. Global warming and higher temperature, sea level rise, increased risk of drought, fire and floods, stronger storms and increased storm damage, changing landscapes, posing risks to wildlife, more heat-related illness and disease, economic losses and many other challenges are some of direct and indirect effects of climate change. Many researchers believe that industrial revolution is the origin of human influences and emission increase. Currently, combustion of fossil energy resources for heat supply, electricity generation and transport, account for around 70% of total Greenhouse Gases (GHGs) emission (IPCC, 2007b). As a result, concentration of GHGs have been rising rapidly (2.3 ppm CO_{2eq} per year). The concentration of CO_2 increased to 408.84 ppm in June 2017 from 280 ppm during pre-industrial era (NOAA, 2017).

The unequivocal scientific evidence in combination with recent extreme events (De'Donato and Michelozzi, 2014; Duchez et al., 2015; Sena et al., 2014) for changing and warming of the climate system has taken this environmental challenge as a center stage in the international debates. Recent studies show that if a limit is set to the total amount of CO_2 emitted globally until 2050 (global carbon dioxide budget), there will be a realistic chance for restricting global warming to 2 °C (Friedlingstein et al., 2014; Kvale et al., 2012; Messner et al., 2010). It is obvious that countries cannot continue to emit carbon dioxide as they did in the past and a 450 ppm CO_{2eq} stabilization target suggested and should be placed as the upper limit on concentrations of heat-trapping emissions to avoid dangerous climate change (Luers et al., 2007). Consequently, international climate efforts have been focused on emission reduction targets to stabilize GHG emissions at a safe level in the atmosphere and a group of studies are analyzing the important factors influence on GHG emissions.

Identifying the factors which influence on carbon emissions is highly challenging because of the wide number of these driving factors. Clearly, population is one of the

* Corresponding author. e-mail: atavakoli@znu.ac.ir

most important ones. Population growth affects the energy demand to supply essential requirements, such as food, water, clothing, shelter, and so on. Birdsall (1992) explains that by two different mechanisms, population growth could contribute to greenhouse gas emissions. At first, an increase in fossil fuel emissions because of more demand for energy by different sectors such as power generation, industry, transportation and so on. At the second, deforestation, land use and combustion of fuel wood which decrease the potential ability of the environment to absorb existing GHG emissions and strongly influenced by the population increase. Many researchers investigated this relationship (Begum et al., 2015; Bin and Dowlatabadi, 2005; Druckman and Jackson, 2009; Sadorsky, 2014; Zhu and Peng, 2012). In addition, economic development pattern can be considered as the other key factor which influence carbon emissions, especially for developing countries. Developing countries carry out this pattern of development relying on fossil fuels while lack of appropriate or commercialized technologies, high initial capital investments and no substantial outside expertise to operate are some of the obstacles the developing countries are faced with. Many researchers have been studying issues related to economic development, fossil fuel emissions or Environmental Kuznets Curve (EKC) (Du et al., 2012; Fodha and Zaghdoud, 2010; Ghosh, 2010; Lotfalipour et al., 2010; Menyah and Wolde-Rufael, 2010; Ozturk and Acaravci, 2010; Pao and Tsai, 2011). The other factors, such as welfare level, affluence, fuel type, buildings size, industries type, and climate circumstances, can be effective on the rate of GHGs emission in a country or region. In order to evaluate emissions of different regions and effective driving factors, comprehensive and measurable parameters should be examined. Many conceptual and mathematical models are suggested and developed for this purpose.

The «Kaya» equation is a conceptual framework employed to characterize the various driving forces of anthropogenic GHG emissions at a global scale. These factors cover demographic, economic, fuel type and energy usage to estimate potential CO_2 emissions. To date, few studies have explored this equation at sub-national or regional scale to predict emission rates or analyzed the most effective influencing factors for mitigation efforts (Duro, 2010; Jung et al., 2012; O'Mahony, 2013; Zhao and Wu, 2010; Ziemele et al., 2015). To the best of our knowledge, no attempt has yet focused on all world›s countries at a national scale, considering all four driving forces.

Kaya Identity, which was developed by Yoichi Kaya (a Japanese energy economist), is meant to estimate global (not national) emissions of CO_2. Therefore, it is interesting to see how it could be downscaled to a national level. The manuscript is novel in the way it applies «Kaya Identity» to individual countries around the world (in the case of data availability) and examines how well Kaya equation can estimate emissions in compare with real data. For this purpose, the expected emissions data for a period of 20 years (1990-2011) are estimated and compared with real data at this period. It seems that despite simplicity and inaccurate appearance of Kaya identity; it has a great potential to estimates CO_2 emissions close to real data.

2. Methodology

A powerful model, extensively used to conduct quantitative analysis on CO_2 emissions, is «Kaya Identity» which was introduced by the Japanese professor Yoichi Kaya during a seminar organized by IPCC in 1989 (Kaya and Yokobori, 1997; Yoichi, 1989). This model established a simple mathematical equation which relates various economic, demographic and environmental factors to estimate global CO_2 emissions of human activities as below:

$$E_{carbon} = Population \times \frac{GDP}{Person} \times \frac{Energy}{GDP} \times \frac{CO_2}{Energy} \quad (1)$$

where,

E_{carbon}: Carbon emission rate (GtC/yr)

$\frac{GDP}{Person}$: Per capita Gross Domestic Product ($/person-yr)

$\frac{Energy}{GDP}$: Energy intensity, primary energy per unit of GDP (EJ/$)

$\frac{Carbon}{Energy}$: Carbon intensity, carbon emissions per unit of primary energy (GtC/EJ)

In more details, this emission equation offers a framework for evaluating the factors shaping GHGs emission, in the form of fuel consumption. The GHGs resulting from fossil fuels combustion (CO_{2eq}) is the function of the amount of fuel consumption and fuel type which the first one itself can be affected by population, economic development pattern, welfare level, fuel dependency of industries, climate circumstances of region and so on.

Population growth is one of the major factors that lead to carbon emissions in all countries; however this impact has been more pronounced in developing countries than the developed ones.

The world population increased from 791 million in 1750 (the beginning of Industrial Revolution) (UN, 2004) to 7.4 billion at the end of 2015. During this period, the people who just started burning of fossil fuels increased carbon dioxide concentrations from about 280 parts per million to 408.84 parts per million in June 2017.

For Kaya Identity, the economic situation of society can be estimated by Gross Domestic Product (GDP) per capita. GDP per capita is a measurement of the total economic output of a country divided by its population and provides a general index for standard of living. This index mostly used for international comparisons. Countries with low GDP per capita and slow growth in GDP per capita are less able to satisfy basic needs for food, shelter, clothing, education, and health (Tucker, 2012) and therefore, this index is a measure of fossil fuel consumption in a society, hence the GHG emissions.

Energy intensity is a measure of the energy efficiency of a country›s economy. In other words, this index is a measure of the amount of energy it takes to produce a dollar›s worth of economic output, or conversely the amount of economic output that can be generated by one standardized unit of energy. Some factors, such as the level of industrialization, the mix of services and manufacturing in economic structure of a country, and the attention paid to energy efficiency, can change the amount of this index (Wang et al., 2005; Wang

et al., 2015).

Carbon intensity is the relative amount of carbon emitted per unit of energy or fuels consumed. It is a measure of how efficiently countries use their polluting energy resources, such as coal, oil and gas. The countries which are ramping up the amount of renewable energies can decrease the carbon intensity but those who still rely on fossil fuels to drive economic growth have less chance for reduction. As a real example, among the top 25 emitter, China had declined its carbon intensity about 51% over 12 years (1990-2002) but carbon intensity rose significantly in Saudi Arabia, Indonesia, Iran, and Brazil (Baumert et al., 2005).

Population and economic growth are considered as ascending factors for emissions. In return, for the world as a whole, energy intensity and carbon intensity are both improving over time, which may help offset some of consequences associated with population and economic growth.

To achieve the goal of the present work, five types of information include population, GDP, energy intensity, carbon intensity and CO_2 emissions from fossil fuels are needed. Population censuses are collected from World Population Prospects- the 2015 revision (UN, 2015). Information related to economic output of countries, such as GDP (constant 2005 US$) and carbon intensity received from the World Bank- World Development Indicators website.

Besides, energy intensity information is calculated based on data provided by U.S. Energy Information Administration (EIA). To determine the amount of real GHG emissions, the amount of all fuel types consumed in a specific country or region are to be estimated. Then, using the emission factors for each fuel, the relevant GHG emissions are determined. In the final step, using the Global Warming Potential (GWP) coefficients, the emissions report based on carbon dioxide equivalent (CO_{2eq}). During the present study, the data related to CO_2 emissions from fossil-fuel burning are received from Carbon Dioxide Information Analysis Center (CDIAC), World Bank Data Center and for some cases, emissions are estimated from fuel consumption data of each country and IPCC 2006 guideline is used for the calculation of emissions.

The amount of CO_2 emissions is estimated by original Kaya Identity as mentioned in equation 1. In this way, no coefficient or special function is considered in the calculations. This calculation includes a period of 20 years (1990-2011) and for about 251 countries around the world. Then, calculated emissions are compared with real data to estimate how successful Kaya Identity to estimate GHG emissions is. It means that the gap between actual and predicted values by the model is evaluated and expressed as percentages. For each year, separate calculations are done. In fact, one year›s steps are considered for each region or country to evaluate this difference. In the present study, Excel 2013 and SPSS 16 software (for calculations and error estimation of the model) and ArcGIS 10.2 (to depict maps) are used. According to the 20 studied years, only the maps of the 1990, 2000, 2005 and 2011 are displayed.

3. Results and Discussion

Analysis results indicate that Kaya Identity, taking into account major factors influencing on emissions (population, GDP, carbon intensity and energy intensity), can be considered among the powerful models to estimate CO_2 emissions. Despite the ease and simple structure of this equation, it could be considered a good estimator of CO_2 emissions, not only at a global level, but also for many countries at national level.

The decomposition of Kaya Identity, in order to evaluate the role of different factors influencing on CO_2, during 1990-2011 for the world as a whole (215 countries), is shown in Figure 1. Based on this diagram, energy intensity has been decreasing rapidly. In addition, carbon intensity follows a decline path but not as steep as energy intensity done. In contrast, population and GDP per capita have a strong increase rate and as a consequence, CO_2 emission is growing. In sum, more attempts are needed on the path of carbon intensity improvement. Development of renewable energies, rapid switch from dirty fossil fuels to clean ones and setting limitations on coal consumption are robust suggestions for this purpose.

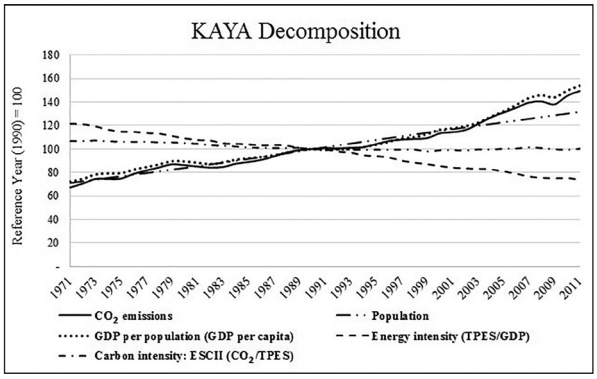

Figure 1. Decomposition of influencing factors on Kaya identity

Another achievement of the present study is the evaluation of the expected CO_2 emissions calculated by Kaya and comparing them with real data during a period of 20-year with one year steps. For a better understanding and summing up, the results of this comparison are shown as global maps only in four time section (including 1990, 2000, 2005 and 2011), presented in Figures 2 to 5. In these figures, the difference of emissions (real - expected) for 1990 to 2011 are categorized.

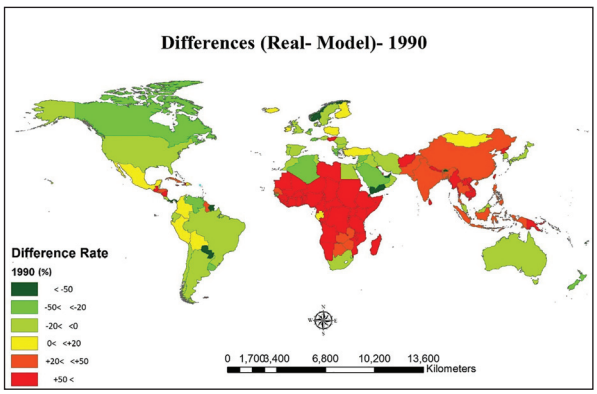

Figure 2. The difference of real and calculated (Kaya) emissions-1990

 - Volume 8, (Number 2), (ISSN 1995-6681)

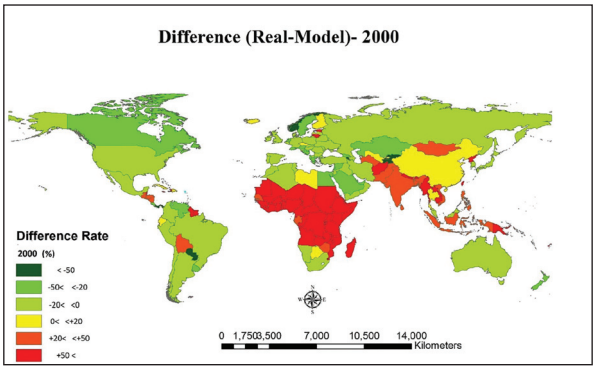

Figure 3. The difference of real and calculated (Kaya) emissions- 2000

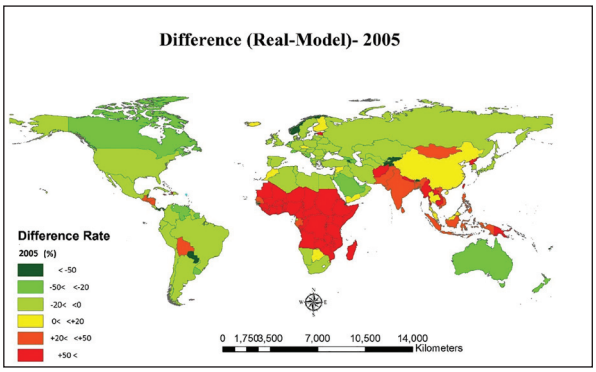

Figure 4. The difference of real and calculated (Kaya) emissions- 2005

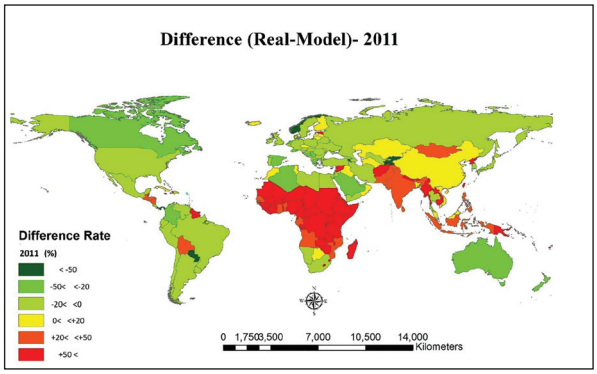

Figure 5. The difference of real and calculated (Kaya) emissions- 2011

Typically, the accuracy estimation of a model can be judged by considering the error values. Models with less than ±20% error are considered accurate and reliable, between 20-50% is acceptable; for higher values, a modification of the model is suggested. Based on this rule of thumb, findings of the present study, from all 251 countries under evaluation, during 1990-2011, are classified into five groups (Table 1). Group 1 includes those with accurate results in comparison with reality (with less than 20% error). Groups 2 to 4 consist of countries with more difference in estimated emissions with real data; and finally small countries or islands with no data availability are placed in group 5. It should be emphasized that despite the large number of countries in group 5, they are accounted for only 1.9% of emissions around the world, which is negligible. Although more than 80% of emissions is related to countries which, according to Kaya Identity are of an acceptable margin of error, are predictable.

Table 1. Statistic of 251 countries estimated by Kaya and compared with real data (1990-2011)

Classification	Difference (%) Real- Kaya	Number of Countries	Population (%)	Share of GDP (%)	Share of Emissions (%)
Group 1	≤ 20	74	54.5	77.4	81.7
Group 2	20 < ≤ 50	27	29.0	12.5	15.7
Group 3	50 < ≤ 100	23	8.5	1.6	0.9
Group 4	more than 100	4	0.3	0.4	0.1
Group 5	no Data	123	8.3	8.4	1.9

The number of countries that Kaya Identity can estimate their emissions close to reality (with less than 20% difference) is increasing and from 56 in 1990 improved to 82 and 71 during next decades. These countries covered about 52% of the total world population in 2011. In addition, about 74% of world›s GDP and more than 80% of CO_2 emissions are related to these countries and are estimated well by Kaya Identity. Table 2 depicts the statistics related to countries that are estimated well (with less than 20% difference) by Kaya and share of population, GDP and CO_2 emission of this group of countries. It could be concluded that the model›s ability to predict emissions has increased over time.

The top emitter countries in 2015 include China, United States, India, Russia, Japan, Germany, Korea, Canada, Iran and Brazil. Another interesting result of the present study is that, except for Canada and India, all the top ten emitter countries are placed in the group of countries which can be estimated accurately by Kaya.

In contrast, five countries (Armenia, Malta, Paraguay, Singapore and Tajikistan) represent a great error in the estimation of emissions by Kaya Identity (more than 100%), so that real emission amounts are far less than the predicted ones. This conclusion is related to the type of economic activities that have been done in a country. For example, agriculture, husbandry, tourism, etc., are effective on the economy of a country or a region but with no direct effect on GHG emissions. Kaya Identity is unable to predict emissions in the other sectors, which are far from fossil fuel consumption and industry. Development of the other models and driving forces with the ability to predict emissions from non-combustion sectors must be put on the agenda.

Table 2. Statistic of countries that follow Kaya identity (with less than 20% difference), Group 1

Year	Number of Countries	Population (%)	Share of GDP (%)	Share of Emissions (%)
1990	56	25	63.8	64.0
2000	57	51.5	75.8	80.6
2005	82	52.2	77.2	82.0
2011	71	52.5	74.3	80.4

Conclusions:

The estimation of the CO_2 emissions and comparing the results with real data among 215 countries for a period of 20 years (1990-2011) are the most important aims of the present study. Based on the amount of errors in the prediction of emissions (%) and data availability, five groups are categorized. It is concluded that this simple estimator can be used for the prediction of future emissions in many countries and may cover about 80% of emissions around the world. In addition, the evaluation of the most important factors influencing on the emission of a country is possible by the decomposition of Kaya influencing factors. For example, during a study done on China (Xiangzhao and Xuechen, 2009), Kaya Identity, in combination with macroeconomic factors, was used for a period of 34 years (1971-2005), indicating that the economic development and population growth are mainly responsible for CO_2 emissions. Based on the results of the present study, during the two past decades, Kaya Identity has worked as a suitable estimator for the prediction of CO_2 emissions of China (with less than 5% error).

Another study applied Kaya Identity as an extended format to identify drivers of CO_2 emissions in the former Soviet Union and among 15 countries (Brizga et al., 2013). It was mentioned that during different stages of economic development (from 1990 to 2010) different factors played different roles on emission rates. The evaluation of this case in the present article revealed that, during this period (1990-2011), Kaya Identity was not followed by all this group. Armenia experienced about -85.6% error between real data and Kaya prediction, Azerbaijan (-21.2%), Belarus (-3.4%), Estonia (+59.1%), Georgia (-36.7%), Kazakhstan (+1.9%), Kyrgyzstan (-94.6%), Latvia (+4.1%), Lithuania (+2.8%), Moldova (-10.2%), Russia (-6.5%), Tajikistan (-145.7%), Turkmenistan (-0.6%), Ukraine (-5.1%) and Uzbekistan (-10.0%) and each country follows a different pattern in emissions.

Decomposition of carbon emissions in the period of 1990-2010 is subject of a study done on Ireland (O'Mahony, 2013). Affluence and population lead to more emissions and are countered by energy intensity and fossil fuel substitution. We found that Ireland›s emission data are in good coordination with Kaya results (with about 12% error).

Economic development, carbon intensity and the change in the composition of the economy are introduced as the most contributors to the rise in CO_2 emissions in Turkey (1980-2003) (Lise, 2006) and we recommend Kaya Identity as a good model for this evaluation (with an average -6.2% error in prediction).

However, the present study can help in giving a better understanding of Kaya Identity for emission prediction. It should be mentioned that, for each country or region, more parameters could be suggested to extend or improve this model. In this way, more accurate predictions may become possible. Governments and policy makers can better analyze the influencing factors, paving the way for achieving more emission reduction.

References

[1] Baumert, K.A., Herzog, T., and Pershing, J., 2005. Navigating the Numbers. World Resources Institute.

[2] Begum, R.A., Sohag, K., Abdullah, S.M.S., and Jaafar, M., 2015. CO2 emissions, energy consumption, economic and population growth in Malaysia. Renewable and Sustainable Energy Reviews, 41, pp. 594-601.

[3] Bin, S., Dowlatabadi, H., 2005. Consumer lifestyle approach to US energy use and the related CO2 emissions. Energy Policy, 33, pp. 197-208.

[4] Birdsall, N., 1992. Another look at population and global warming. World Bank Publications. Vol 1020.

[5] Brizga, J., Feng, K., and Hubacek, K., 2013. Drivers of CO2 emissions in the former Soviet Union: a country level IPAT analysis from 1990 to 2010. Energy, 59, pp. 743-753.

[6] De'Donato, F., Michelozzi, P., 2014. Climate change, extreme weather events and health effects. In: The Mediterranean Sea. Springer, pp. 617-624.

[7] Druckman, A., Jackson, T., 2009. The carbon footprint of UK households 1990–2004: a socio-economically disaggregated, quasi-multi-regional input–output model. Ecological economics, 68, pp. 2066-2077.

[8] Du, L., Wei, C., and Cai, S., 2012. Economic development and carbon dioxide emissions in China: Provincial panel data analysis. China Economic Review, 23, pp. 371-384.

[9] Duchez, A., Forryan, A., Hirschi, J., Sinha, B., New, A., Freychet, N., Scaife, A., and Graham, T., 2015. Impact of climate change on European weather extremes. In: EGU General Assembly Conference Abstracts, p 2828.

[10] Duro, J.A., 2010. Decomposing international polarization of per capita CO2 emissions. Energy Policy, 38, pp. 6529-6533.

[11] Fodha, M., Zaghdoud, O., 2010. Economic growth and pollutant emissions in Tunisia: an empirical analysis of the environmental Kuznets curve. Energy Policy, 38, pp. 1150-1156.

[12] Friedlingstein, P., Andrew, R.M., Rogelj, J., Peters, G.P., Canadell, J.G., Knutti, R., Luderer, G., Raupach, M.R., Schaeffer, M., and Van-Vuuren, D.P., 2014.` Persistent growth of CO2 emissions and implications for reaching climate targets. Nature geoscience, 7, pp. 709-715.

[13] Ghosh, S., 2010. Examining carbon emissions economic growth nexus for India: a multivariate cointegration approach. Energy Policy, 38, pp. 3008-3014.

[14] IPCC, 2007a. Climate change 2007: the physical science basis Agenda 6.

[15] IPCC, 2007b. The Fourth Assessment Report of the Intergovernmental Panel on Climate Change Geneva, Switzerland.

[16] Jung, S., An, K.J., Dodbiba, G., and Fujita, T., 2012. Regional energy-related carbon emission characteristics and potential mitigation in eco-industrial parks in South Korea: Logarithmic mean Divisia index analysis based on the Kaya identity. Energy, 46, pp. 231-241.

[17] Kaya, Y., Yokobori, K., 1997. Environment, energy, and economy: strategies for sustainability. United Nations University Press Tokyo, Japan.

[18] Kvale, K., Zickfeld, K., Bruckner, T., Meissner, K., Tanaka, K., and Weaver, A., 2012. Carbon Dioxide Emission Pathways Avoiding Dangerous Ocean Impacts. Weather, Climate, and Society, 4, pp. 212-229.

[19] Lise, W., 2006. Decomposition of CO2 emissions over 1980–2003 in Turkey. Energy Policy, 34, pp. 1841-1852.

[20] Lotfalipour, M.R., Falahi, M.A., and Ashena, M., 2010. Economic growth, CO2 emissions, and fossil fuels consumption in Iran. Energy, 35, pp. 5115-5120.

[21] Luers, A.L., Mastrandrea, M.D., Hayhoe, K., and Frumhoff, P.C., 2007. How to Avoid Dangerous Climate Change. Union of Concerned Scientists.

[22] Menyah, K., Wolde-Rufael, Y., 2010. Energy consumption, pollutant emissions and economic growth in South Africa. Energy Economics, 32, pp. 1374-1382.

[23] Messner, D., Schellnhuber, J., Rahmstorf, S., and Klingenfeld, D., 2010. The budget approach: a framework for a global transformation toward a low-carbon economy. Journal of Renewable and Sustainable Energy, 2:031003.

[24] Earth›s CO2 Home Page, 2017. www.http://co2now.org/. Accessed 13 August 2017.
[25] O'Mahony, T., 2013. Decomposition of Ireland›s carbon emissions from 1990 to 2010: An extended Kaya identity. Energy Policy, 59, pp. 573-581.
[26] Ozturk, I., Acaravci, A., 2010. CO2 emissions, energy consumption and economic growth in Turkey. Renewable and Sustainable Energy Reviews, 14, pp. 3220-3225.
[27] Pao, H.T., Tsai, C.M., 2011. Modeling and forecasting the CO2 emissions, energy consumption, and economic growth in Brazil. Energy, 36, pp. 2450-2458.
[28] Sadorsky, P., 2014. The effect of urbanization on CO2 emissions in emerging economies. Energy Economics, 41, pp. 147-153.
[29] Sena, A., Corvalan, C., and Ebi, K., 2014. Climate Change, Extreme Weather and Climate Events, and Health Impacts. In: Global Environmental Change. Springer, pp. 605-613.
[30] Tavakoli, A., Shafie-Pour, M., Ashrafi, K., and Abdoli, G., 2016. Options for sustainable development planning based on «GHGs emissions reduction allocation (GERA)» from a national perspective. Environment, Development and Sustainability, 18, pp. 19-35, DOI 10.1007/s10668-015-9619-0.
[31] Tucker, I., 2012. Microeconomics for today. Cengage Learning.
[33] UN, 2004. United Nations, The World at Six Billion.
[34] UN, 2015. Population Division, Department of Economic and Social Affairs.
[35] Wang, C., Chen, J., and Zou, J., 2005. Decomposition of energy-related CO2 emission in China: 1957-2000. Energy 30(1), pp. 73-83.
[36] Wang, Z., Wang, C., and Yin, J., 2015. Strategies for addressing climate change on the industrial level: affecting factors to CO2 emissions of energy-intensive industries in China. Natural Hazards 75(2), pp. 303-317.
[37] Xiangzhao, F., Xuechen, W., 2009. Analysis of Impact Factors on China›s CO2 Emission Trends During 1971-2005. Advances in Climate Change Researche, 5, pp. 66-72.
[38] Yoichi, K., 1989. Impact of carbon dioxide emission on GNP growth: interpretation of proposed scenarios. Paris: Presentation to the energy and industry subgroup, response strategies working group, IPCC.
[39] Zhao, A., Wu, C., 2010. Analysis of decomposition of influencing factors of variation in CO2 emission of China–Based on improved Kaya identity and LMDI method. Soft Science, 24, pp. 55-59.
[40] Zhu, Q., Peng, X., 2012. The impacts of population change on carbon emissions in China during 1978–2008. Environmental Impact Assessment Review, 36, pp. 1-8.
[41] Ziemele, J., Gravelsins, A., and Blumberga, D., 2015. Decomposition analysis of district heating system based on complemented Kaya identity. Energy Procedia, 75, pp. 1229-1234.

JJEES
Jordan Journal of Earth and Environmental Sciences

Volume 8, (Number 2), Dec, 2017
ISSN 1995-6681
Pages 97 - 103

The Use of GIS Techniques and Geophysical Investigation for Flood Management at Wadi Al-Mafraq Catchment Area

Hani Al-Amoush[1*], Abdel Rahman Al-Shabeeb[1], Rida Al-Adamat[1], A'kif Al-Fugara[2], Saad Al Ayyash[2], Akram Shdeifat[3], Eid Al-Tarazi[4] and Jafar Abu Rajab[4]

[1] *Institute of Earth and Environmental Sciences, Al al-Bayt University, Mafraq, Jordan*
[2] *Faculty of Engineering, Al al-Bayt University, Mafraq, Jordan*
[3] *Water, Environment and Arid Regions Research Center, Al al-Bayt University, Mafraq, Jordan*
[4] *Natural Resources Faculty, Hashemite University, Zarqa, Jordan*

Received 25 July, 2017; Accepted 25 August, 2017

Abstract

The rapid expansion of urban areas over the past two decades within Mafraq City has affected the surface hydrology runoff. Developments in Mafraq City have changed the land coverage from vegetation to impervious surface (Asphalt and Buildings) which covers most of the urban areas within Mafraq City. This reduced the ability of the land to absorb rainfall and force the excess rainfall-runoff to flow faster over the surface. As a result, the West and central regions of Mafraq City recently experienced floods that have affected hundreds of people. In order to control flood and minimize its impacts on local people, it is necessary to manage such floods. The present study aims at identifying the potential sites for water harvesting dam within the Wadi Al-Mafraq watershed to control the flood that pass through the city using GIS techniques. In order to select the potential site for the water-harvesting dam, five physical criteria that affect the water harvesting were identified based on a literature review. These criteria are rainfall, soil texture, slope, material of vadoze zone and drainage density. Based on the use of the Weighted Linear Combination (WLC) method, a water harvesting potential map was generated. The outcome of the GIS analysis was validated by fieldwork investigations carried out using Time Domain Electromagnetic Geophysical method (TDEM). The TDEM results show that (10 - 25) m of silty clay, soil and alluvium deposits are dominated the proposed site as the topmost layer. Moreover, three to four distinctive subsurface geo-electrical layers were identified in terms of their resistivity, thicknesses and structures. The present study proves the importance of the integration of different techniques GIS and TDEM in water harvesting and flood management studies.

Keywords: Flood management, TDEM, Wadi Al-Mafraq, GIS, Water harvesting.

1. Introduction

The rapid expansion of urban areas over the past two decades within Mafraq City has impacted the surface hydrology runoff. Developments in Mafraq City have changed the land coverage from vegetation to impervious surface. Impervious concrete and asphalt surfaces cover most of the urban areas within Mafraq City, which reduces the ability of the land to absorb rainfall and force the excess rainfall-runoff to flow faster over the surface.

Accumulation of water in certain areas can be the main causes of localized flooding problems. The west and central regions of Mafraq City have recently experienced floods that have affected hundreds of people. Although no inhabitants appear to have been physically harmed, many homes and roads were affected. According to reports published in national newspaper, Wadi Al-Hussein passing through Mafraq City attained high floodwater levels that constitute a significant danger in particular, where the main road crossing the Wadi. The road was closed as sections were swamped by up to a three meter of water, and flash floods overwhelmed drainage system, forcing the closure of most road tunnels and grid locking traffic (Addustour newspaper, 10/10/2011) (Figures 1a and b). Most importantly, this disaster will continue with time and the Wadi is widening and forming a dangerous problem on the surrounding houses in center of the city (Figure 1a).

* Corresponding author. e-mail: hani1@aabu.edu.jo

 - Volume 8, (Number 2), (ISSN 1995-6681)

Figure 1. Flashflood in Mafraq City (a. Addustour newspaper, 10/10/2011 , b. 2016)

In order to counter flood effects, it is very crucial to operate the surface water system for flood control efficiently to minimize the impacts of flood during real-time flood events (Jha et al., 2012). Many flood mitigation structures in the city projects have been implemented in a phased program to rehabilitate and upgrade the existing drainage infrastructure (Charlesworth, 2010).

The early phases were operated on a traditional approach that involved channel improvement works to speed up the flow of the flood wave through the city and the construction of storage facilities upstream to regulate the magnitude of floodwaters flowing into the city (Zevenbergen et al., 2010). There is, however, minimal impacts of such solutions; this is because such flooding still causes a threat to the residential and commercial buildings or other public and private infrastructures (Zevenbergen et al., 2010). A completely new approach for flood control is deemed necessary for the Mafraq City. As a result, a comprehensive flood mitigation system. This system involves a set of structural flood control measures to divert the flood runoff from the catchment through a bypass channel before it is being directed back to the Mafraq City centre downstream and/or construction storage ponds and dams upstream of the city to detain floodwater and attenuate the flood flow into the city. Local planners and decision makers are in dire need for accurate information on the spatial distribution, magnitude and depth of flooding, and on the land use affected. The integration of GIS, remote sensing and Digital Elevation Models (DEMS) with multi criteria decision support system is an active area of research. In recent years, Geographic Information Systems (GIS) and Multi Criteria Decision Analysis (MCDA) have been widely used for water harvesting site selection studies. Several researchers have used GIS and MCDA for water harvesting studies (e.g., Al-Shabeeb, 2015; Al-Shabeeb, 2016; Srivastava, 2001; Gupta et al., 1997; Al-Amoush et al., 2016; El-Awar et al., 2000; Baban and Wan-Yusof, 2003; Shatnawi, 2006; Al-Adamat, 2008; Al-Adamat et al., 2010 and Al-Adamat et al., 2012).

Those researchers used GIS in selecting the best sites for water harvesting projects at various parts of the world. In their search to find the best sites, they applied the Weighted Linear Combination (WLC) within GIS on various thematic layers including geology, land use/land cover, soil types, slope, rainfall and drainage density. WLC is a method of MCDA that is implemented within GIS environment, which defines weights for criteria selected.

In the present study, five physical criteria were used, including the rainfall, the slope, the drainage density, materials of vadose zone and soil texture to select an optimum site for a dam in Wadi Al-Mafraq catchment area to control the flood that passes through Mafraq City. WLC was used for determining the best sites for water harvesting dam in the present study. The selected sites were then validated using Time Domain Electromagnetic Geophysical method in order to investigate the subsurface layering.

2. Study Area

The study area is located in the Northern part of Jordan to the West of Mafraq City (Figures 2 and 3). Figure 3 shows the Wadis that enter Mafraq City from the West and cause the flooding problem. It shows also the corresponding watershed for each Wadi. In the present study, the catchment area of Wadi Al-Mafraq has been thoroughly investigated to establish a flood control system because Wadi Al-Mafraq is the major contributor to the flooding problem within the city. The study area is inhabited by more than 200.000 people (DOS, 2015). The soil clay percentages in the study area is 29% and the soil texture is silty loam (Al-Adamat et al., 2007). The study area topography is predominated with regions of high elevation (918m) in the west and north west and low elevation (675 m) in the eastern parts of the study area (Figure 4). The annual rainfall ranges between 150 mm in the eastern parts to 250 mm in the western parts of the study area (Al-Adamat et al., 2007) (Figure 5). Surface water flows towards Mafraq City from the west and north west (Figure 3).

The study area is situated in an area classified as an arid to semi-arid climate zone with hot summer and cold winter with average temperatures 38°C (Summer) and 14°C (Winter) (Department of Meteorology DOM, 2015). The mean annual rainfall is estimated to be 161 mm and is fairly evenly distributed throughout the winter season (Department of Meteorology DOM, 2015).

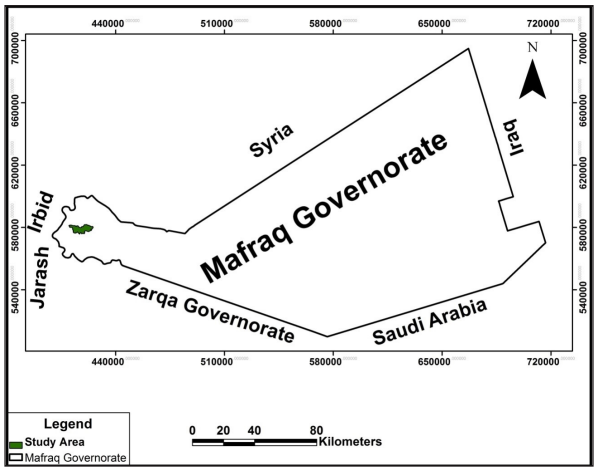

Figure 2. Location map of the study area

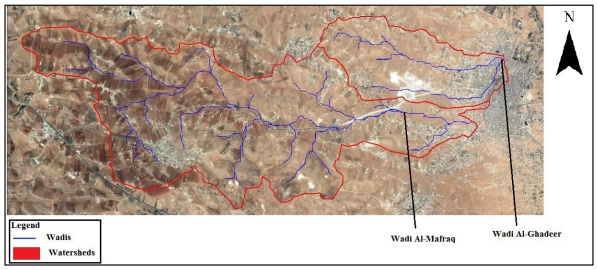

Figure 3. Major Wadis and their watersheds

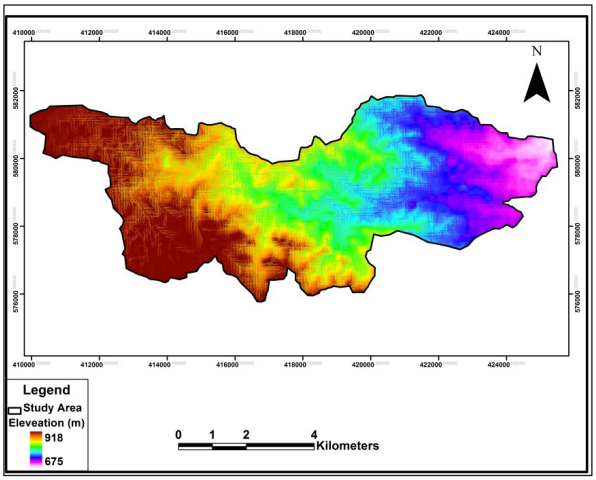

Figure 4. Elevations within the study area (Based on ASTER DEM)

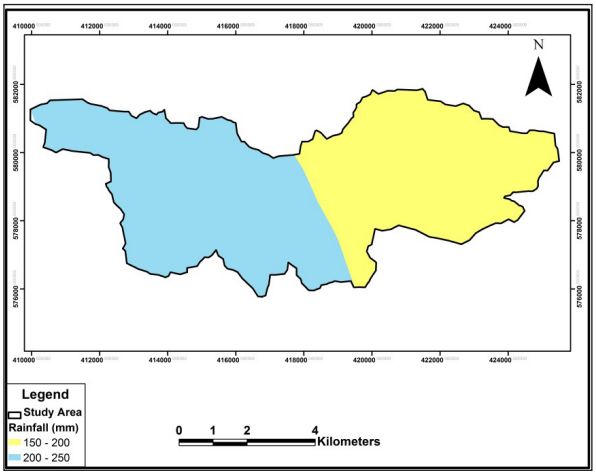

Figure 5. Average annual rainfall within the study area (Modified from Al-Adamat et. al., 2007)

3. Methodology

The methodology adopted for determining the suitable water harvesting sites in the selected areas of the Wadi-Al-Mafraq is presented in Figure 6.

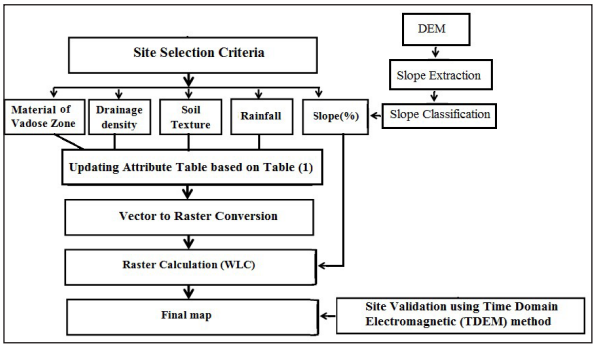

Figure 6. Flowchart of the methodology adopted in this study

Table 1 lists the rates of each parameter and its associated weight score. This table lists only the ratings appropriate for the study area. The attribute table of the rainfall layer (Figure 5) was updated according to Table 1 and then converted to raster format (Figure 7). Based on Figure 6, the Advanced Space borne Thermal Emission and Reflection Radiometer (ASTER) DEM (spatial resolution of 30 m) (Figure 4) has been used to derive the slopes for the study area and classify them according to Table 1 (Figure 8). It appears, from this table, that the material of vadose zone and soil texture have only one value each to represent the weight by ratings. The entire study area of the same vadose zone material (Limestone). Also, the entire study area of the same soil texture (silt loam). The material of vadose zone has the value of 6 and the soil texture has the value of 2. The ASTER DEM has been also used to derive the drainage network for the study area through the use of Flow Direction and Flow Accumulation calculation techniques within ESRI ArcGIS® (Figure 3). The resulted GIS layer was subjected to density calculation and classification based on Table 1 and the result is shown in Figure 9.

Table 1. The used weights ratings in this study (after Al –Shabeeb, 2016)

Criteria	Condition	Weight (W)	Rating (R)	W×R
Rainfall (mm)	100-200	5	2	10
	200-300		3	15
Slope (%)	> 8%	4	1	4
	4-8%		2	8
	2-4%		3	12
	0-2%		4	16
Material of Vadose Zone	Limestone	3	2	6
Drainage density (km/ km^2)	> 2.55	2	1	2
	1.5 - 2.25		2	4
	0.75 - 1.5		3	6
	0 - 0.75		4	8
Soil Texture	Silt Loam	1	2	2

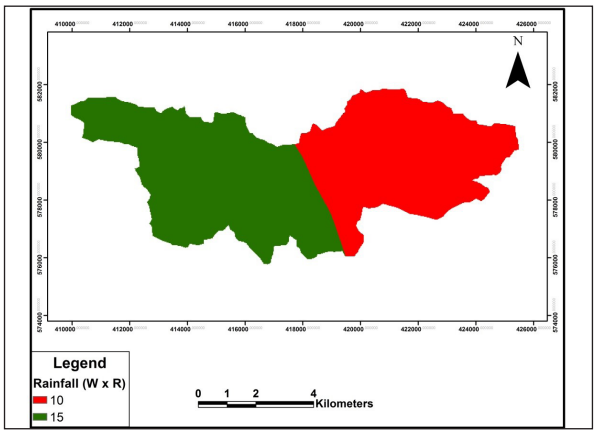

Figure 7. Rainfall (Weight × Ratings)for the study area

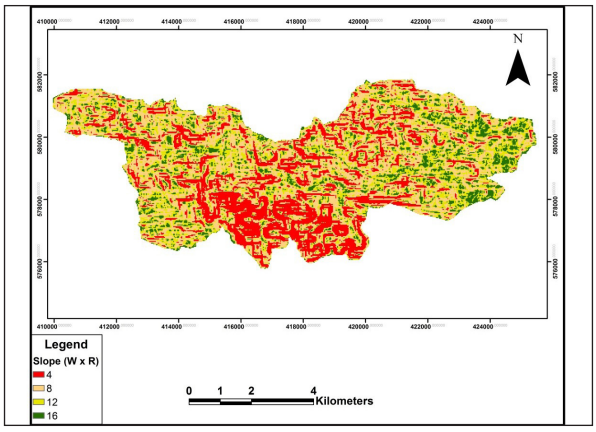

Figure 8. Slope (Weight × Ratings) for the study area

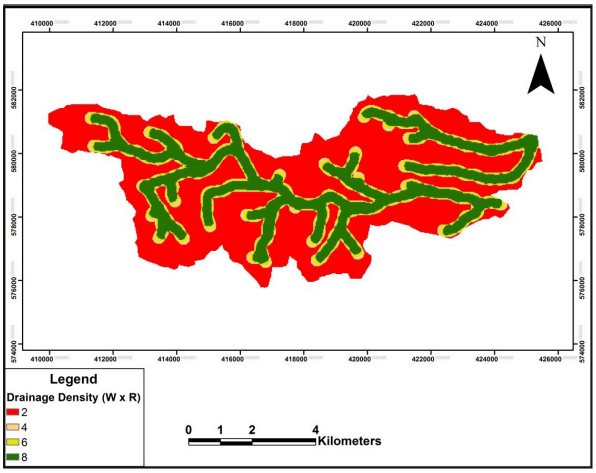

Figure 9. Drainage Density (Weight × Ratings) for the study area

4. Results and Discussion

The GIS layers (Figures 7, 8 and 9) were combined using the raster calculation techniques within ESRI ArcGIS® together with a fixed number of 8 that represents the material of vadose zone and soil texture. Table 2 describes the combination of the GIS layers. The numbers listed in this table represent the cells values of each layer. Figure 10 shows the water harvesting potential within the study area. The map has been classified into four potential classes (Low, Moderate, High and Very High). It is clearly appear from this figure that the most western part of the study area is characterized by a high and very high suitability regions for water harvesting, particularly along the major course of the Wadi and within the Wadi bed.

Table 2. The conducted arithmetic operation for the site selection of water harvesting dam

Rainfall (W×R)	+	Slope (W×R)	+	Material of Vadose Zone (W×R)	+	Drainage density (W×R)	+	Soil Texture (W×R)
10		4		6		2		2
15		8				4		
		12				8		
		16				12		

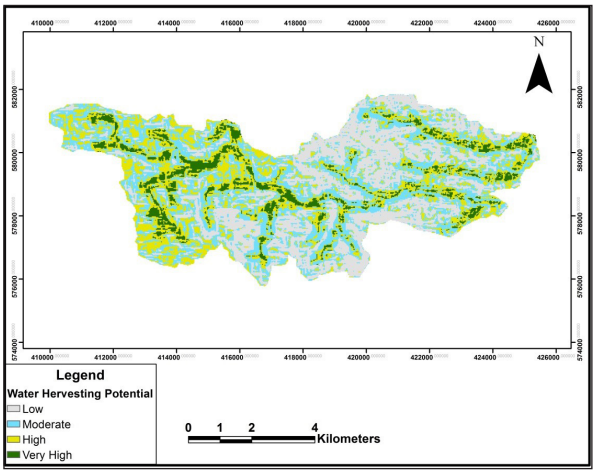

Figure 10. Water Harvesting Potential map

5. Validating the Selected Site Using Time-Domain Electromagnetic Geophysical Method (TDEM)

TDEM method has been widely used for hydro-geological studies (e.g., Danielsen et al., 2003; Goldman et al., 1994; Al-Amoush et al., 2015; Al-Amoush et al., 2016). It was used for environmental applications (e.g., Hoekstra and Blohm, 1990; Mauldin-Mayerle et al., 1998). TDEM was combined with DC electrical resistivity method to investigate the groundwater contamination (e.g., Buselli et al., 1990), for geological mapping (e.g., Jorgensen et al., 2005). For hydro-geophysical and mapping larger structural formation investigations (e.g., Christensen and Sorensen et al., 1995). The theoretical background of TDEM is described in many books (e.g., Reynolds, 2011; Sharma, 1997; Telford et al., 1990; Kirsch, 2006; Keary et al., 2002) as well as in several published articles.

The principle of TDEM is based on generated a primary field which is not continuous but that consists of a series of pulses separated by periods when it is inactive (Keary et al., 2002). During the period of current-on, a static magnetic field is established in the earth (Sharma, 1997; Keary et al., 2002). The eddy currents induced in a subsurface conductor tend to diffuse inward outwards its center when the inducing field is removed and gradually dissipate by resistive heat loss (Keary et al., 2002). This causes a decaying of the magnetic field at the earth surface (Sharma, 1997). The secondary magnetic field can be measured easily. Within highly conductive bodies, the decay of eddy currents (secondary magnetic fields) is significantly slower than that in poor conductors. Measurements of the rate of decay of the secondary magnetic field thus provides a means of detecting subsurface conductive bodies and estimating their conductivities (Sharma, 1997)

In the present study, Time-Domain Electromagnetic (TDEM) method was carried out at specified locations in Wadi Al-Mafraq catchment area as determined by Geographical Information System (GIS) modeling tools based on a pre-defined criteria (include soil texture, slope, material of vadose zone, rainfall and drainage density). The objective of TDEM survey is to investigate the shallow subsurface layering›s (stratigraphy) and structures and to build a 2D - hydro-geophysical models along and across the Wadi course to investigate its suitability for water harvesting dam.

5.1. Field Survey and Geometry

In the present study, eight TDEM sounding points were carried out at the proposed location for water harvesting structure construction (Figure 11). A square transmitter loop (dipole Tx-Rx) configuration with dimension (50m * 50m) was used for data acquisition. The estimated depth penetration was (~130m). The measurements were acquired using a typical TEM-FAST 48HPC system comprising a transmitter (Tx), a receiver (Rx) and unit control managed by HP-IPAQ Pocket system. The measurements were made by transmitting a direct current up to 4 Ampere using 12V batteries with 48 active time gate. A stacking time was set to 7 minutes with 50Hz filter to eliminate aliasing effects. Data processing and modeling was performed using attached software called TEM-RESEARCHER to obtain 1-D models and to construct a 2-D geo-electromagnetic models over the study area. Figure 12 shows the 1-D modeling soundings for the 8-TDEM carried out in the proposed site.

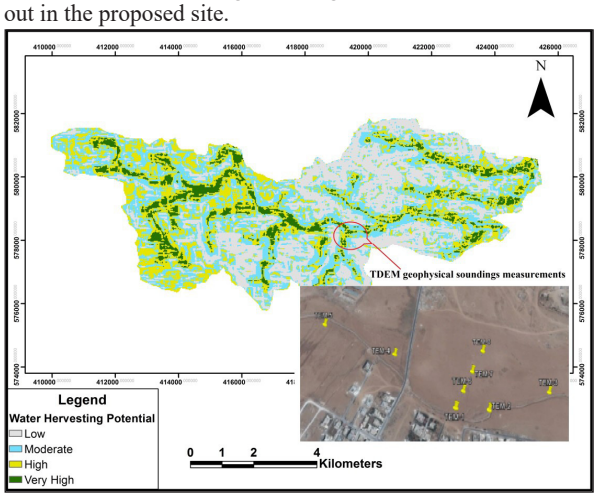

Figure 11. Water Harvesting Potential map and enclosed Google earth map shows the locations of TDEM geophysical soundings measurements

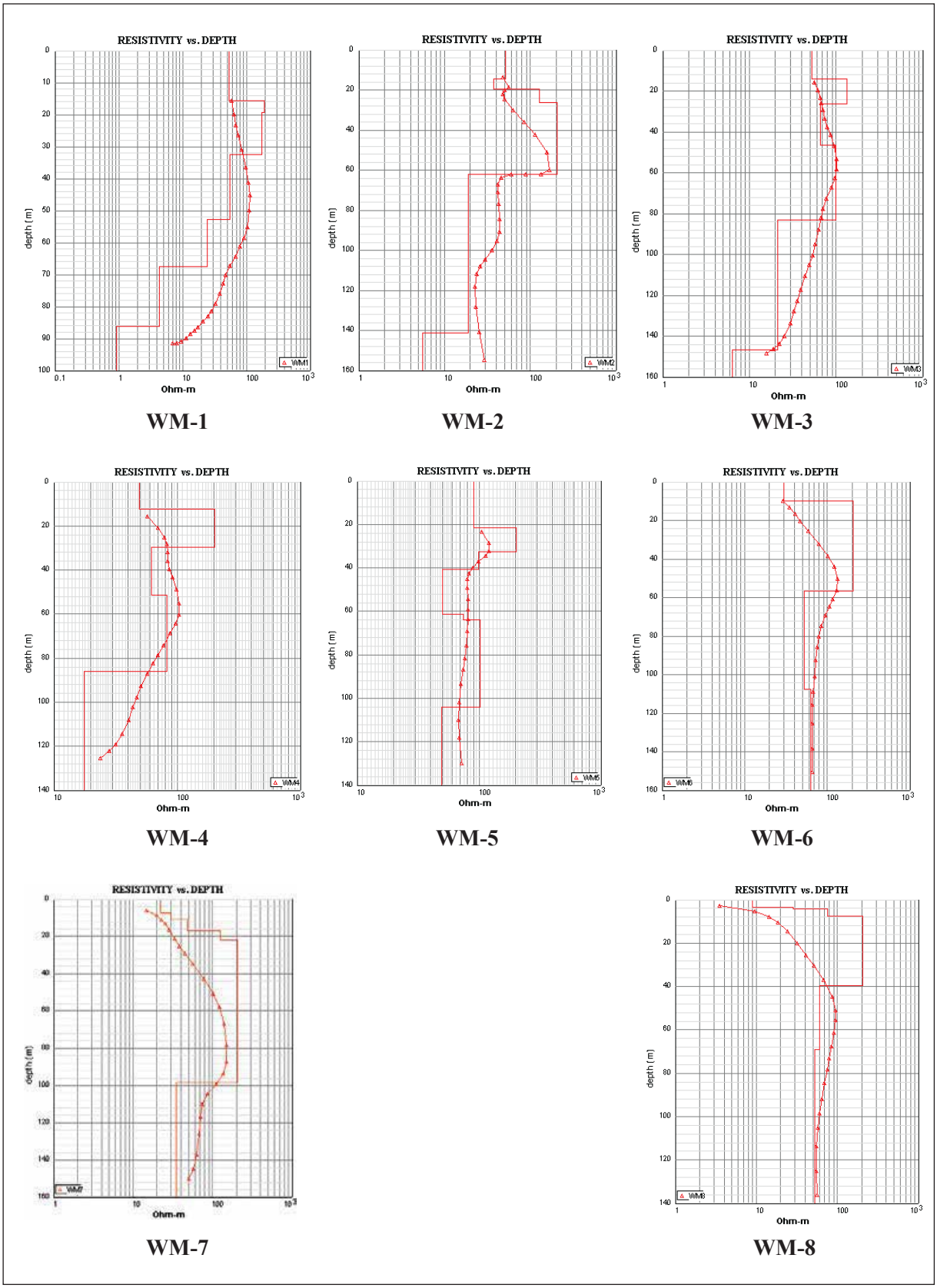

Figure 12. 1- D TDEM modeling soundings at proposed site dam within Wadi Al-Mafarq catchment area

5. 2. Geophysical Data Interpretation

The study area was classified as a dry zone and there was no close boreholes to the proposed dam site investigation. Therefore, the Generalized geological Vertical Section (GVS) and surface geological map as well as the available geological cross sections for the study area were used for interpreting and calibrating the various TDEM soundings and models (Table 3). The TDEM soundings were used to build 2-D geo-electromagnetic resistivity cross-sections in order to investigate the subsurface stratigraphy and structures.

Table 3. a) TDEM measurements and modeling results of sounding TDEM-2 b) Generalized geological Vertical Section(GVS) (Columnar section, Map sheet 3254IV, Geological map of Al-Mafraq) of the study area (Modified after Al-Smadi, 1997)

a)TDEM-2	b) Generalized geological Vertical Section (GVS)

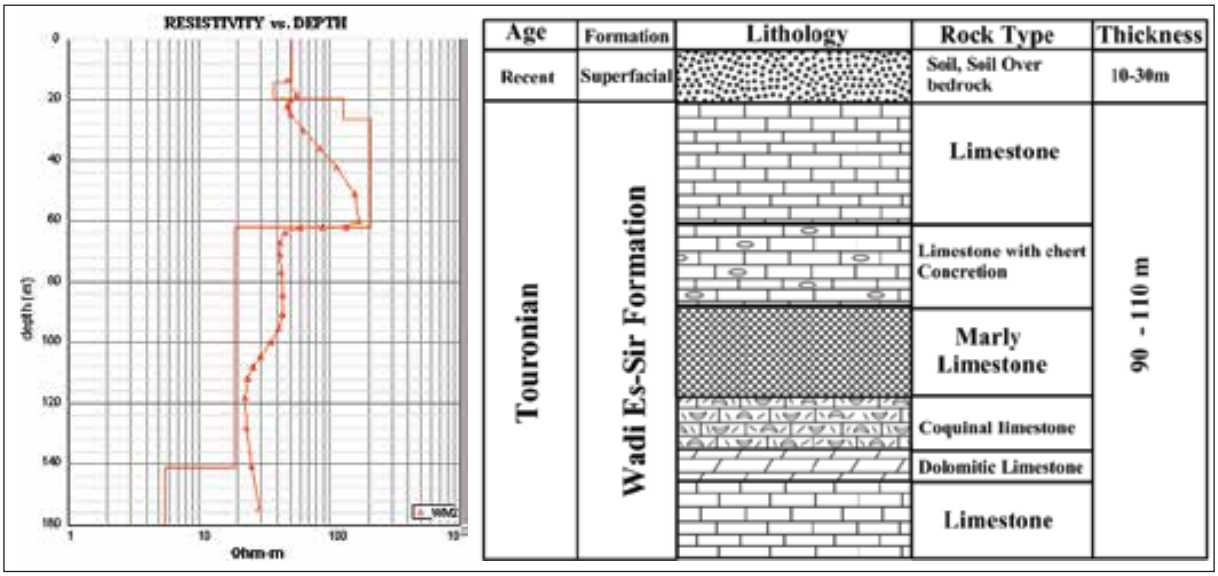

5.2.1. WNW-ESE 2-D Geo-Electromagnetic Cross-Section

Figure 13 shows an E-W 2-D geo-electromagnetic cross-section extending along the course of the Wadi. This model links the soundings TDEM-5, TDEM-4, TDEM-2, TDEM-6 and TDEM-3. The inverted model was correlated with the generalized geological vertical section (GVS) of the study area. Four distinctive subsurface units can be recognized in this model. The upper most unit has a low resistivity layer (20-40) Ohm.m, it has thickness in the range of 10 to 20m over the section; this unit correlates with the predominantly impermeable silty clay - soil and alluvium sediments. The second subsurface unit is a resistive layer (180 - 200) Ohm.m. Its thickness is 20m in the western part and 40m in the most eastern part of the model. It can be correlated with the massive-fractured limestone of Wadi Es-Sir formation (WSL). The third subsurface unit has an intermediate to high resistivity (100 - 140) Ohm.m. It is correlated with limestone and marly limestone of WSL. The fourth subsurface unit has low resistivity values (30-70) Ohm.m, extending to a depth down to 140m and could indicate to saturated zone of limestone or marly-limestone of WSL. The geo-electromagnetic model exhibits lateral variations in resistivity and unit thicknesses, which indicates a change in stratigraphical facies along the course of the Wadi. Moreover, significant faults and fractures have been identified between TDEM-4 and TDEM-6, and between TDEM-6 and TDEM-2 (Figure 13).

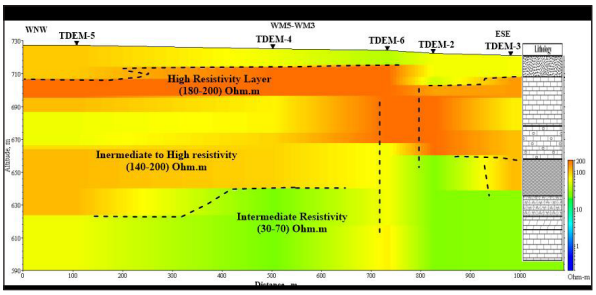

Figure 13. WNW- ESE 2-D Geo-electromagnetic section along Wadi Al-Mafraq based on models of TDEM Soundings (TDEM-5, TDEM-4, TDEM-6, TDEM-2 and TDEM-3). Lithology is interpreted based on a correlation with Generalized geological Vertical Section (GVS) of the study area (see Figure 11 for location)

5.2.2. N-S 2-D Geo-Electromagnetic Cross-Section

Figure 14 shows a N-S 2D geo-electromagnetic cross-section extending a cross the Wadi. The section links the soundings TDEM-1, TDEM-6, TDEM-7 and TDEM-8. The inverted model is correlated with the generalized vertical section (GVS) of the study area. In this model, three distinctive subsurface units can be recognized; the first subsurface is a low resistivity subsurface unit (20-40) Ohm.m.; it has a thickness in the range 15-25m. This unit can be correlated with the predominantly impermeable silty-clay, soil and soil over bedrock. The second subsurface unit is a high resistivity (150 - >200) Ohm.m unit. Its thickness varies along the model (40 - 60)m. It can be interpreted as a paleo-channel deposits composing of blocks of limestone, gravel and wadi sediments especially under TDEM-7. Another explanation for this unit is a layer consisting of massive-fractured limestone corresponding to WSL formation bounded by vertical faults and joints. The third subsurface unit has an intermediate resistivity (40-90) Ohm.m with 70m -100m in thickness. It correlates with limestone to marly limestone of Wadi Es-Sir limestone (WSL).

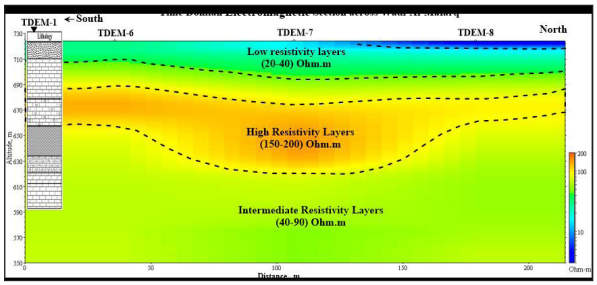

Figure 14. N-S 2-D Geo-electromagnetic cross section across Wadi Al-Mafraq based on models of TDEM Soundings (TDEM-1, TDEM-6, TDEM-7 and TDEM-8). Lithology is interpreted based on a correlation with generalized vertical section (GVS) of the study area (see Figure 11 for location)

6. Conclusions:

The main aim of this study is to map the potential sites for water harvesting suitability and to select an optimum site for a dam in Wadi Al-Mafraq catchment area to control the flood that pass through Mafraq City during winter times. In order to achieve the objectives of the study, different thematic maps (e.g., rainfall, soil texture, drainage density, slope derived DEM and vadose zone materials) were gathered from different resources and organized, incorporated within Geographical Information System tools (GIS). The final harvesting suitability model map for the study area was produced based on the use of Weighted Linear Combination (WLC) techniques, where each GIS layer has its ratings and weights. Water harvesting potential to control flood within the Mafraq City caused by Wadi Al-Mafraq runoff was classified into four classes (Low, Moderate, High and Very high). A significance site located within the high water harvesting potential to the West of Mafraq City was selected to perform a Time Domain Electromagnetic geophysical method as a validation to investigate the subsurface geological layering. The TDEM results show that three distinctive subsurface geo-electrical layers were identified in the proposed site. The topmost layer, composed of (10 - 25) m, is interpreted as a silty clay, soil and alluvium with resistivity of (20-40) Ohm. m. The second subsurface layer, composed of 20m to 60m and resistivity of (150 - >200) Ohm.m, is interpreted as a massive fractured limestone and/or a paleo-channel deposits. The third subsurface layer, with resistivity of (40-140) Ohm.m and depth reaches 140m, is interpreted as a massive fractured limestone of Wadi Es Sir Limestone (WSL).

References

[1] Addustour newspaper, 2011. Issue No (15892), 10, October, Monday, Newspaper Archives.

[2] Al-Adamat, R., Diabat, A., and Shatnawi, G., 2010. Combining GIS with multicriteria decision making for siting water harvesting ponds in Northern Jordan, Journal of Arid Environments, 74(11): 1471-1477.

[3] Al-Adamat, R., 2008. GIS as a decision support system for siting water harvesting ponds in the Basalt Aquifer/NE Jordan, Journal of Environmental Assessment Policy and Management, 10(02): 189-206.

[4] Al-Adamat, R., Al Ayyash, S., Al-Amoush, H., Al-Meshan, O., Rawajfih, Z., Shdeifat, A., and Al-Farajat, M., 2012. The combination of indigenous knowledge and geo-informatics for water harvesting siting in the Jordanian Badia, Journal of Geographic Information System, 4(4): 366-376.

[5] Al-Adamat, R., Rawajfih, Z., Easter, M., Paustian, K., Coleman, K., Milne, E., and Batjes, N. H., 2007. Predicted soil organic carbon stocks and changes in Jordan between 2000 and 2030 made using the GEFSOC Modelling System, Agriculture, ecosystems & environment, 122(1): 35-45.

[6] Al-Amoush, H., Al-Shabeeb, A.R., Al-Ayyash, S., Al-Adamat, R., Ibrahim, M. and Rajab, J.A., 2016. Geophysical and Hydrological Investigations of the Northern Wadis Area of Azraq Basin for Groundwater Artificial Recharge Purposes, International Journal of Geosciences, 7(5): 744-760.

[7] Al-Amoush, H., Al-Tarazi. E., Abu Rajab, J., Al-Dwyeek, Y., Al-Atrash, M., Shudiefat. A., 2015. Geophysical Investigation Using Time Domain Electromagnetic Method (TDEM) at Wadi Deir Al-Kahaf Area/Jordan for Groundwater Artificial Recharge Purposes, Journal of Water Resource and Protection, 7: 143-151

[8] Al-shabeeb, A., 2016. The Use of AHP within GIS in Selecting Potential Sites for Water Harvesting Sites in the Azraq Basin—Jordan, Journal of Geographic Information System, 8(1): 73-80

[9] Al-shabeeb, A., 2015. A modified analytical hierarchy process method to select sites for groundwater recharge in Jordan, Unpublished PhD thesis, Department of Geography, University of Leicester, UK.

[10] Al-Smadi, A., 1997. Map sheet No.3254IV, Geological map of Al-Mafraq Report

[11] Baban, S., and Wan-Yusof, K., 2003. Modelling optimum sites for locating reservoirs in tropical environments, Water Resources Management, 17(1): pp.1-17

[12] Buselli, C., Barker, C., Davies, G., and Salama R., 1990. Detection of groundwater contamination near waste disposal sites with transient electromagnetic and electrical methods, In Geotechnical and Environmental Geophysics, V (2). SEG., Tulsa, pp.27-41.

[13] Charlesworth, S. M., 2010). A review of the adaptation and mitigation of global climate change using sustainable drainage in cities, Journal of Water and Climate Change, 1(3): 165-180.

[14] Christensen, N., and Sorensen, K., 1995. New strategies for surface and borehole electromagnetic methods in hydro-geophysical investigations, extended abstract, proceeding, EEGS, Torino, pp 356-359.

[15] Danielsen J., Auken, E., Lorgensen, F., Sondergaard, V., Sorensen, K., 2003. The application of the transient electromagnetic method in hydrogeophysical surveys, Journal of Applied Geophysics, 53:181-198.

[16] Department of Statistics (DOS), 2015. Open files and reports

[17] Department of Meteorology (DOM), 2015. Open files and reports.

[18] El-Awar, F., Makke, M., Zurayk, R., and Mohtar, R., 2000. A hydro-spatial hierarchical method for siting water harvesting reservoirs in dry areas, Applied Engineering in Agriculture, 16(4): 395-404.

[19] Goldman, M., Rabinvich, B., Rabinovich, M., Gilad, D., Gev. I. and Shrov, M., 1994. Application of the integrated NMR-TDEM method in groundwater exploration in Israel, Journal of Applied .Geophysics, 31: 27-52

[20] Gupta, K., Deelstra, J., and Sharma, K., 1997. Estimation of water harvesting potential for a semiarid area using GIS and remote sensing, IAHS Publications-Series of Proceedings and Reports-Intern Assoc Hydrological Sciences, 242(63): p.63.

[21] Hoekstra, P., and Blohm, M. W., 1990. Case histories of time-domain electromagnetic soundings in environmental geophysics. In: WARD, S. H. (Ed.): Geotechnical and environmental geophysics, II. Society of Exploration Geophysicists, Tulsa, 1-15.

[22] Jha, A., Bloch, R., and Lamond, J., 2012. Cities and flooding: a guide to integrated urban flood risk management for the 21st century. World Bank Publications.

[23] Jorgensen, F., Sandersen, P., Auken, E., Lykke - Anderesen, H., and Sorensen K. 2005). Contribution to the geological mapping of Mors, Denmark- A case study on Large scale TEM Surveys, Bulletin of the geological society of Denmark, 52: 53-75

[24] Keary, P., Brooks, M., and Hill, I. 2002. An Introduction to Geophysical Exploration. 3rd edition., Blackwell Publishing, 262p.

[25] Kirsch, R. 2006. Groundwater Geophysics: A Tool for Hydrogeology. Springer-Verlag, Berlin Heidelberg, 493 p. http://dx.doi.org/10.1007/3-540-29387-6

[26] Mauldin – Mayerle, C., Carlson, N., and Zonge, K., 1998. Environmental apploications of high resolution TEM methods, proceedings, EEGS, Barcelona, pp.829-833.

[27] Reynold, M. 2011. An Introduction to Applied and Environmental Geophysics, 2nd edition., Wiely Blackwell, UK, 696p.

[28] Sharma, V. 1997. Environmental and Engineering Geophysics. 2nd edition, Cambridge University Press, 475p.

[29] Srivastava, R., 2001. Methodology for design of water harvesting system for high rainfall areas, Agricultural Water Management, 47(1): 37-53.

[30] Shatnawi G., 2006. Determine the Best Sites for Water Harvesting Projects (Dams &Hafirs) in Northeastern Badia Using GIS Applications. Unpublished MSc., Al al-Bayt University, Mafraq, Jordan.

[31] Telford, W., Geldart, L., and Sheriff, R.1990. Applied Geophysics 2nd edition, Cambridge University Press.

[32] Zevenbergen, C., Cashman, A., Evelpidou, N., Pasche, E., Garvin, S., and Ashley, R. 2010. Urban Flood Management. CRC Press.

المملكة الأردنية الهاشمية

صندوق دعم البحث العلمي

الجامعة الهاشمية

المجلة الأردنية
لعلوم الأرض والبيئة

JJEES

مجلة علمية عالمية محكمة

المجلد (٨) العدد (٢)

http:// jjees.hu.edu.jo/

ISSN 1995-6681

المجلة الأردنية لعلوم الأرض والبيئة

مجلة علمية عالمية محكمة

المجلة الأردنية لعلوم الأرض والبيئة: مجلة علمية عالمية محكمة ومفهرسة ومصنفة، تصدر عن عمادة البحث العلمي في الجامعة الهاشمية وبدعم من صندوق البحث العلمي - وزارة التعليم العالي والبحث العلمي، الأردن.

ترسل البحوث إلكترونيا إلى البريد الإلكتروني التالي:

رئيس تحرير المجلة الأردنية لعلوم الأرض والبيئة

jjees@hu.edu.jo

لمزيد من المعلومات والأعداد السابقة يرجى زيارة موقع المجلة على شبكة الانترنت على الرابط التالي:

www.jjees.hu.edu.jo

المملكة الأردنية الهاشمية

صندوق دعم البحث العلمي

الجامعة الهاشمية

المجلة الأردنية لعلوم الأرض والبيئة

JJEES

مجلة علمية عالمية محكمة

تصدر بدعم من صندوق دعم البحث العلمي

http://jjees.hu.edu.jo/

المجلد (٨) العدد (٢) ISSN 1995-6681 كانون الأول ٢٠١٧ / ربيع الأول ١٤٣٩